

A MODEL OF A MAGNETIC STAR

by

RAYMOND G. CARLEBERG

A THESIS SUBMITTED IN PARTIAL FULFILMENT OF
THE REQUIREMENTS FOR THE DEGREE OF
MASTER OF SCIENCE

in the Department
of
Astronomy and Geophysics

We accept this thesis as conforming to the
required standard

THE UNIVERSITY OF BRITISH COLUMBIA

March, 1975

In presenting this thesis in partial fulfilment of the requirements for an advanced degree at the University of British Columbia, I agree that the Library shall make it freely available for reference and study. I further agree that permission for extensive copying of this thesis for scholarly purposes may be granted by the Head of my Department or by his representatives. It is understood that copying or publication of this thesis for financial gain shall not be allowed without my written permission.

Department of Geophysics and Astronomy

The University of British Columbia
Vancouver 8, Canada

Date May 7 / 1975

ABSTRACT

A method of computing the effects of a magnetic field on the structure of a star is discussed. The field is restricted so that the magnetic force is derivable from a potential, which allows the development of a simple expression for the field and distortion to the star. The J^2 technique is used to derive the perturbed equations of stellar structure, the only difference from the unperturbed equations being an alteration to the effective gravity as a function of radius. This method is applied to the computation of the structure of an upper main sequence star containing a dipolar magnetic field. The cases of the flux penetrating the convective core, and the flux excluded from the core are considered. The changes in the structure of the star, the distortion of the surface and the expected changes in the observable quantities are calculated.

TABLE OF CONTENTS

Abstract	i
Figures	iii
Tables	iv
1. Introduction and Review	1
1.1 Observations	1
1.2 Empirical Models	3
1.3 The Theoretical Problem	3
1.3.1 The Surface Effects	4
1.3.2 The Interior Field Structure	5
1.3.3 The Dynamics	7
1.3.4 Convection	10
1.3.5 Static Field Models	11
1.4 The Purpose of This Investigation	16
2. The Model of a Magnetic Star	17
2.1 The Equations of Stellar Structure	18
2.2 The Magnetic Field	20
2.3 The Magnetic Field Force Potential	22
3. The Equations Of Stellar Structure	28
3.1 Expansion of Potential And Variables	28
3.2 The Perturbed Stellar Structure Equations	29
3.3 The Distortion	31
4. Results and Discussion	34
4.1 The Field Structure	34
4.2 The Flux Free Convective Core	44
4.3 The Rotating Magnetic Star	45
4.4 Effects of the Field on the Star	47
4.5 The Perturbation to the Structure	51
4.6 The Validity of the Approximation	59
5. Conclusions	60
6. Acknowledgments	61
Bibliography	62
Appendix I: Stellar Structure Equations	69
Appendix II: The Distortion Terms	80
Appendix III: The Larson-Demarque Equations	82
Appendix IV: The Grey Atmosphere	92
Appendix V: Computer Programs	97

FIGURES

1. The Ap Stars	2
2. The Stream Function $b(r)$	35
3. Stream Function Derivative $b'(r)$	36
4. Streamlines for the Flux Penetrating the Core	37
5. Streamlines for the Flux Excluded from the Core	38
6. Components of the Magnetic Field	39
7. Ratio of Magnetic to Gravitational Force	40
8. Central Radial Field <u>vs.</u> Polar Field	41
9. Central Density Change <u>vs.</u> Polar Field	48
10. Central Temperature Change <u>vs.</u> Polar Field	49
11. Stellar Radius Change <u>vs.</u> Polar Field	50
12. The Magnetic Star in the HR Diagram	52
13. Equatorial And Polar Radii Difference	53
14. Polar And Equatorial Temperature Difference	54
15. The Distortion	55
16. Changes in B and V Indices	56
17. Geometry of Star's Surface	91

TABLES

I : Comparison of Initial Models	31
II : Comparison of Magnetic Stream Functions	42
III : Comparison of Changes to Structure	51

1. INTRODUCTION AND REVIEW

1.1 Observations of Stellar Magnetic Fields

Stellar magnetic fields were first observed in sunspots by Hale in 1908, and general high intensity stellar fields were discovered by Babcock in 1946. Since then a large amount of observational data has been accumulated on magnetic stars. The measured quantity is the effective longitudinal magnetic field, i.e. the component of the field in the observer's line of sight, averaged over the visible surface. The effective field is inferred from the Zeeman shift between right and left circularly polarized components of a spectral line (4). The extremely small displacements produced by the Zeeman effect are only measurable because the magnetic stars have very sharp lines, which is taken to mean that they are slow rotators (29). The quoted fields have to be viewed with some caution. Borra (10,11) has shown that there may be significant errors in the measurement of the effective field if one only measures the centroid of the line, while disregarding the shape of the line. In addition, the fields are found from an average over several spectral lines which reflect significant intrinsic variation in the field strength. The magnetic fields found in this way vary between the limit of observation, about 100 Gauss, and 34kG (4,5,50) which is the largest field measured for a main sequence star.

Magnetic stars are confined to the narrow range of spectral

types from B8 to A0. Due to their anomalous abundances relative to other stars in this temperature range, they are classified as Ap stars (29,50).

Figure 1 : The Ap Stars

Underlining indicates a magnetic field

(from Deutsch (11))

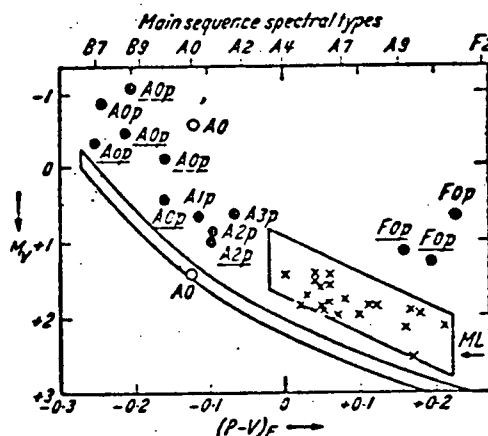


Fig. 6. The color-absolute-magnitude-spectral type diagram in the region of the peculiar A stars (Ap) and metallic-line stars (ML). [Adapted from O. Eggen: Astronom. J. 62, 45 (1957).] See text.

Depending on the surface temperature different elements are over or underabundant (44) sometimes as much as one thousand times with respect to a normal star. Ap stars were long known to exhibit photometric variations in their brightness and colour, usually with an extremely regular period. In addition they exhibit spectral variations, particularly of the peculiar elements.

The discovery of a magnetic field which in most Ap stars varied regularly with essentially the same period as the spectral and photometric variations was hailed as the unifying characteristic. Of course there are many exceptions, some Ap stars show no magnetic field, and some magnetic stars show no regularity of field variation. A number of excellent reviews of the magnetic stars can be found in the references (4,5,21,29,37,49).

1.2 Empirical Models of Magnetic Stars

The empirical model which has been best elucidated, and which provides an extremely neat and efficient framework for the observations is the oblique rotator model. It was first proposed by Stibbs (102) and later elaborated by Deutsch (29). One of the best recent uses of the model is Pyper's analysis of α^2 Canum Venaticorum, which includes detailed maps of the magnetic field and element distribution over the the surface of the star.

A simple dipole field in the oblique rotator model gives only sinusoidal variations of the field and hence cannot explain the assymmetrical shapes of the magnetic field variation. Consequently Landstreet (48) proposed a decentred dipole (decentred as much as $2/3$ of the stellar radius for 53 Cam) which provides a much nicer fit to the observations. However this may be mostly due to the introduction of an additional free parameter. Chiam and Monaghan (16) provided an equally close fit by mixing a quadropole component with the dipole.

1.3 The Theoretical Problem

The theoretical problem posed by magnetic stars is more or less separated into two areas; the explanation of the observed characteristics of the spectrum, which means consideration of surface effects of the magnetic field; and the investigation of

the unobservable interior field structure.

1.3.1 The Surface Effects

Preston (84) has written an excellent summary of the surface effects of magnetic fields. Only the major points will be discussed here.

Michaud (60) proposed that the magnetic field would stabilize patches against any small tendencies to mix the atmosphere, thus allowing the radiation pressure to drive a diffusion process. There is also the possibility of surface nuclear reactions (35). Particles accelerated to very high energies by the magnetic field surrounding the star would come crashing in at the poles to react with the surface elements. It is interesting to note that Aller and Cowley (4) tentatively identified Pm in a magnetic star, the most stable isotope of Pm having a half life of about 18 years. Other current theories involve binary supernovae and accretion.

The photometric characteristics are now generally believed to be a consequence of the non-uniform distribution of elements, which redistributes the flux through backwarming and line blanketing. Specific computations were made by Peterson (81) for a range of Si abundances and Wolff and Wolff (114) for the different ionization states of the rare earth elements. Both of these were able to produce variations of the proper magnitude, although there are problems with respect to specific types of Ap

stars. Trasco (107) has magnetic flux tubes emerging over the surface, and the magnetic pressure creates local hot spots. Also the distortion of the star by the magnetic field would produce light and colour fluctuations.

Strittmatter and Norris (103) have tried to unify the surface effects of magnetic fields to present a plausible outline of the evolutionary history of a magnetic Ap star. They consider how the magnetic field interacts with rotation, circulation, convection, accretion, mass loss, and diffusion. In brief, they find that if the magnetic field exceeds an initial critical value the external field will not vanish beneath the surface, thus allowing magnetic braking to slow the star. As the star slows the driving force for circulation lessens until the magnetic field is able to entirely suppress it, and a diffusion process can establish the abundance inhomogeneities.

1.3.2 The Interior Field Structure

The interior fields of magnetic stars are speculative quantities since there is no direct observational evidence to guide one through an extremely complex and intractable problem. There are several immediate questions; how the field got there in the first place, what the detailed structure of the field is, and how the internal field is related to the observable surface field.

The only general theoretical equation which covers real

stars with magnetic fields is the virial theorem. Invoking the global stability condition that the total energy must be negative Chandrasekhar and Fermi (22) showed that the maximum RMS magnetic field is limited by:

$$\sqrt{\langle H^2 \rangle} \lesssim 2 \times 10^8 \frac{M/M_0}{(R/R_0)^2} .$$

What is the origin of the field within the star? For strong magnetic fields the fossil theory seems to be the most likely answer. During the collapse of the protostar from the interstellar clouds the gas becomes ionized and the magnetic field lines are "frozen" into the collapsing cloud. The interstellar magnetic field of 10^{-6} G is more than sufficient to provide the maximum field allowed by the virial theorem. With simple arguments for a poloidal field Cowling (21) showed that the decay time is of the order of 10^{10} years. Since a fossil field would provide magnetic braking, this theory provides a mechanism for the explanation of the generally slow rotation of the magnetic stars. It is possible that fossil fields may be present in many stars, but the interior and exterior fields have been separated and the exterior field later lost.

The dynamo theory provides a magnetic field by transforming the kinetic energy of large scale mass motions into magnetic energy, but the dynamo requires a "seed" field for its initial operation. This mechanism is not particularly simple, since Cowling's celebrated anti-dynamo theorem precludes the maintenance of an axisymmetric field by symmetric mass motions.

The battery effect (91) converts thermal energy into magnetic energy, through the gravitational and rotational forces pro-

ducing a slight charge separation between the electrons and ions. This is the only mechanism envisioned so far which requires no initial field for its operation. Unfortunately the mechanism will not work at all if any poloidal magnetic field component is present, and in any case it is only capable of generating very weak fields.

1.3.3 The Dynamics

The discussion of the origin of the magnetic field serves to introduce the crucial interaction between the magnetic field and the mass motions within the star. The problem is essentially dynamic and static solutions may impose too great a restriction on the field to be representative of the true field. In spite of a desire to provide truly general solutions the problem rapidly becomes so hopelessly complex that little can be done.

The stability of a star with a magnetic field has been discussed in a number of recent papers. Wright (119) and Markey and Tayler (53) both used Bernstein's energy principle (6) to find that a purely poloidal field is unstable to "kink" and "sausage" type instabilities. A purely toroidal field with a non-zero current density on the axis of the star is found to be unstable to interchanges of the flux tubes (105, 109). This would occur near the centre of the star where convective motions are important, the interaction being unclear. These pure fields are unstable, but if a poloidal and toroidal field of roughly

equal magnitudes are mixed, the resulting field is likely to be stable. It may be noted that their analyses made a number of simplifying assumptions which may lessen the impact of these instabilities. The equations were incapable of saying anything about the size of the oscillations, merely whether or not the state was stable. Consequently the oscillations, although present, may be quite small. In addition the geometry was simplified so that any significant departure from equilibrium would severely strain the assumed field structure. It is interesting to note that the predicted period of oscillation is of the order of the size of the region, divided by the Alfvén wave velocity. This period is of the order of an hour, which is roughly the period of the high frequency oscillations observed in the light variations (49). Only the most rapidly occurring, largest scale instabilities were investigated. In addition there are resistive instabilities and micro-instabilities which may have an important role. These instabilities put added restrictions on the interior field structure on a real star, and require more complex models to fulfil the stability criterion. In particular they suggest that probably a toroidal and poloidal field coexist.

The most common theoretical models of the magnetic stars follow from the oblique rotator model, i.e. a magnetic field fixed in a rotating star. Mestel and Takhar (59) have investigated the internal dynamics of the oblique rotator. By considering energy dissipation it is found that the angle between the magnetic axis and the rotation axis decreases for an oblate star and increases for a prolate star. The time scale of the process

is easily capable of changing the angle of obliquity within the time scale of a star. The internal motions also lead to mixing of material between the evolutionary core and the surface layers.

Rotating stars are well known to exhibit meridian circulation, and in general one would expect that even a non-rotating magnetic star would have some circulation. It is possible that the magnetic field is sufficiently well frozen into the material that no circulation across field lines is allowed. For a rotating magnetic star the two fields may interact in such a way the circulation is entirely suppressed, in which case Ferraro's law of isorotation requires that the angular velocity be constant on stream lines (34). Maheswaran (57) has calculated the evolution of a prescribed magnetic field in a prescribed circulation field and finds that the flux is expelled from the middle of the circulation zone, leading to a concentration of the flux towards the poles of the star.

The specific effects of rotation have different qualitative features dependent on the ratio of the rotational to magnetic energies, and on the geometry of the field. Of particular interest is Mestel's remark (57) that a weak magnetic field, which constrains a star to uniform rotation, sets up a circulation which destroys the initially conservative, i.e. curl free, centrifugal force.

1.3.4 Convection

The problem of stellar convection is quite difficult, even without the complicating effects of a magnetic field, rotation, or a combination of the two. If initially there is a magnetic field in a zone which is unstable to convection then the work of Weiss (111) suggests that the eddying motions of the convection would expel the field. This process results in the destruction of some flux at the centre of the eddy through resistive dissipation, and a concentration of the expelled flux at the borders of the eddy. This process occurs on a time scale of a few times the eddy turnover time, which for a convective core would be considerably shorter than the main sequence lifetime of the star.

Taylor, his co-workers (74, 75, 105), and Kovetz (16) have discussed criteria for convective stability. Gough and Taylor obtained a relation for stability in an infinitely conductive plane parallel compressible fluid. The simplified stability equation is:

$$\frac{B_{\text{vertical}}^2}{\gamma P + B_v^2} > \nabla - \nabla_{\text{ad}}.$$

It is readily seen that the field has a stabilizing influence on convection, but for typical central stellar pressures of 10^{17} dynes/cm², very large magnetic fields are required to suppress

convection in the core. This criterion may be useful in the core where the gradient can be set equal to the adiabatic gradient to very high accuracy, but provides no equation for stellar structure in the envelope, where some dynamical theory, e.g. mixing length theory is required.

Stothers and Chin (104) and Moss and Tayler (75) have computed models of upper main sequence stars with convection completely suppressed in the cores, although it is possible that the magnetic field may interfere with the convection only to the extent of making it a less efficient energy transport mechanism. The models found have evolutionary histories incompatible with observations of clusters. Hence radiative cores do not seem to be viable.

1.3.5 Static Field Structure Models

To make any progress in the construction of models of magnetic stars a great number of simplifying approximations must be made. The earliest models were very simple indeed, but served to outline many of the qualitative features of more complex models, and also provided a path of analysis which could be extended to more realistic cases. Several excellent reviews are available (21,55).

Briefly the first models assumed that the star was barytropic. This implies that the magnetic force/unit mass must be derivable from a potential, i.e.

$$\nabla \times \left\{ \frac{(\nabla \times \vec{H}) \times \vec{H}}{4\pi \rho} \right\} = 0.$$

Ferraro applied this condition to a liquid star model (34). Later Wentzel added a toroidal field component (112) to a liquid star with a poloidal field. These two components of the field in concert with the barytropic condition greatly restrict the possible field structures. Wentzel was confronted by the problem of surface boundary conditions for the field. Either force free fields give rise to large surface stresses, which must be balanced by an external field; or the surface field must vanish. An exact solution with the surface field vanishing was found by Prendergast (87), which has the interesting property of being spherical. Woltjer (115,116,117) and Wentzel (113) extended these results to include more realistic density distributions. Attempts were made to establish the stability of the field structure, but since thermal equilibrium is entirely ignored these analyses have little applicability to realistic stars.

Any non-spherical perturbing force is capable of driving circulation, which in turn is capable of distorting the original perturbing force. Roxburgh looked for solutions where the circulation and magnetic field had come into equilibrium. Solutions were obtained only for two cases: a dominant rotational force with a weak magnetic field maintaining the star in nearly uniform rotation, and a dominant toroidal field.

Roxburgh (90) presents fields for realistic, non-polytropic stars which are made self-consistent by restricting the perturbing magnetic field to be independent of the circulation which

it drives. This is done for a weak toroidal field dominated by rotation and for a toroidal field which dominates the rotation and the poloidal field.

Roxburgh also examines a mixed toroidal and poloidal field in a polytrope (92). This results in an eigenvalue equation for the magnetic stream function. The field is forced to vanish at the surface to meet the condition of being derivable from a stream function. Van der Borcht has extended Roxburgh's results, in particular calculating the shape of the star.

Monaghan has extensively investigated of polytropes with large dipole magnetic fields. He sets out the perturbation technique for the calculation of the change in the star's structure (61). Any variable $Q(r, \theta)$ is expanded as

$$Q(r, \theta) = Q_0(r) + \lambda_M [Q_{10}(r) + Q_{12}(r) P_2(\cos \theta)],$$

where $Q_0(r)$ is the unperturbed zero order value, λ_M a parameter of order of the ratio of the magnetic field energy to the gravitational energy, Q_{10} is the first order spherical perturbation, and Q_{12} the nonspherical term.

The resulting polytropes are distorted into oblate spheroids, contracted with respect to the original non-magnetic model. Later Monaghan (64) repeated the analysis with polytropes with a simplified and improved perturbation expansion which incorporates some of the magnetic effects in the spherical model (not the zero order model).

The basic type of perturbation expansion has been extended by Monaghan to more realistic stellar models (63), i.e. they include thermal equilibrium. In turn this has been extended

again to rotating magnetic stars by Davies (28), Wright (118), and Monaghan and Robson (70). None of these models include circulation. The first order terms comprise a coupled set of non-linear differential equations, involving the non-spherical perturbations to the pressure, density, temperature, and gravitational field. The magnetic field stream function is found by using an iterative technique on the set of non-linear equations. The so-called pseudo-polytropic magnetic field obtained from

$$\frac{d^2 b}{dr^2} - \frac{2b}{r^2} = k f_0 r^2,$$

is used as a starting approximation. Note that f_0 implies that the field is only dependent on the spherical model. The final field found exhibits a quantitative change of about 25% from the starting approximation, but retains the basic qualitative features.

For the case of rotating star, if the surface polar field strength is held constant as the rotation velocity is increased, then the ratio of central field to polar field strength increases from about 30 for a non-rotating star, to about 1200 for a star with a ratio of rotational to magnetic force of about 10%. Similarly if the interior magnetic flux is held constant as the rotation velocity increases, the emergent flux decreases to zero at some finite limit less than the break up velocity. These results are dependent only on the ratio of rotational to magnetic force and not on their absolute values relative to the total energy of the star (for weak fields anyway). The shape of the star as determined by Monaghan and Robson is dependent on what one takes the surface to be, a surface of constant pressure or

constant temperature, which are not coincident surfaces in these models. In fact the constant pressure surfaces are considerably more oblate.

This type of model has been extended to more complex field structures. Monaghan (67) has placed the dipolar field at an angle to the rotation axis and found that for a given surface field the maximum central field occurs when the angle of obliquity is zero. Unfortunately these results are not very complete because of a problem of convergence. Chiam and Monaghan (16) incorporated a multipole magnetic field in a polytrope, using the same basic analysis as Monaghan's earlier work, but with a stream function extended to higher multipoles.

These types of calculations were further extended to simple realistic stars by Monaghan (68) and Moss (72). The set of equations which result from the perturbation expansions are an extensive set of nonlinear differential equations, which are solved by recourse to the pseudo-polytropic approximation for a starting solution. The resulting field structure is similar to the rotating dipolar magnetic stars; the interior concentration of the field increases with rotation, for a given flux there is a maximum rotation rate for the existence of a solution, and there is a minimum value that the ratio of magnetic field energy to rotational energy can have as the rotation increases. In contrast, the surface field need not vanish above a certain rotation velocity, since the quadrupole component does not vanish with the dipole component.

Recently attempts have been made to move on from these static models to more realistic dynamic models. Monaghan (69)

has calculated the decay of the field and Moss (73) tried to include some circulation.

A different type of model has been put forth by Trasco (106). He assumes that the star contains a random magnetic field which introduces an isotropic magnetic pressure. The field is obtained from a flux freezing consideration, where $H \propto \rho^{2/3}$. Trasco's model is spherical and therefore amenable to standard stellar model computer programs modified only by including a magnetic pressure term to the gas pressure. There are no "first order" or "non-spherical" terms to be explicitly calculated.

1.4 The Purpose of This Investigation

This thesis calculates the magnetic field and the stellar structure by a method in the spirit of Trasco, and similar to the one used for rotating stars. That is, a realistic prescribed dipole field, based upon the star's spherical structure is used to provide a magnetic force which incorporates the basic structural changes in the spherical model, thereby avoiding the problem of explicitly calculating the non-spherical terms. The Henye technique for calculating stellar models is nearly trivially adapted to this. In addition it can be easily expanded to include dynamical and evolutionary changes. All these possibilities are of great practical value for a model of a magnetic star.

2. THE MODEL OF A MAGNETIC STAR

2.1 The Equations of Stellar Structure

The full set of equations which must be satisfied for a complete dynamical description of a magnetic star are described in Roxburgh (90) and elsewhere. Only the equations which are left after making the various simplifying assumptions will be repeated here.

First, the greatest simplification. This model has no dynamical features, which immediately means all quantities are independent of time, and hence all time derivatives are zero. Next, there are no large scale, ordered fluid motions within the star, such as circulation currents. This assumption of a static model greatly alleviates the computational burden by allowing us to ignore such diverse effects as viscous energy dissipation, energy transport by circulation, balance of the toroidal forces, angular momentum transfer, and differential rotation. These effects although important in themselves, can be investigated separately and are not necessarily crucial to understanding how the magnetic field would effect the star. To simplify the electrostatic equations we assume the star is a perfect conductor, which considering the high densities and temperatures is not unreasonable. These assumptions leave us with the following equations.

Hydrostatic equilibrium,

$$\frac{\nabla P}{\rho} = -\nabla \Phi + \Omega^2 \tilde{\omega} + \frac{1}{c} \vec{J} \times \vec{H}.$$

(2.1)

P is the pressure, ρ is the density, Ω is the rate of angular rotation, $\tilde{\omega}$ is the distance from the axis of rotation, \vec{J} is the current density, \vec{H} is the magnetic field vector, and Φ is the potential field acting on the star, which is usually only self gravitation.

The gravitation potential is given by Poisson's equation,

$$\nabla^2 \phi = 4\pi G \rho.$$

(2.2)

For energy transport by radiation the flux is

$$\vec{F} = -\frac{4ac}{3} \cdot \frac{T^3 \nabla T}{\kappa \rho}.$$

(2.3)

The energy can be transferred by convection if,

$$\nabla = \frac{d \ln T}{d \ln P} > \nabla_{ad} = \frac{8 - 6\beta}{32 - 24\beta - 3\beta^2}.$$

(2.4)

The ratio of gas pressure to total pressure is given by β .

The equation of state for a perfect gas gives the gas pressure

$$p_g = \frac{R}{\mu} \rho T.$$

(2.5)

The radiation pressure is

$$p_r = \frac{a}{3} T^4.$$

(2.6)

Energy conservation, with the above assumptions is simply

$$\nabla \cdot \vec{F} = \epsilon \rho,$$

(2.7)

where ϵ is the local energy generation rate per gram of material.

Perfect conductivity implies $\vec{E} = 0$ everywhere in the star so Maxwell's equations reduce to

$$\nabla \times \vec{H} = \frac{4\pi}{c} \vec{J},$$

(2.8)

$$\nabla \cdot \vec{H} = 0.$$

(2.9)

2.2 The Magnetic Field

The Lorentz force produced by the magnetic field,

$$\vec{F}_L = \frac{\vec{J} \times \vec{H}}{c}, \quad (2.10)$$

can be decomposed by using (2.8) and splitting the field into toroidal (H_t) and poloidal (H_p) components, then

$$\mu_0 \vec{F}_L = (\nabla \times \vec{H}_p) \times \vec{H}_p + (\nabla \times \vec{H}_t) \times \vec{H}_t + (\nabla \times \vec{H}_t) \times \vec{H}_p. \quad (2.11)$$

The last term in (2.11) is the only toroidal force and can only be balanced by the convection of angular momentum by circulation. Since circulation has been explicitly assumed not to exist, the toroidal force must vanish. Therefore,

$$(\nabla \times \vec{H}_t) \times \vec{H}_p = 0, \quad (2.12)$$

which implies

$$H_p = f(r, \theta) \nabla \times \vec{H}_t \quad (2.13)$$

With (2.9) this means that the field is derivable from a stream function.

Now (2.8) when decomposed says

$$\nabla \times \vec{H}_t = \frac{4\pi}{c} \vec{J}_p .$$

(2.14)

We require that J_p goes to zero at the surface. Consequently (2.13) combined with (2.14) implies that for a mixed poloidal-toroidal field, the poloidal field must go to zero at the surface. Hence it cannot match onto an external field. This condition on the poloidal component of the current can also be satisfied if H_t or H_p are zero throughout the star.

This boundary condition causes the magnetic fields to be partitioned into three distinct sets;

- 1) a purely toroidal field,
- 2) a mixed toroidal-poloidal field which is confined to the star,
- 3) a purely poloidal field which matches onto an external field.

To obtain an observable field, the third choice was taken. At the outset it should be pointed out that Wright and Markey and Tayler have shown that a purely poloidal field is unstable to MHD instabilities in the star. The instabilities occur at the O type neutral point, which is located at about 1/3 the stellar radius from the centre. Thus the oscillations may be greatly damped in the overriding layers of the star.

In spite of these instabilities it was felt that purely poloidal fields were a realistic approximation worth doing. Other research has been done on magnetic fields of this type so

that at least the method of computing the changes to the stellar structure could be compared. Additionally the technique can be easily extended to toroidal and mixed poloidal and toroidal fields.

2.3 The Magnetic Field Force Potential

For simplicity of calculation of the stellar structure, where methods exist to handle perturbations due to rotational forces derivable from potential functions, we restrict the field to that subset for which the force per unit mass is derivable from a potential function, that is

$$\nabla \times \left(\frac{\vec{F}_L}{\rho} \right) = 0.$$

(2.15)

Then the equation of hydrostatic equilibrium reduces to

$$\frac{\nabla P}{\rho} = -\nabla \Phi,$$

(2.16)

where Φ can be decomposed into a gravitational potential, ϕ plus a potential for the perturbing field, ψ ,

$$\Phi = \phi + \psi.$$

(2.17)

Consequently all physical structure quantities $P, T,$ and ρ are constant on surfaces of constant Φ , and hence the opacities and energy generation rates are constant also. This considerably simplifies the calculation of stellar structure.

How realistic can a magnetic field this restricted be? This field is not intended to give a representation of the detailed internal structure of the field, rather it is proposed as a simple and computationally quick way to calculate the gross effects of a magnetic field on a star, and the gross features of that field. This restriction of potential derivable disallows only non-conservative magnetic force fields, and still leaves a vast selection which should adequately perform the functions we require of them.

Now as noted from (2.13) the magnetic field is derivable from a stream function, Ψ , such that

$$\vec{H}_p = f(r, \theta) \nabla \Psi \times \hat{\phi}. \quad (2.18)$$

Taken with (2.9) this specifies $f(r, \theta)$ and therefore in spherical co-ordinates,

$$\vec{H}_p = \left(-\frac{1}{r^2 \sin \theta} \frac{\partial \Psi}{\partial \theta}, \frac{1}{r \sin \theta} \frac{\partial \Psi}{\partial r}, 0 \right). \quad (2.19)$$

The major contribution to the observed fields is assumed to be a dipole field. Therefore we choose Ψ to represent a field which will match onto an external dipole. A dipole has a stream function $\Psi \propto r^{-1} \sin^2 \theta$ so for the internal field we chose

$$\Psi = B b(r) \sin^2 \theta,$$

(2.20)

where B is chosen so that $b(R_*) = 1$.

Substituting (2.20) into (2.19) gives

$$\frac{\vec{F}_L}{\varphi} = \frac{B^2}{4\pi} \frac{\frac{1}{r^2} (b'' - \frac{2b}{r^2})}{\varphi} \left[-\sin^2 \theta b', -\frac{2 \cos \theta \sin \theta}{r} b, 0 \right]. \quad (2.21)$$

Noting that the vector term in brackets in (2.21) is the gradient of $b(r) \sin^2(\theta)$, all we require for the potential is that

$$\nabla \left(\frac{1}{r^2} \frac{b'' - \frac{2b}{r^2}}{\varphi} \right) \times \nabla (b \sin^2 \theta) = 0. \quad (2.22)$$

We require a general $b(r)$ which satisfies this nonlinear equation (and note that φ is coupled to b in a first order correction). Monaghan's work with polytropes showed that an exact solution for $b(r)$ from the first order perturbation expansion, is given by

$$\frac{\frac{1}{r^2} (b'' - \frac{2b}{r^2})}{\varphi_{\text{polytrope}}} = \text{constant}. \quad (2.23)$$

This has been successfully used as a starting point for the solution of the nonlinear equations resulting from the same expansion made to first order for real stars. These solutions

were found to differ little from the initial approximation to $b(r)$, the so called pseudo-polytropic stream function, given by

$$\frac{\frac{1}{r^2} \left(b'' - \frac{2b}{r^2} \right)}{\rho_0(r)} = \text{constant.} \quad (2.24)$$

This is what is used herein to obtain the magnetic field, with the added distinction that $\rho_0(r)$ is no longer the zero order density distribution, rather it is the spherical part of the density, now perturbed by the magnetic field.

Substituting (2.24) into (2.21) and integrating we obtain for the magnetic force potential,

$$\psi_H = \frac{B^2}{4\pi k} b(r) \sin^2 \theta \quad (2.25)$$

It should be noted that (2.24) does not give a completely consistent equation for the field, since the forcing function ρr^2 and the boundary conditions are evaluated on the spherical part of the model, not on the oblate spheroid which the magnetic field causes the star to assume.

The boundary conditions for the magnetic field are quite simple. The field must match onto an external dipole, so at the surface we have

$$b(R_*) + R_* b'(R_*) = 0. \quad (2.26)$$

At the centre we require that the magnetic force vanish, so

$$b(0)=0, \quad b'(0)=0.$$

(2.27)

Equation (2.24) is linear and the solution can be expressed as a particular solution plus a constant times the solution to the homogenous equation. The solution of the homogenous equation is

$$b_h = a_1 r^2 + \frac{a_2}{r}.$$

(2.28)

Consequently if the field extends to the centre of the star the boundary condition (2.28) requires that $a_2=0$. On the other hand the field may not extend to the centre and another field structure arises. Although the influence of convection on the magnetic field is not well understood, there are several equilibrium possibilities. The field may suppress convection, the field may be expelled by the convective motions, or there may be some sort of coexistence. As mentioned above it seems that a star with totally suppressed convection in the core is not very plausible (104). Weiss (111) conducted investigations into the expulsion of flux by eddies, which indicated that the field may be expelled from the core. To represent a magnetic field which has been expelled we set

$$b(r)=0 \quad \text{for} \quad 0 \leq r \leq r_c$$

(2.29)

where r_c is the radius of the convective core. For the solution of the homogenous equation we match (2.28) onto (2.29) which eliminates one of the constants, and

$$b_h = a \left(r^2 - \frac{r_c^3}{r} \right). \quad (2.30)$$

Unfortunately (2.30) implies that at the boundary,

$$b'_h = 3a r_c^3, \quad (2.31)$$

which results in a discontinuity in radial force across the boundary of the convective core. But as the results of Weiss show there is an extremely high concentration of flux at the edge of the eddies. Thus while there are no discontinuities we might expect an extremely rapid rise in $b'(r)$ across the boundary. A discontinuity is not very palatable, but it was felt that the alternative of fitting a polynomial to smooth it out, or any other artificial device would be even less acceptable. Also the discontinuity in total force, magnetic plus gravitation is relatively small, so as long as the stellar structure program was able to converge, the approximation was deemed adequate.

3. THE EQUATIONS OF STELLAR STRUCTURE

3.1 Expansion Of Potential and Variables

The magnetic force potential of (2.25) combined with the gravitational potential can now be written as,

$$\Phi = \phi(r, \theta) + \frac{2}{3} \frac{B^2}{4\pi k} b(r) [1 - P_2(\cos \theta)]. \quad (3.1)$$

To specify this potential completely, we need to know ϕ which is computed from Poisson's equation. Note the perturbation is composed of a spherically symmetric term plus a $P_2(\mu)$ term, where $\mu = \cos \theta$. Any variable Q can be expanded in a Legendre series,

$$Q = Q_0(r) + \sum_{n=1}^{\infty} Q_n(r) P_n(\cos \theta). \quad (3.2)$$

We would expect that the dominant perturbation to be that one forced by the $P_2(\mu)$ term of the magnetic potential. We will explicitly make this assumption. P , T , and χ will be expanded as

$$Q = Q_0(r) + Q_2(r) P_2(\mu). \quad (3.3)$$

If Q_0 is of order 1 then Q_2 is of order

$$\lambda_H = \frac{\frac{2}{3} \frac{B^2}{4\pi k}}{\frac{G M_*}{R_*^2}} \quad . \quad (3.4)$$

With the expansion for ϕ as above the Poisson's equation for the gravitational potential becomes

$$\nabla^2 \sum_{n=0}^{\infty} \phi_n P_n(u) = 4\pi G (\rho_0 + \rho_2 P_2(u)). \quad (3.5)$$

Only the ϕ_0 and ϕ_2 terms are left with ρ expanded as above.

3.2 The Perturbed Stellar Structure Equations

The perturbation is handled in a manner similar to that used by Faulkner, Roxburgh and Strittmatter (32) and the J^2 method of Papaloizou and Whelan (77). The spherical terms are found by evaluating the equations at the point $P_2(u)=0$, on a surface of constant potential. This is an exact treatment of the perturbation, except for approximations later made when evaluating the integrals over the nonspherical surface. The full development of the equations is given in Appendix I. The resulting equations are, to first order,

$$\frac{1}{\rho} \frac{d\rho}{dr_0} = - \frac{G M_r (1 + \lambda)}{r_0^2} , \quad (3.6)$$

$$\frac{dm_r}{dr_0} = 4\pi r_0^2 \rho(r_0),$$

(3.7)

$$\frac{dT}{dr_0} = \frac{-3\kappa\rho L_r}{16\pi ac r_0^2 T^3}, \quad (\text{radiative})$$

(3.8)

$$\frac{d \ln T}{d \ln P} = \frac{8 - 6\beta}{32 - 24\beta - 3\beta^2}, \quad (\text{convective})$$

(3.9)

$$P = \frac{R}{\mu\beta} \rho T,$$

(3.10)

$$\beta = \frac{P_g}{P} = 1 - \frac{\frac{3}{8} T^4}{P},$$

(3.11)

$$\lambda = \frac{\frac{3}{8} \frac{\beta^2}{4\pi k} \frac{db}{dr}}{c m_r / r_0^2}.$$

(3.12)

The essence of this method of calculation of the stellar structure is simplicity. By taking the distance to a potential surface along the line $P(\cdot)=0$ as the radial coordinate, the stellar structure equations retain their original form. The only

change is a first order correction to the mass. Similarly the various perturbations to the stars structure are easily calculated. The details of the calculation are outlined in Appendix II.

The energy generation rate was taken from Larson and Demarque (47). The opacities were found from the analytic fit to the Keller-Meyerott opacity tables used by Sackmann and Arand (96). The equations were integrated using the relaxation technique outlined by Larson and Demarque although the equations were changed to neglect degeneracy pressure and to include radiation pressure. The composition chosen was $X=.80$ and $Z=.02$, corresponding to a population I star. The spherical, non-magnetic starting models calculated agree well with the results of other calculations.

Table I: Comparison of Initial Models

M/M_{\odot}	$\log(L/L_{\odot})$	$\log(T_e)$	$\log(R/R_{\odot})$
Iben's Models $X=.708$ $Z=.02$			
9	3.65	4.41	.54
5	2.80	4.29	.35
3	1.97	4.14	.24
Unperturbed Models Used Here $X=.80$ $Z=.02$			
10	3.61	4.36	.61
5	2.26	4.19	.42
3	1.69	4.05	.28

3.3 The Distortion

Substituting the expanded physical variables into the stellar structure equations and equating the nonspherical terms, i.e. those with a coefficient of $P_2(\mu)$, or its derivative, gives a set of equations in $\rho_1, \rho_2, T_1, \phi_1$, and ψ_2 . We point out that the nonspherical part of the magnetic perturbing potential is determined from the spherical model alone. Since all quantities are constant on surfaces of constant Φ , we only need to use these quantities to determine the shape of the surface of constant Φ . These surfaces are easily found by making a simple Taylor's expansion about a spherical surface. The radial distance from the centre to any point is given, to first order, by

$$r = r_0 [1 + \epsilon(r_0) P_2(\mu)]. \quad (3.13)$$

The expansion is made on the potential, the only part of which needs to be specially determined is the nonspherical part of the gravitational potential.

The effective temperature of the star is easily determined from

$$4\pi R_*^2 \sigma T_e^4 = L_* . \quad (3.14)$$

To find the variation of the temperature over the surface of the star we use Von Zeipel's theorem which states that the radiated flux is directly proportional to the effective gravity at that point. Hence

$$\frac{T_e^4(r, \theta)}{T_e^4(R_0, P_2=0)} = \frac{g(r, \theta)}{g(R_0, P_2=0)} \quad (3.15)$$

Using this temperature distribution a simple plane parallel grey atmosphere was fitted to the surface, from which the V and B indices could be obtained. The U index was not attempted since the grey approximation is not valid for stars of $T_e > 10^4 \text{ K}$. The calculation is outlined in Appendix III.

4. RESULTS AND DISCUSSION

4.1 The Field Structure

The stream function for the magnetic field was calculated from the pseudo-polytropic approximation (2.24). The density was taken from the spherical part of the model. This stream function was then used in the magnetic force potential to obtain a new spherical model, from which a new $b(r)$ was calculated, and so on until the magnetic field converged. For a reasonable step size from the previous field, fields of order 10^7 G converged to 0.1% in about 5 iterations.

Equation (2.25) obviously implies that the accuracy of the stream function is dependent on the accuracy of the run of the density from the spherical model, which in turn is dependent on the reality of the model used. The judgement of the model can be separated into two parts; first, the method of calculation of the perturbed structure; and second, the input physics for the quantities required by the structure calculation. The physics for the opacity was a curve fit to detailed tables. The energy generation rate was found from formulas based upon step by step reactions, using experimentally determined cross-sections.

It is interesting to compare the stream function, $b(r)$ found here to the stream function found by Monaghan and Robson (MR ref.70) and Davies (28) for a dipolar field. These authors used a nonlinear calculation and $b(r)$ was not restricted to be a po-

Figure 2 : Streamlines of the Magnetic Field

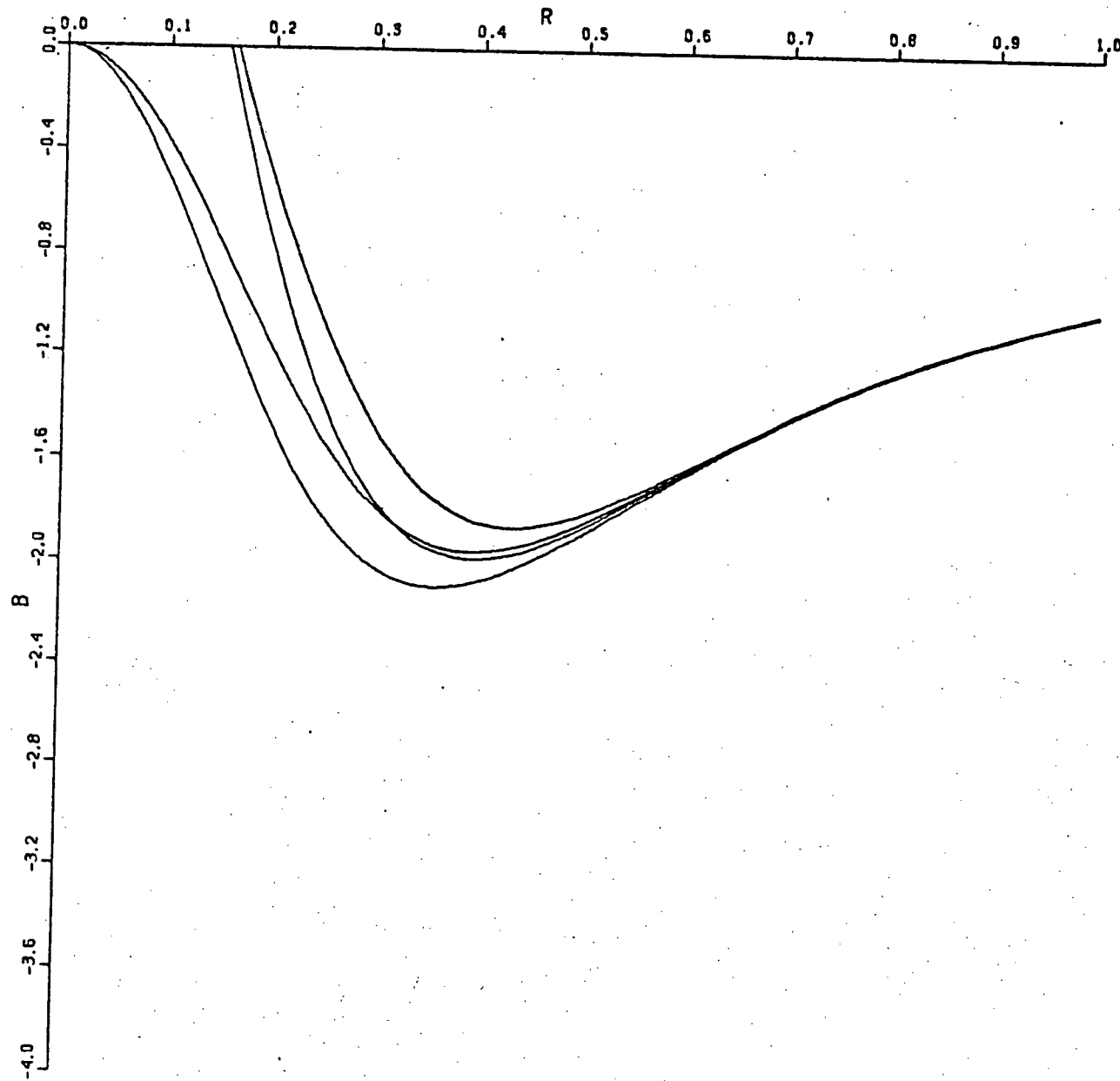


Figure 3 : Derivative of Stream Function

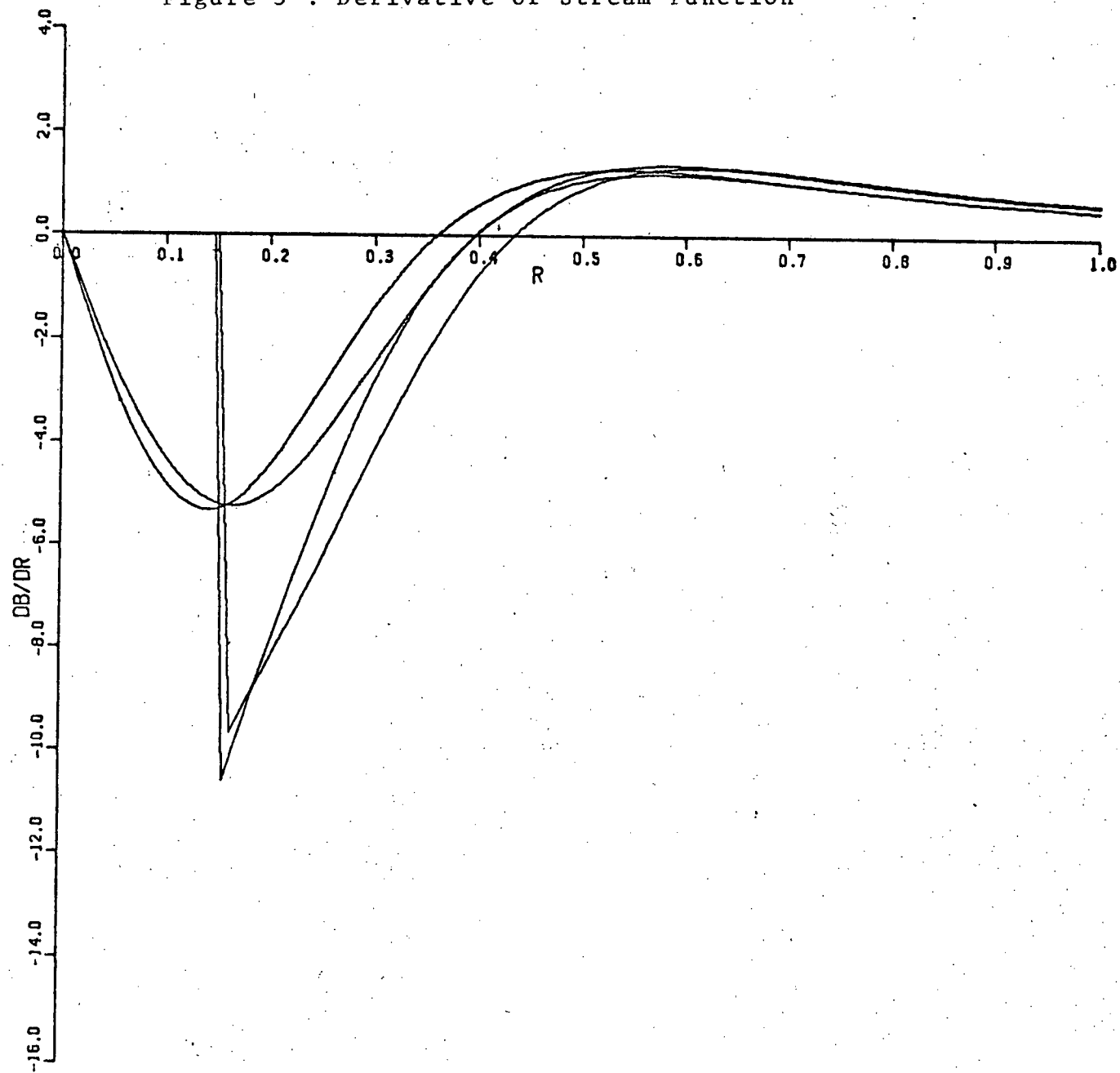


Figure 4 : Streamlines for the Flux Penetrating the Core

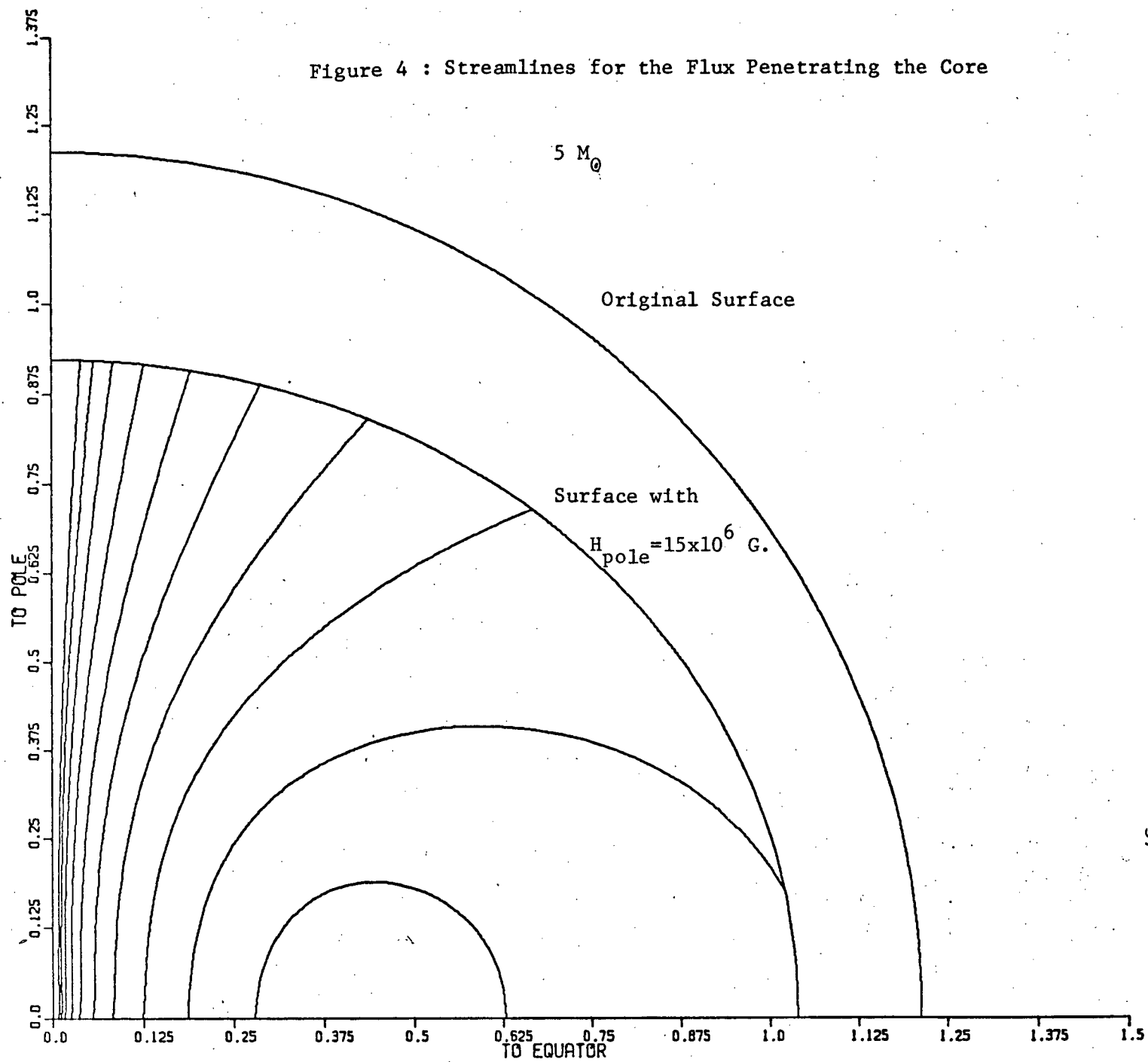


Figure 5 : Streamlines for the Flux Excluded from the Core

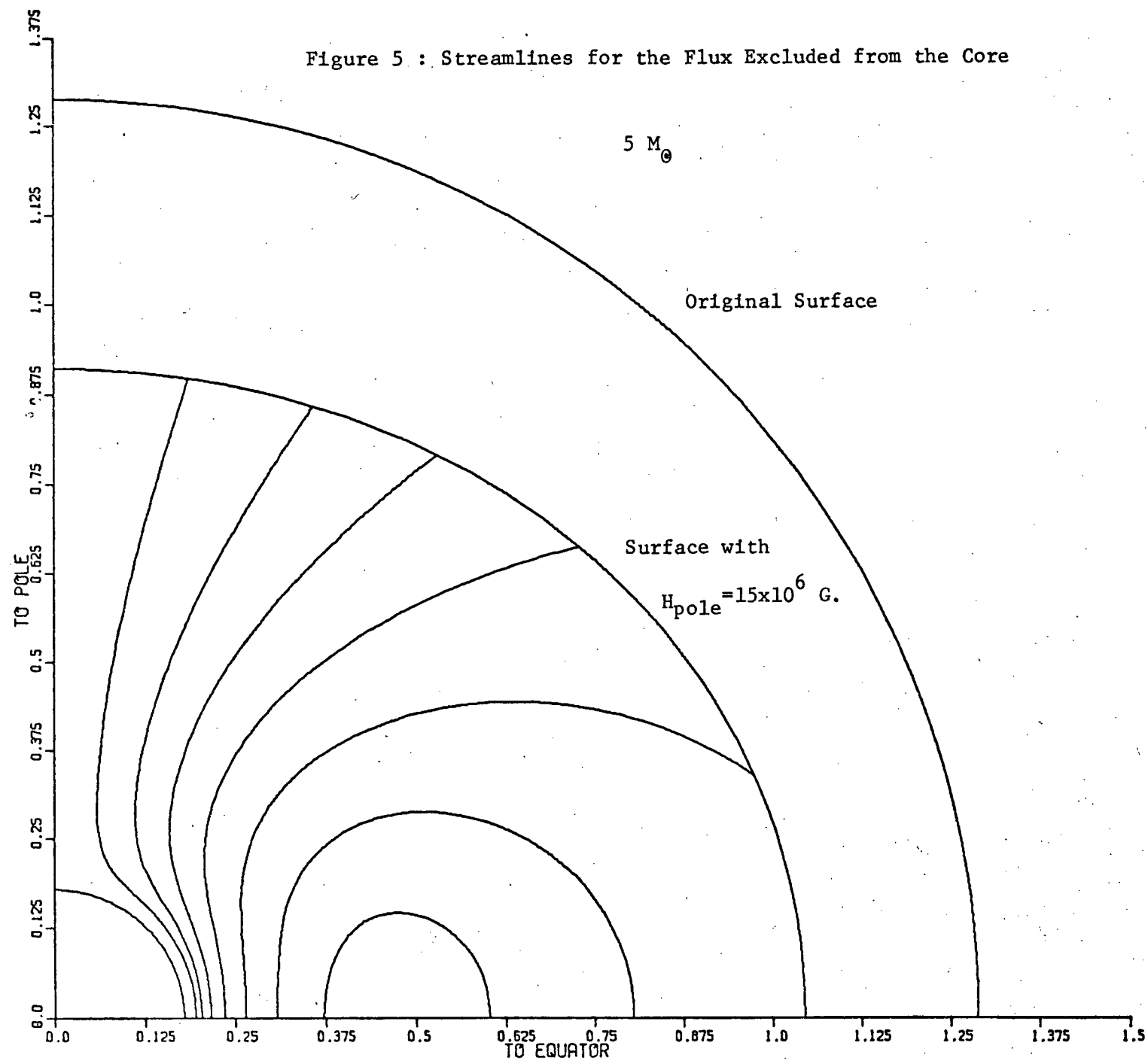
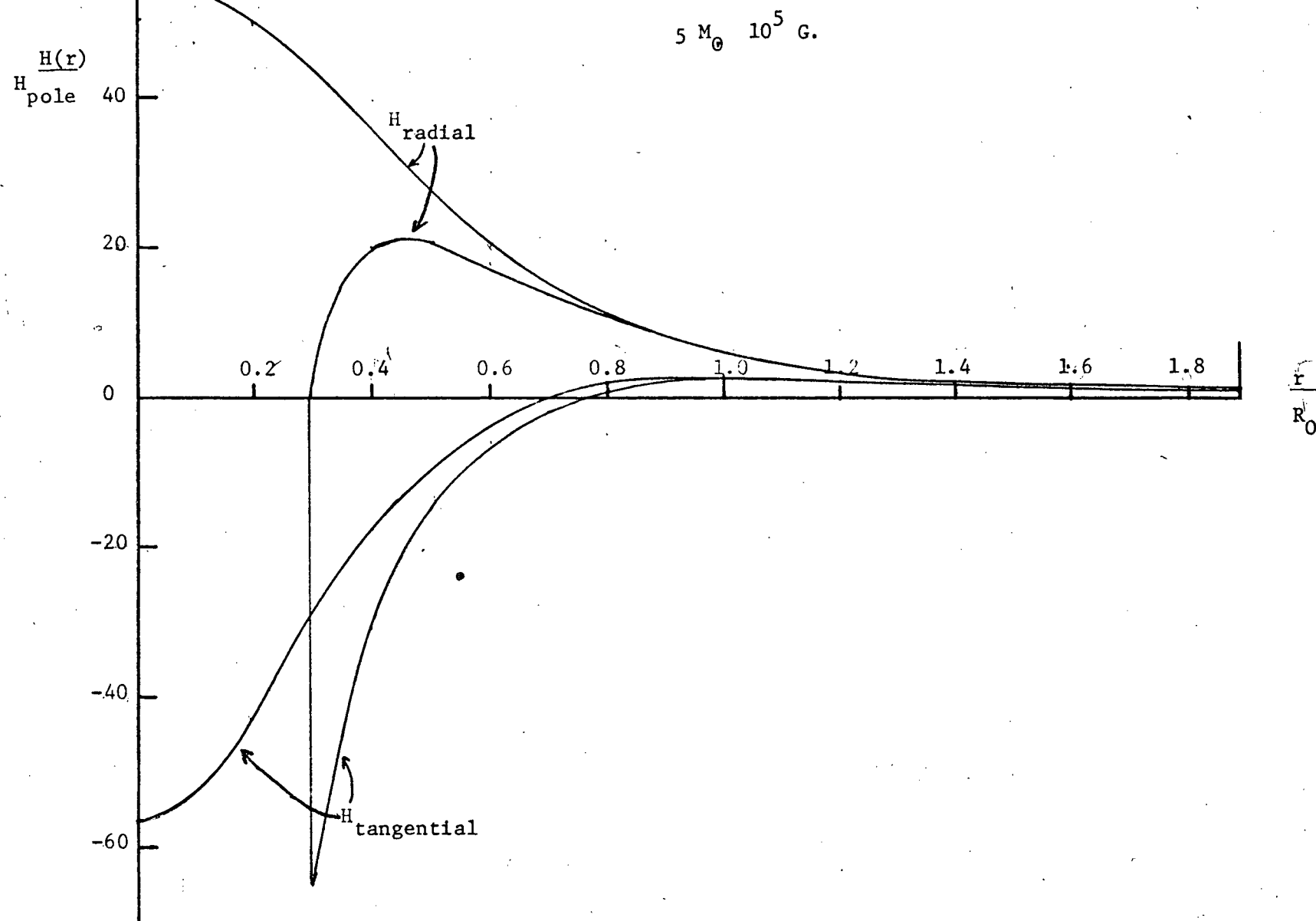


Figure 6 : Components of the Magnetic Field



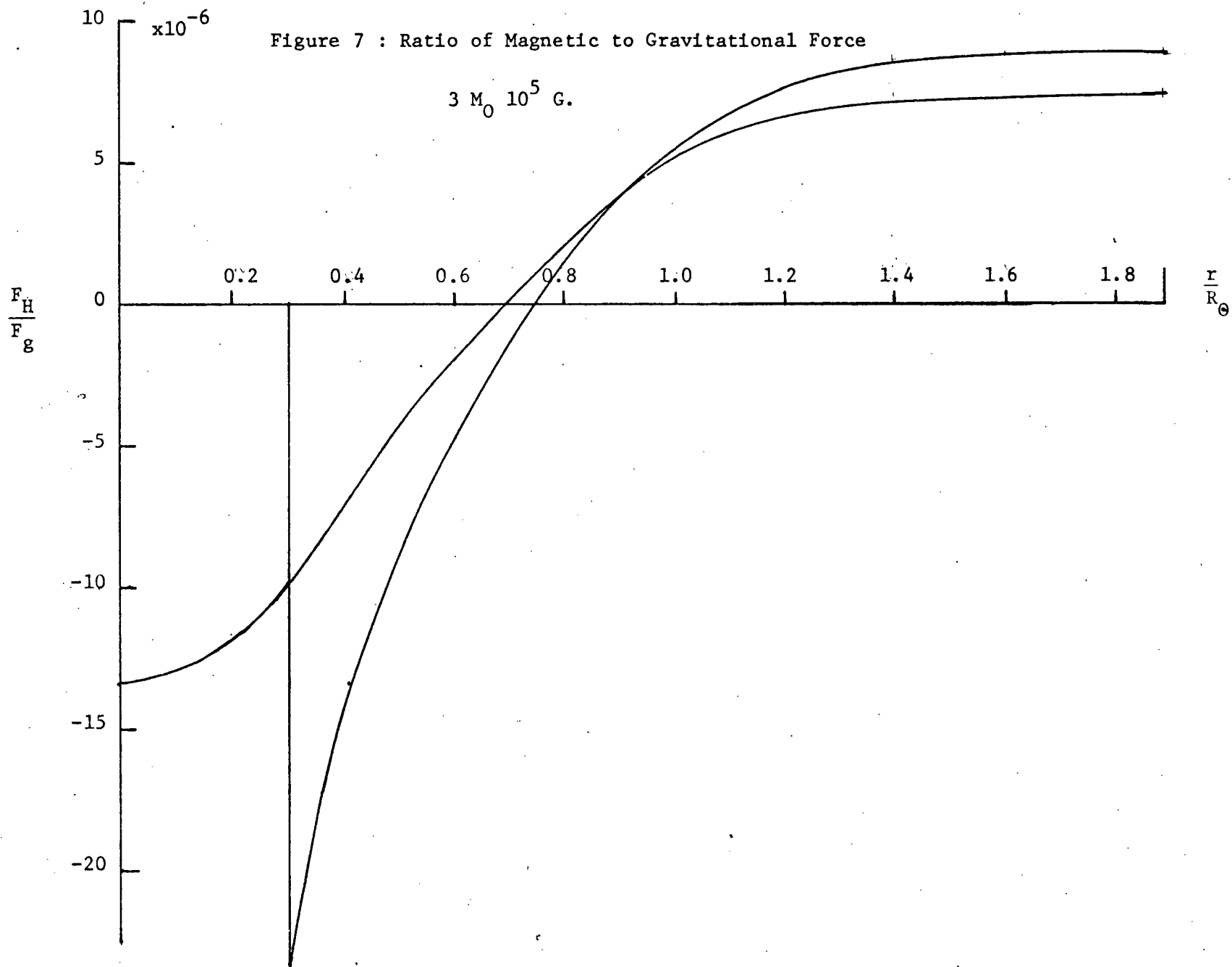
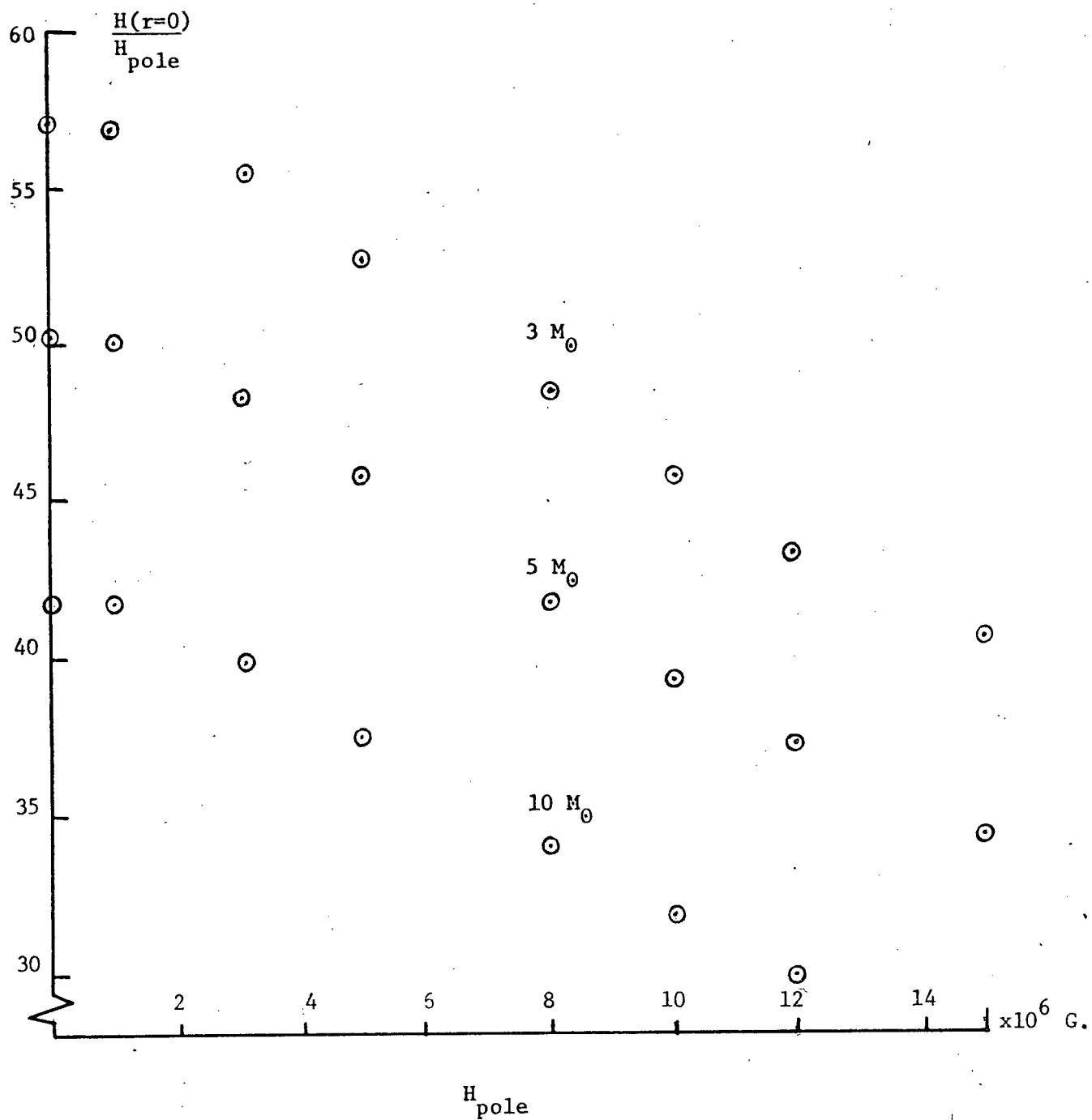


Figure 8 : Central Radial field vs. Polar Field



tential function. MR used the pseudo-polytropic stream function as an initial approximation. This is given in the column labelled PP in Table II. Note there is considerable difference between the stream functions of this paper and MR, the only difference in calculation being the spherical model used. Both MR and Davies used a very simple energy generation formula ($\epsilon \propto T^{17}$) and electron scattering opacities. Since the change to the nonlinear solution is only a small fraction (25%) from the initial pseudo-polytropic solution, it can be seen that one does not need to go to nonlinear calculations for a valid model of a non-rotating magnetic star.

Table II: Comparison of Magnetic Stream Functions

	This Paper	MR (70)		Davies (28)
$x=r/R$	$ b(r) $	PP	non-linear	non-linear
0	0	0	0	0
0.1	.537	.206	.258	.22
0.2	1.51	.706	.864	.78
0.3	2.02	1.24	1.47	1.34
0.4	2.07	1.57	1.78	1.66
0.5	1.87	1.65	1.77	1.69
0.6	1.63	1.56	1.61	1.56
0.7	1.42	1.40	1.42	1.38
0.8	1.23	1.25	1.25	1.22
0.9	1.13	1.11	1.11	1.09
1.0	1.0	1.0	1.0	1.0

The solutions are remarkably different in the central regions, where λ , the ratio of magnetic to gravitational force, is the highest, and therefore the region where magnetic forces are especially important (see fig. 7). The stream functions found here in this region are at least twice the value found by the others. This difference is attributed to the greater central

density concentration of the more detailed models used. Note the location of the 0 type neutral point is slightly closer to the origin in the models found here, which may be of importance when considering the magnitude of the instability of the poloidal field.

Figure 8 shows that as the surface magnetic field grows in strength, the central concentration of the field, i.e., $H_{radial}(r=0)/H_{radial}(r=pole)$, is reduced. Also the neutral point moves outward slightly with respect to the radius of the star, with increasing field.

These results can be understood on an intuitive physical basis. As the surface field increases, the star contracts and the surface is then slightly closer to the major current source. Near the surface the magnetic field varies with r^{-3} so for a given increase in surface field, only part of the increase need come from a directly proportional increase in the internal current, the rest coming from the contraction of the star. Thus the central field, which varies directly with the interior current, rises less rapidly than the surface field and therefore the ratio of the two falls. Similarly the outward move of the neutral point can be viewed as a result of the increased density of field lines in the core. The field lines repel each other and try to expand away in order to minimize the field energy; consequently the neutral point moves out slightly.

4.2 The Flux Free Convective Core

Figure 2 shows the stream function for the case of the magnetic field excluded from the convective core and figure 4 shows the streamlines of the field. For $r \geq 1/2 R$ the field rapidly converges to the core penetrating field. For identical values of the surface field the total flux contained between the centre and the neutral point in the equatorial plane is given by

$$\begin{aligned} F_t &= \int_0^{r_0} b_{\max} H_0 2\pi r dr, \\ &= \int_0^{r_0} \frac{H_p R_*^2}{2} \frac{b'}{r} 2\pi r dr, \\ &= H_p \pi R_*^2 |b_{\max}|. \end{aligned}$$

(4.1)

This flux is about 10% lower for the flux excluded case.

The magnetic field energy is taken as

$$\begin{aligned} E_H &= \int_0^R \int_0^\pi \frac{H_p^2}{8\pi} [h_r^2 \cos^2 \theta + h_\theta^2 \sin^2 \theta] 2\pi r^2 \sin \theta d\theta dr, \\ &= \frac{H_p^2}{4} \int_0^R \left[\frac{2}{3} h_r^2 + \frac{4}{3} h_\theta^2 \right] r^2 dr. \end{aligned}$$

(4.2)

where the magnetic field is given by

$$\vec{H} = H_p (h_r \cos \theta, h_\theta \sin \theta, 0),$$

where
$$h_r = -\frac{R_*^2}{F^2} b(r),$$

$$h_\theta = \frac{R_*^2}{2r} b'(r).$$

(4.3)

The ratio of the magnetic field energy to the gravitational energy is always lower for the flux excluded field, given equal surface field.

4.3 The Rotating Magnetic Star

Fields were calculated for a rotating star with a poloidal field which penetrates the core, with the axis of rotation parallel to the magnetic axis. The technique of calculation used requires only that the perturbing potential be expressible in terms of a spherically symmetric term plus a term with angular dependence $P_2(\cos\theta)$. If β is the angle of obliquity, then the perturbing potential is

$$\psi = \frac{1}{2} \Omega^2 r^2 \sin^2(\theta + \beta) + \frac{B^2}{4\pi K} b \sin^2 \theta, \quad (4.4)$$

which reduces to $\sin^2\theta$ and $\cos^2\theta$ terms only for $\beta=0$ and $\beta=\pi/2$. Only the $\beta=0$ case was done at this time.

Rotation was not added to the flux excluded from the core

case because it was felt that this treatment of the interaction of rotation with the discontinuity in $b'(r)$ at the core boundary would be completely lacking in any physical meaning.

A very significant difference between this calculation of a rotating magnetic star and others (MR, Wright, and Davies) is that the only coupling between the rotation and the magnetic field is through the spherical model. Consequently this coupling is always fairly small. On the other hand, MR's and Davies' models are coupled through the nonspherical, distortion terms. These terms are of order of the strongest perturbing force acting, so if rotation is dominant, the magnetic field will be grossly altered from the field of a non-rotating model. As a result of their method MR find that their star is cooler at the poles, whereas the star found here is hotter at the poles, as are most oblate stars. The models found here do not exhibit the vast increase in interior field concentration, nor the vanishing of the surface flux at some finite rotational velocity.

The central field concentration is expected to rise, due to the same effect of the change in radius as before with a non-rotating star, except that here there will be an expansion due to rotation, rather than a contraction, which will cause the ratio to rise rather than fall. For a fairly weak field of 10^5 G it is found that $H_r(r=0)/H_r(r=R_*)$ approximately doubles as goes from zero to a value such that the ratio of the rotational force to gravitational force at the equator is about 75%. Monaghan and Robson, and Wright find that this ratio increases about 20 times for a similar change in Ω .

4.4 Effects of the Field on the Star

All the well known results for a poloidal field are confirmed for both the magnetic field structures, magnetic flux permeating the core and flux excluded from the core. The differences are largely quantitative. The changes in the spherical model as a function of field strength are shown in the accompanying figures (9,10,11). The luminosity of the star is reduced with increasing magnetic field. The added magnetic force in the radial direction at the centre allows the equilibrium to exist with a lower $P_{\text{gas}} + P_{\text{rad}}$, so the central temperature drops, with a consequent drop in the thermonuclear reaction rate. From the neutral point outwards the field reinforces the gravitational force, which brings about a net compression of the star, and a rise in the central density. Since $\epsilon \propto T^{17}$, the slight rise in ρ is insufficient to offset the fall in T . For the effective temperature, $T_e \propto \left[\frac{L}{R^2} \right]^{1/4}$, the change in the luminosity must be offset against the change in radius. For the flux excluded magnetic field, the high forces at the core boundary are propagated through the structure sufficiently that the luminosity is reduced to a greater extent than for the flux penetrating case. On the other hand, since the two field b functions converge strongly beyond the neutral point, the net inward force when averaged over the star is greater for the flux penetrating case, than the flux excluded case. Consequently, the star contracts less for the flux excluded field. The contraction in both cases is more than enough to offset the fall in the luminosity, so T rises, the effect being less for the flux excluded case. These changes in the luminosity and effective temperature

Figure 9 : Central Density Change vs. Polar Field

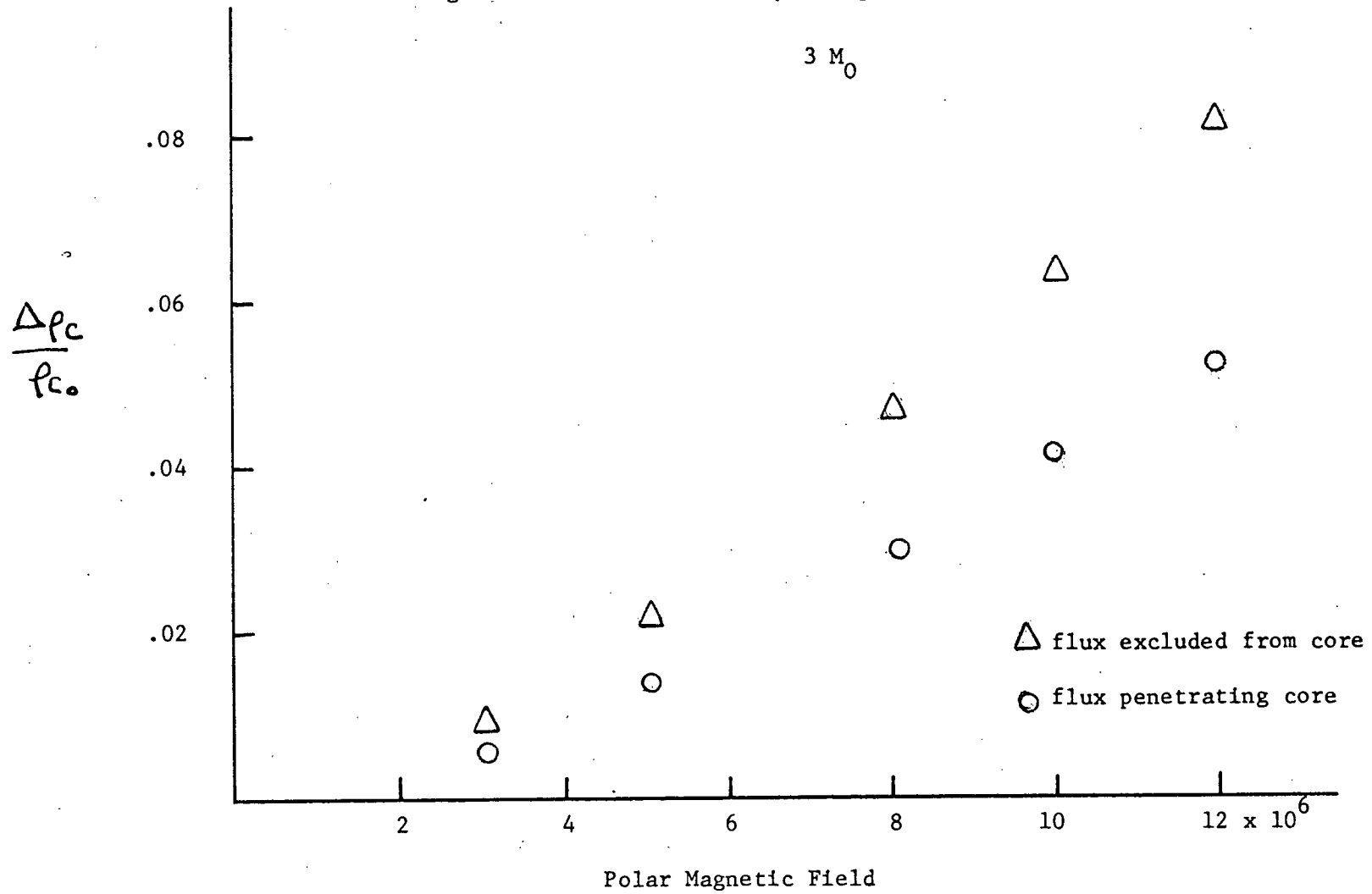


Figure 10 : Central Temperature Change vs. Polar Field

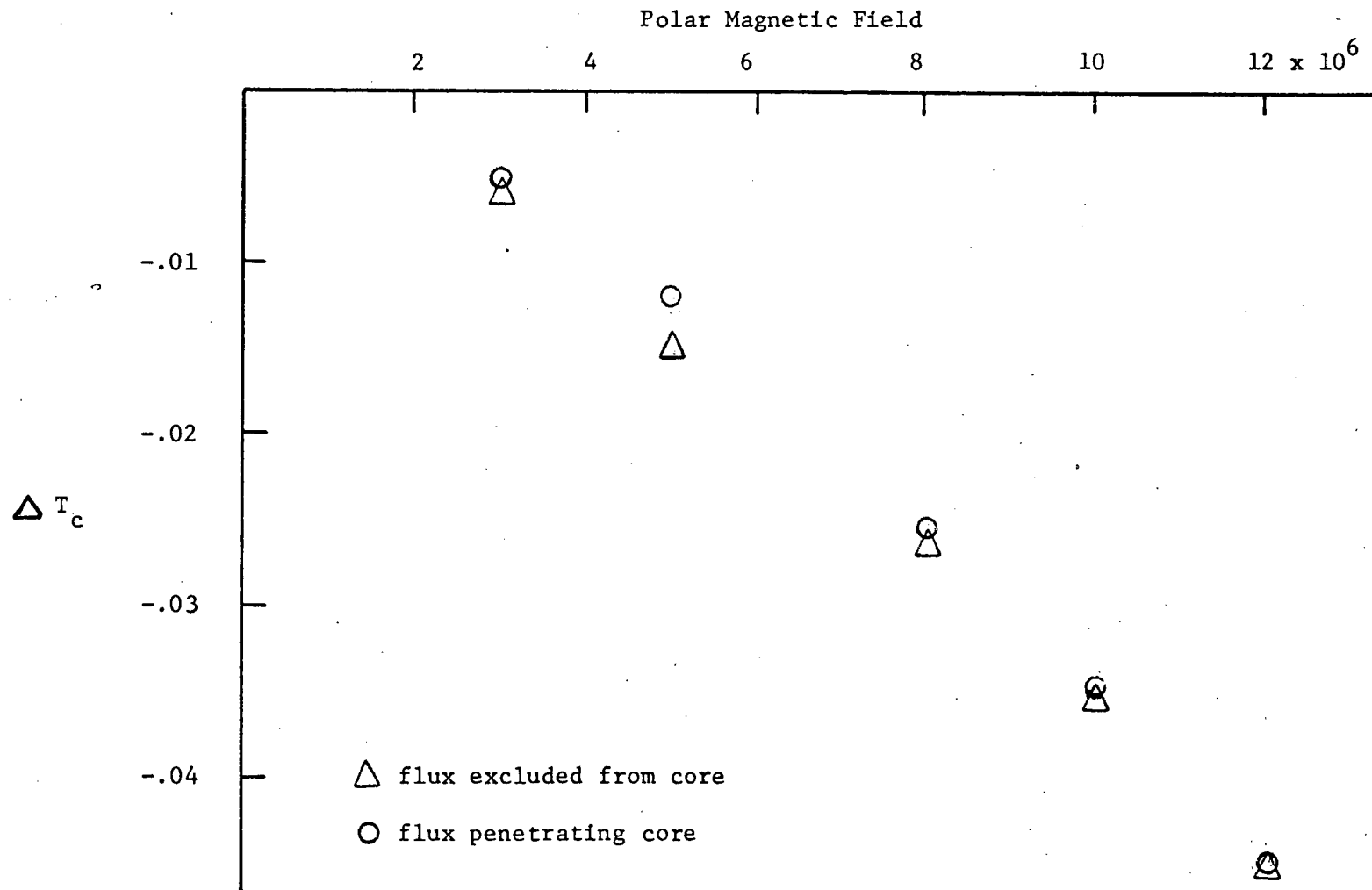
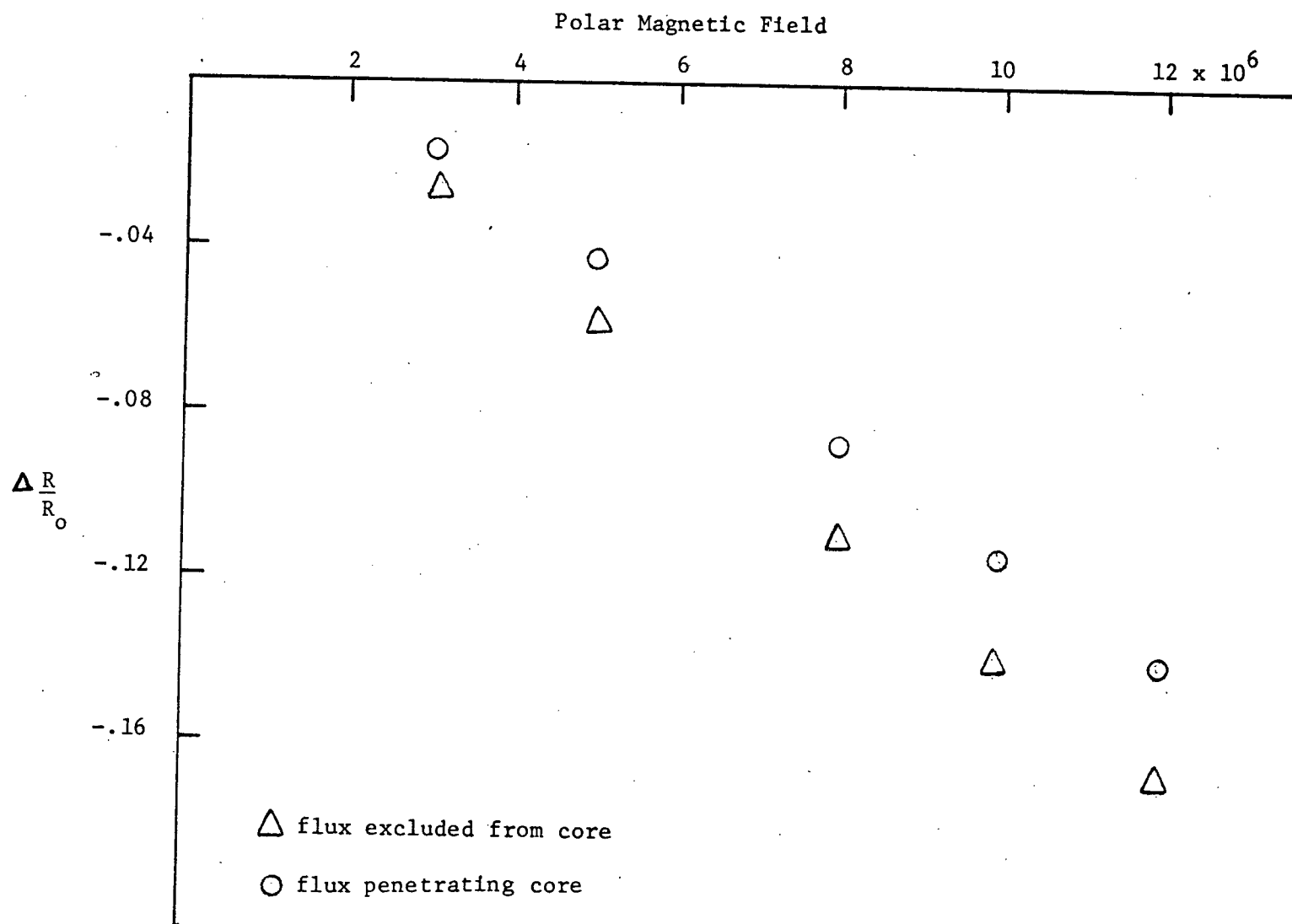


Figure 11 : Stellar Radius Change vs. Polar Field



mean that the star moves to the left and down in the HR diagram, i.e. below the main sequence. This is in contrast to Trasco's models. His stars have a random field which adds an everywhere positive magnetic pressure, which causes the stars to expand. Trasco's stars have a reduced luminosity, but an increased radius, so that they move to the right and down, which is above the main sequence.

For a comparison of results, Monaghan and Robson's perturbations against those found here are presented below.

Table III: Comparison of Changes to Structure

H_{pole}	$\Delta \log L$	$\Delta \log R$	$\Delta \log T_e$
Monaghan and Robson			
6×10^6	-.029	-.042	.008
11×10^6	-.082	-.110	.045
14×10^6	-.127	-.162	.068
This Paper			
5×10^6	-.013	-.049	.0053
10×10^6	-.037	-.121	.014
15×10^6	-.061	-.185	.022

MR's results indicate larger changes to the spherical model than those presented here. This is perhaps due to the use of simpler input physics for the opacity and energy generation rate.

4.5 The Perturbations to the Structure

Figure 12 : The Magnetic Star in the HR diagram

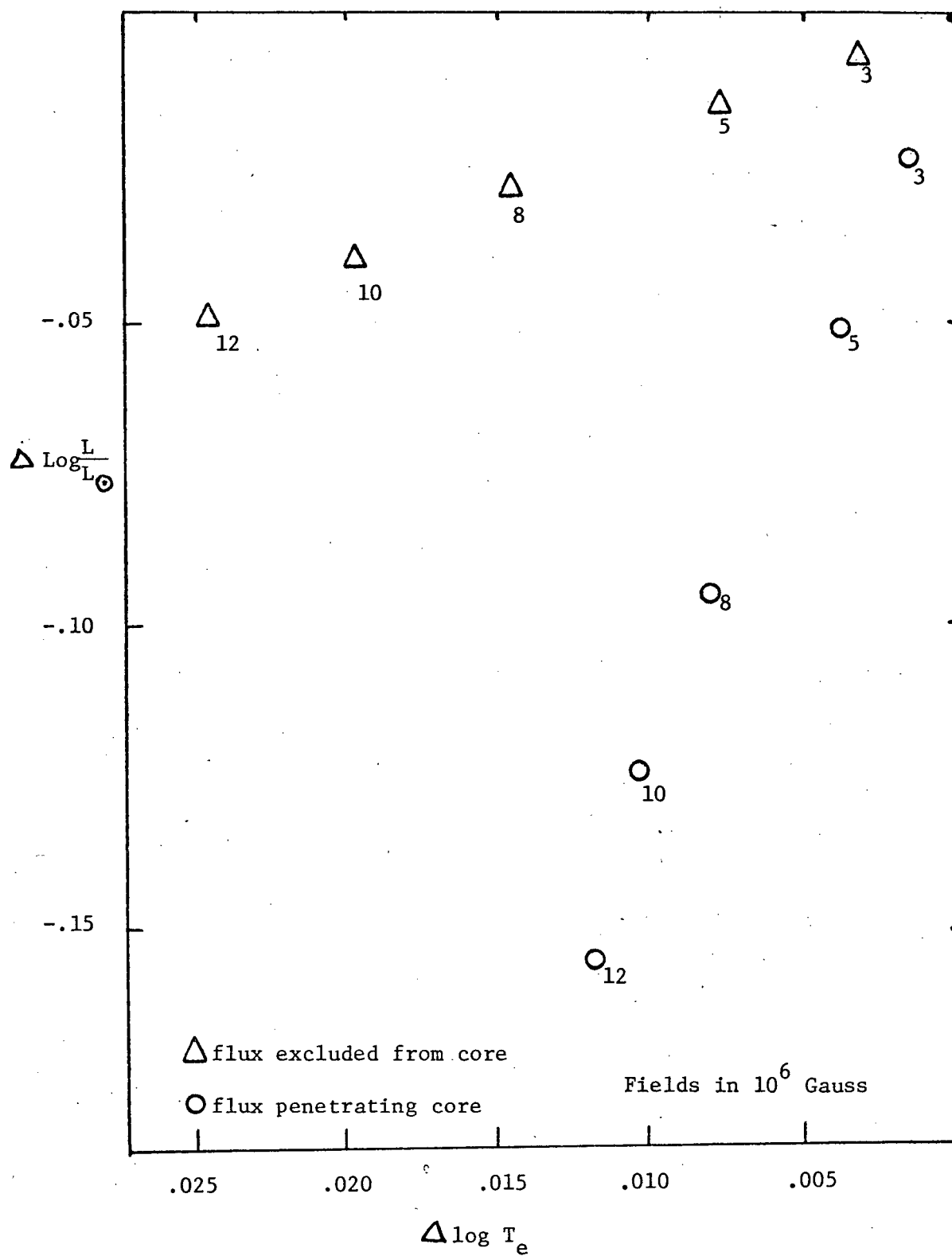


Figure 13 : Oblateness of Star vs. Polar Field

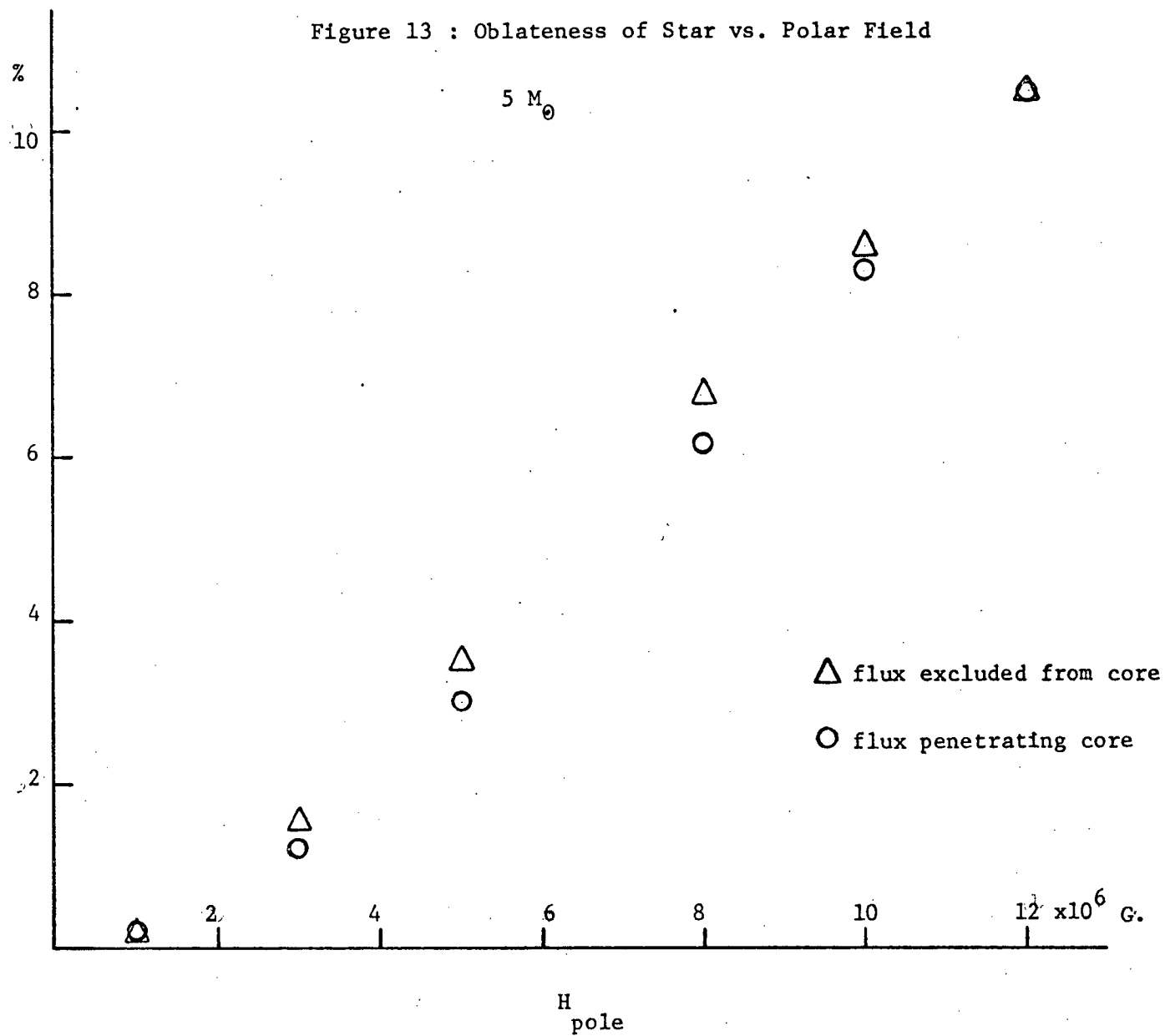


Figure 14 : Polar minus Equatorial Temperature Difference

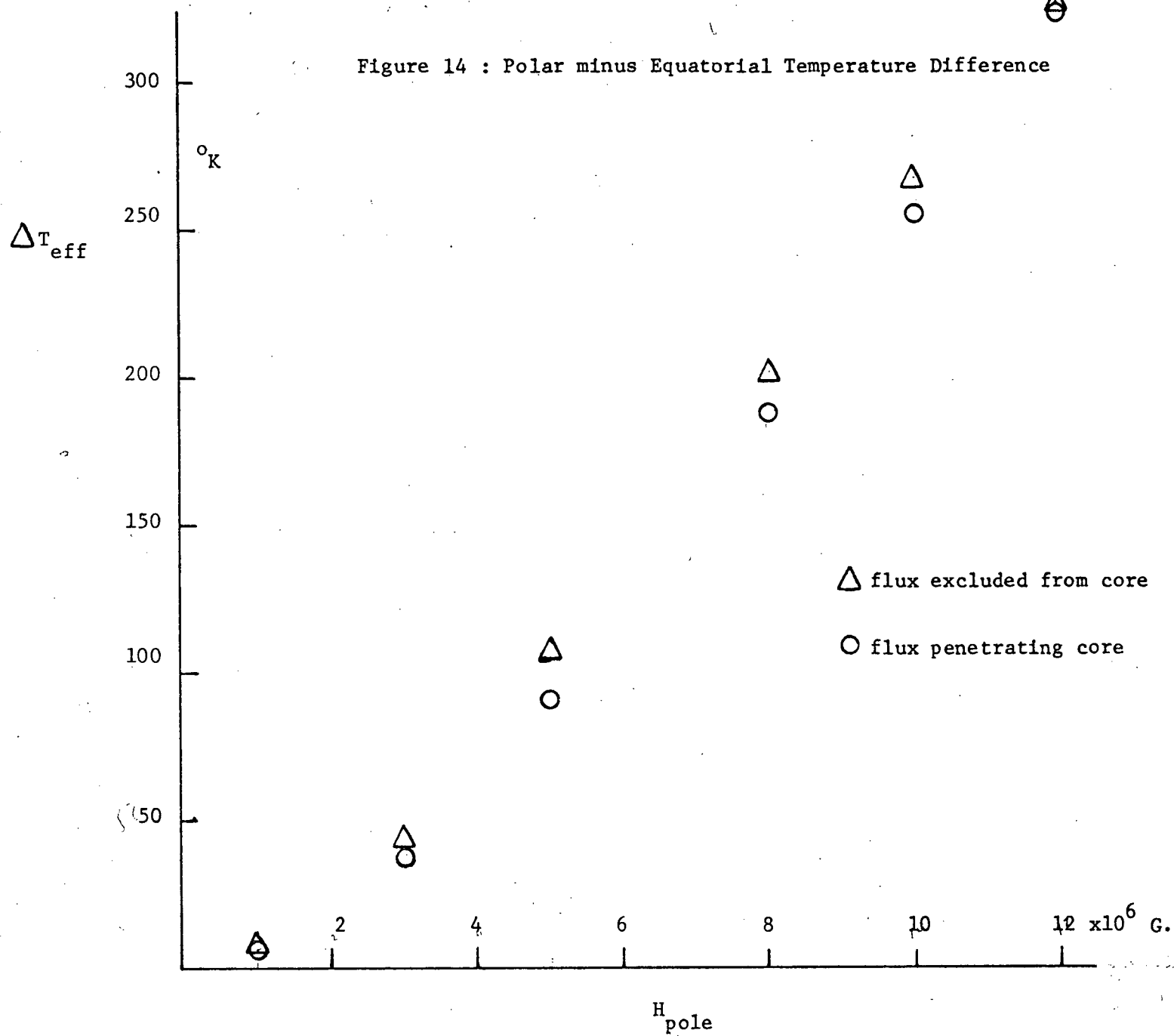


Figure 15 : The Distortion as a Function of Radius

$5 M_0$ 10×10^6 G.

$|\epsilon|$

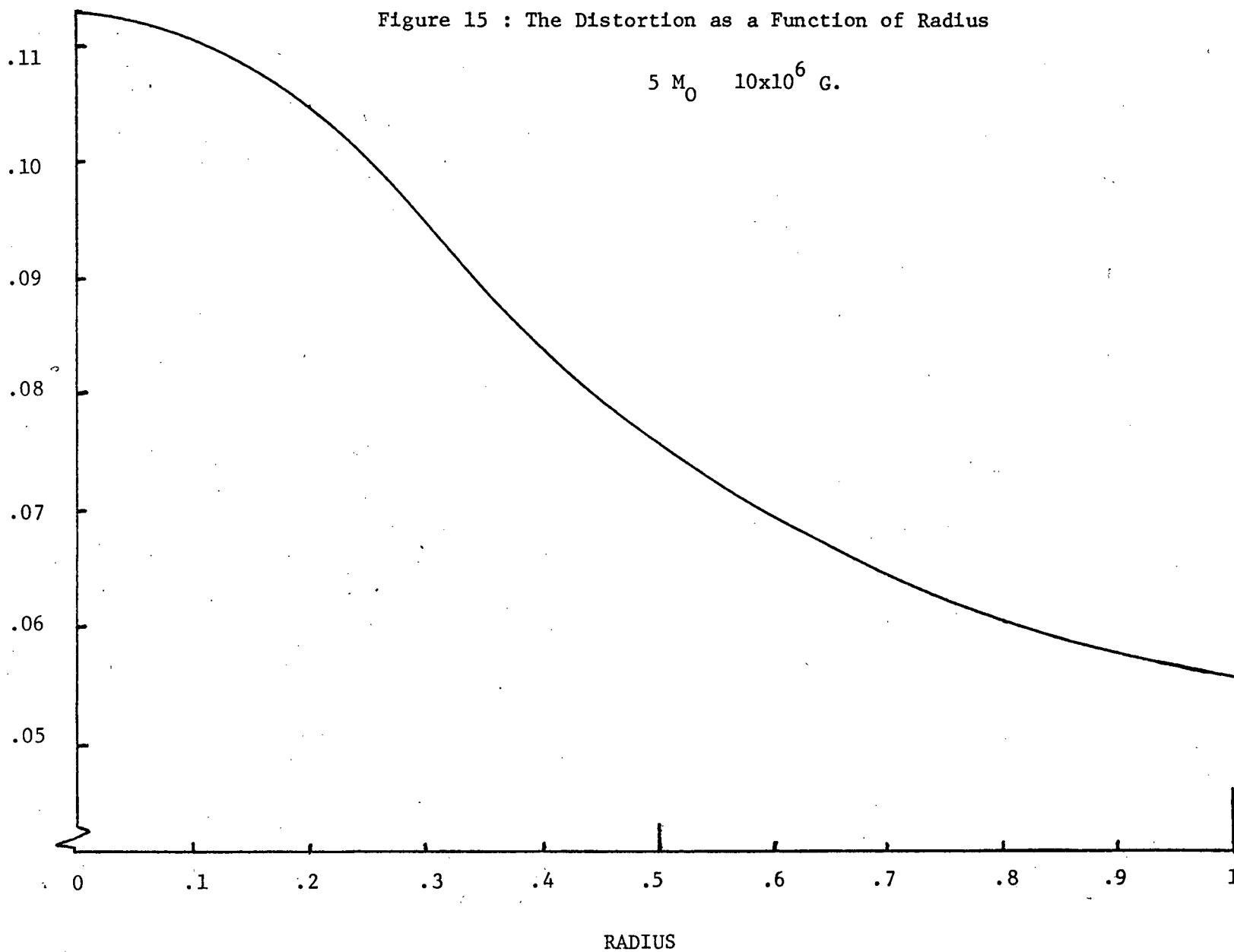
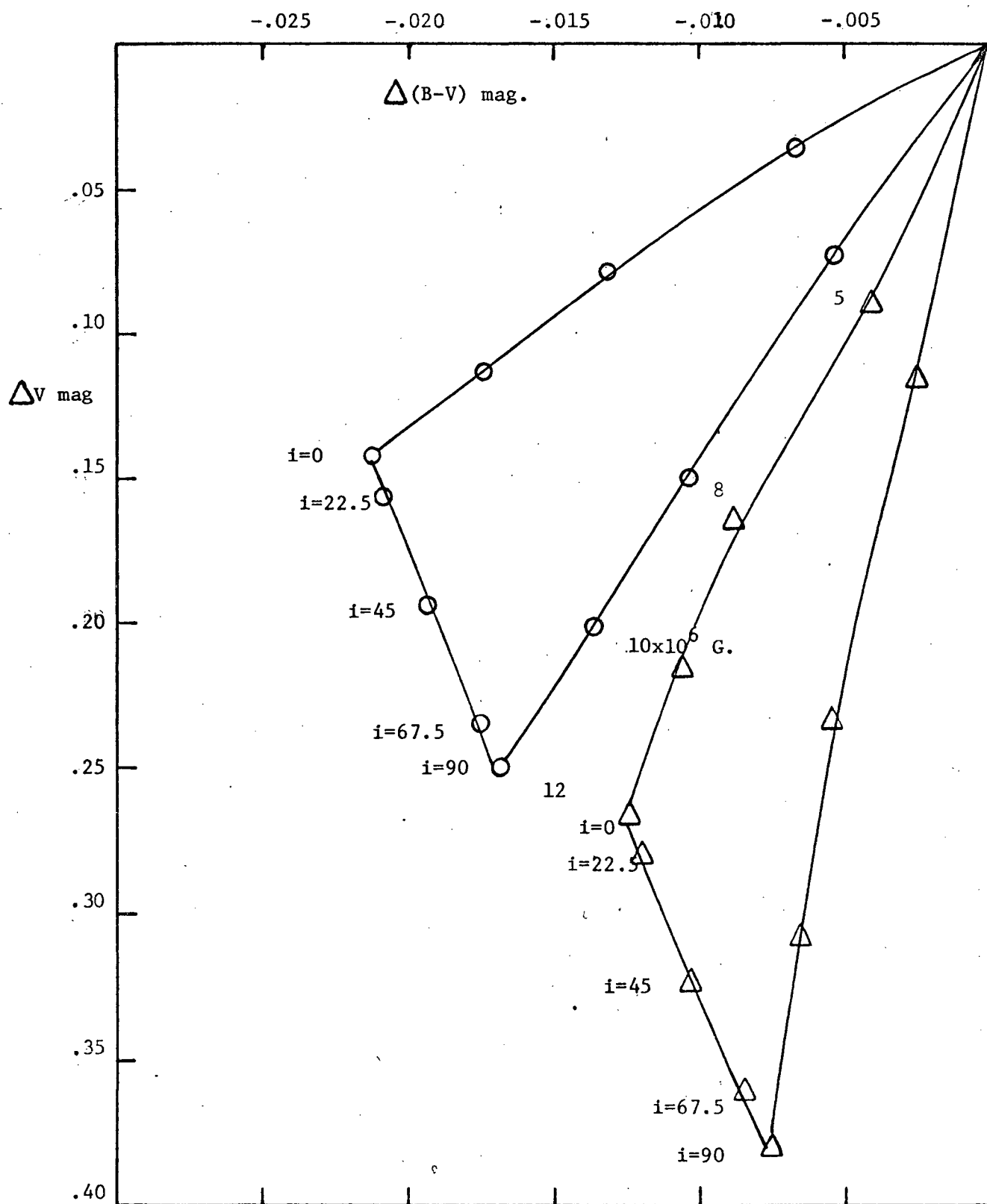


Figure 16 : Changes in B and V indices



Both poloidal magnetic fields produce forces which perturb the star into an oblate spheroid. The differences between the equatorial and polar radii is plotted in Figure 13. For weaker fields the difference is considerably greater for the flux excluded field. With larger fields, the field is sufficiently strong to produce perturbations in the spherical structure which react back on the field structure. This produces sufficient "spreading" of the field, i.e. b_{max} is reduced, and the position of b_{max} moves outward somewhat, such that the difference between the equatorial and polar radii and the temperature change converge towards a common value for the two field structures.

The graph of T_e between the pole and the equator clearly indicates that the observed magnetic fields (maximum H of about 10^5 G) does not produce sufficient perturbation to the structure to be the explaining factor for the light variation of magnetic stars. For a $5 M_\odot$ star with the flux penetrating the core the difference in temperature is about $0.05^\circ K$, whereas the required temperature difference is of the order of $10^3^\circ K$ (107). It is possible that very large internal fields do exist, but that there is some surface mechanism which traps most of the flux within the star. All of these stars have radiative envelopes, and the observations indicate long period stability of the non-homogenous distribution of elements over the surface so any flux containing mechanism must be a relatively quiet process. It is possible that significant circulation might develop somewhere below the surface which would tend to shear the field lines and suppress the flux through the surface, or the influence of rotation itself may operate to suppress the flux as shown by MR,

Wright and Davies.

The changes in the radius, and the effective temperature over the surface of the star produce differences in the UBV indices as the magnetic axis is tilted with respect to the observer. Because of the oblate figure of the star the surface "gravity" is higher at the poles which gives rise to a higher T_e at the poles, in addition the surface visible to the observer has a larger cross-sectional area when viewed pole on. Consequently these two effects combine to make the star appear brighter and hotter when viewed pole on than when viewed equator on. For a field of 15×10^6 G the difference between $V_{\text{pole}} - V_{\text{equator}}$ is about .15 magnitude, and the pole minus equator (B-V) change is about .008 magnitude. In the $\Delta V - \Delta(B-V)$ diagram the line representing the change in the indices for various angles of inclination is virtually a straight line, as opposed to the case of rotation (95), where a shallow curve is described between the pole on an equator on values. Similarly for an inferred maximum observed poloidal field of 10^5 G the variations are $\Delta V_p = 0.67 \times 10^{-5}$ mag. and $\Delta(B-V) = -0.75 \times 10^{-6}$ mag., hardly sufficient to account for the observed variations, which are of order 0.1 magnitude.

4.6 The Validity of The Approximation

The expansion of the variables was only made to first order, and all second order terms were neglected. In order to satisfy the approximation conditions, calculations of the field structure were only carried to a maximum ratio of the magnetic field energy to the gravitational energy of 10%, hoping that at this point the second order effects would be about $(.1)^2$ or 1% and hence still easily discardable. For the field of 10×10^6 G in a $5 M_{\odot}$ star the highest force encountered was at the centre where $\lambda = F_H / E = -.10$ for flux penetrating and $-.16$ for the flux excluded field. The second order correction terms in all the equations involved terms in $\bar{\epsilon}^2(r)$ or $\bar{S}(r)$, which are of order ϵ^2 . Figure 15 shows that for a field with an energy ratio of 6.9%, the maximum value of $\bar{\epsilon}$ is only .113 and hence ϵ^2 is .012.

Since all physical variables are constant on surfaces of constant potential, no explicit problem of the perturbation expansion arose at the surface where the pressure and temperature go to zero. But it was necessary to make an expansion of the potential into spherical and $P_2(\mu)$ terms in order to calculate the distortion, $\epsilon(r)$. The other variables can be left aside once the potential surfaces are known.

5. CONCLUSIONS

A dipole magnetic field in an upper main sequence star was calculated by a quick and simple method. The force produced by the magnetic field was constrained to be curl free. The field was chosen to match onto an external dipole, so that the stream function was made up of only spherical and $P_2(\cos\theta)$ terms. This allowed great simplifications of the equations of stellar structure, in fact the only change is an alteration of the effective mass as a function of radius. The field itself is calculated from a "pseudo-polytropic" equation, dependent only upon the spherical part of the model. Two types of fields were calculated, one where the flux penetrates the convective core, the other where the flux is excluded from the core. The resulting perturbation of the star, and the changes of the field with increasing strength are explainable on an intuitive physical basis.

When rotation was added to a star with a magnetic field, it was found that the effects were almost strictly additive, since the only coupling was through the spherical model.

In the future this technique will be extended to cover fields with toroidal and mixed poloidal-toroidal fields. Being a very quick way to calculate the field, it will also be an efficient way to follow the evolution of a star with a magnetic field.

6. ACKNOWLEDGMENTS

I am deeply grateful for the valuable discussions and assistance of Prof. G.G. Fahlman.

BIBLIOGRAPHY

1. Abramowitz, M. and Stegun, I.A., Handbook of Mathematical Functions, NBS, U.S. Government Printing Office, Washington, D.C. (1964).
2. Alfven, H. and Falthammar, C.-G., Cosmical Electrodynamics, 2nd ed., Clarendon Press, Oxford, 1963.
3. Aller, M.F., and Cowley, C.R., Astrophys. Journ. 162, L145 (1970).
4. Babcock, H.W., Stars and Stellar Systems 2, p. 107 (Hiltner, R.W. ed., Univ. Chicago Press, Chicago, 1962)
5. Babcock, H.W., The Magnetic and Related Stars p. 97 (Cameron, R.C. ed., Mono Book Corp., Baltimore, Md., 1967).
6. Bernstein, I. B., Freeman, E. A., Kruskal, M.D., and Kulsrud, R.M., Proc. Roy. Soc. London A244, 17 (1958).
7. Bidelman, W.P., The Magnetic and Related Stars p. 29 (Cameron, R.C. ed., Mono Book Corp., Baltimore, Md., 1967).
8. Bohm-Vitense, E., Modern Astrophysics, p. 97 (Hack, M. ed. Gauthier-Villars, Paris, 1967).
9. Bohm-Vitense, E., Magnetism and the Cosmos p. 179 (Hindmarsh, W.R., et.al. eds., American Elsevier Pub. Co., New York, 1965).
10. Borra, E.F., Astrophys. Journ. 187, 271 (1974).
11. Borra, E.F., Astrophys. Journ. 188, 287 (1974).
12. Chandrasekhar, S., An Introduction to the Study of Stellar Structure, rpt. Dover, New York (1959).
13. Chandrasekhar, S., Proc. National Acad. Sci. U.S.A., 42, 1 (1956).
14. Chandrasekhar, S., Hydrodynamic and Hydromagnetic Stability, Oxford University Press, Oxford (1961).
15. Chandrasekhar, S and Prendergast, K., Proc. National Acad. Sci. U.S.A. 42, 5 (1956).
16. Chiam, T.C. and Monaghan, J.J., Monthly Notices Roy. Astron. Soc. 155, 153 (1971).

17. Chitre, S.M., Ezer, D., and Stothers, R., Astrophys. Lett., 14, 37 (1973).
18. Clayton, D.D., Principles Of Stellar Evolution And Nucleosynthesis, McGraw-Hill, New York, 1968.
19. Collins, G.W., Astrophys. Journ. 138, 1134 (1963).
20. Collins, G.W., Astrophys. Journ. 142, 265 (1965).
21. Cowling, T.G., Stars and Stellar Systems 8, p. 425 (Aller, L.H. and McLaughlin, D., eds., Univ. Chicago Press, Chicago, 1965)
22. Cowling, T.G., I.A.U. Symp. #22, Stellar and Solar Magnetic Fields p.405 (Lust, R., ed., North Holland Pub. Co., 1965).
23. Cowling, T.G., Magnetohydrodynamics, Interscience, New York, 1955.
24. Cowling, T.G., Monthly Notices Roy. Astron. Soc. 94, 39 (1933).
25. Cox, A.W. and Stewart, J.W., Astrophys. Journ. Supp. Ser. 19, 243 (1970).
26. Cox, A.W. and Stewart, J.W., Astrophys. Journ. Supp. Ser. 19, 261 (1970).
27. Cox, J.P. and Giuli, R.T., Principles of Stellar Structure, 2 vols, Gordon and Breach, New York (1968).
28. Davies, G.F., Australian Journ. Phys. 21, 293 (1968).
29. Deutsch, A.J., Handbuch Der Physik Bd. II, 689, Springer Verlag, Berlin, 1958.
30. Fahlman, G.G., Astrophys. and Sp. Sci. 12, 424 (1971).
31. Faulkner, J., Griffiths, H. and Hoyle, F., Monthly Notices Roy. Astron. Soc. 129, 363 (1965).
32. Faulkner, J., Roxburgh, I.W., and Strittmatter, P.A. Astrophys Journ. 151, 203 (1968).
33. Fermi, E. and Chandrasekhar, S. Astrophys. Journ. 118, 116 (1953).
34. Ferraro, V.C.A., Astrophys. Journ. 119, 407 (1954).
35. Fowler, W.A., Burbidge, E.M., Burbidge, G., and Hoyle, F., Astrophys. Journ., 142, 423 (1965).

36. Gilman, P.G., Astrophys. Journ. 162, 1019 (1970).
37. Gollnow, H., I.A.U. Symp. #22, Stellar and Solar Magnetic Fields p. 23 (Lust, R., ed., North Holland Pub. Co., 1965).
38. Gough, D.O. and Tayler, R.J. Monthly Notices Roy. Astron. Soc. 133, 85 (1966).
39. Hack, M., Magnetism and the Cosmos p. 163
(Hindmarsh, W.R., et.al. eds., American Elsevier Pub. Co., New York, 1965).
40. Hindmarsh, W.R., Magnetism and the Cosmos p. 151
(Hindmarsh, W.R., et.al. eds., American Elsevier Pub. Co., New York, 1965).
41. Hildebrand, F.B., Introduction to Numerical Analysis, McGraw-Hill, New York (1956).
42. Iben, I., Astrophys. Journ. 141, 993 (1965).
43. Khoklava, V.L., Soviet Astron. AJ 15, 419 (1971).
44. Kodaira, K., Astron. Astrophys. 26, 385 (1973).
45. Kopal, Z., Numerical Analysis, Chapman and Hall, London (1961).
46. Kovetz, A., Monthly Notices Roy. Astron. Soc. 137, 169 (1967).
47. Larson, R.B. and Demarque, P.R., Astrophys. Journ. 140, 524 (1964).
48. Landstreet, J.D., Astrophys. Journ. 159, 1001 (1970).
49. Ledoux, P., The Magnetic and Related Stars p. 65
(Cameron, R.C. ed., Mono Book Corp., Baltimore, Md., 1967).
50. Ledoux, P. and Renson, P., ARAA 4, p. 293 (Goldberg, L. ed., Annual Reviews Inc., Palo Alto, Ca., 1970).
51. Lust, R. and Schluter, A., Zeitschr. f. Astrophys. 34, 263 (1954).
52. Maheswaran, M., Monthly Notices Roy. Astron. Soc. 145, 197 (1969).
53. Markey, P. and Tayler, R.J. Monthly Notices Roy. Astron. Soc. 163, 77 (1973).
54. Mestel, L., Monthly Notices Roy. Astron. Soc. 122, 473 (1961).

55. Mestel, L., I.A.U. Symp. #22, Stellar and Solar Magnetic Fields p., 87 (Lust, R., ed., North Holland Pub. Co., 1965).
56. Mestel, L., Magnetism and the Cosmos p. 194 (Hindmarsh, W.R., et.al. eds., American Elsevier Pub. Co., New York, 1965).
57. Mestel, L., Zeitschr. f. Astrophys. 63, 196 (1966).
58. Mestel, L. and Strittmatter, P.A., Monthly Notices Roy. Astron. Soc. 137, 95 (1967).
59. Mestel, L., and Takhar, H.S., Monthly Notices Roy. Astron. Soc. 156, 419 (1972).
60. Michaud, G., Astrophys. Journ. 160, 641 (1970).
61. Modern Computing Methods, National Phys. Lab. Notes on Appl. Sci. No. 16, 2nd ed., HMSO, London (1962).
62. Monaghan, J.J., Monthly Notices Roy. Astron. Soc. 131, 105 (1965).
63. Monaghan, J.J., Monthly Notices Roy. Astron. Soc. 132, 1 (1966).
64. Monaghan, J.J., Monthly Notices Roy. Astron. Soc. 134, 275 (1966).
65. Monaghan, J.J., Zeitschr. f. Astrophys. 68, 461 (1968).
66. Monaghan, J.J., Zeitschr. f. Astrophys. 69, 146 (1968).
67. Monaghan, J.J., Monthly Notices Roy. Astron. Soc. 163, 423 (1973).
68. Monaghan, J.J., Astrophys. Journ. 186, 631 (1973).
69. Monaghan, J.J., Monthly Notices Roy. Astron. Soc. 167, 16 (1974).
70. Monaghan, J.J. and Robson, K.W., Monthly Notices Roy. Astron. Soc. 155, 231 (1971).
71. Monaghan, J.J. and Roxburgh, I.W. Monthly Notices Roy. Astron. Soc. 131, 13 (1965).
72. Moss, D.L., Monthly Notices Roy. Astron. Soc. 164, 33 (1973).
73. Moss, D.L., Monthly Notices Roy. Astron. Soc. 168, 61 (1974).

74. Moss, D.L. and Tayler, R.J., Monthly Notices Roy. Astron. Soc. 145, 217 (1969).
75. Moss, D.L. and Tayler, R.J., Monthly Notices Roy. Astron. Soc. 147, 133 (1970).
76. Ostriker, J.P., and Hartwick, F.D.A., Astrophys. Journ. 153, 797 (1968).
77. Papaloizou, J.C.B. and Whelan, J.A.J., Monthly Notices Roy. Astron. Soc. 164, 1 (1973).
78. Parker, E.N., Astrophys. Journ. 138, 226 (1963).
79. Parker, E.N., Astrophys. Journ. 138, 552 (1963).
80. Parker, E.N., ARAA 8, p. 1 (Goldberg, L. ed., Annual Reviews Inc., Palo Alto, Ca., 1970).
81. Peterson, D.M., Astrophys. Journ. 161, 685 (1970).
82. Piddington, J.H., Astrophys. and Sp. Sci. 24, 259 (1974).
83. Prendergast, K.H., Astrophys. Journ. 123, 498 (1956).
84. Preston, G.W., The Magnetic and Related Stars p. 3
(Cameron, R.C. ed., Mono Book Corp., Baltimore, Md., 1967).
85. Preston, G.W. Publ. Astron. Soc. Pacific 83, 571 (1971).
86. Pyper, D.M., Astrophys. Journ. Supp. Ser. 18, 347 (1969).
87. Raadu, M.A., Astrophys. and Sp. Sci. 14, 464 (1971).
88. Rakosch, Sexl, and Weiss, Astron. Astrophys. 31, 441
(1974).
89. Roxburgh, I.W., Monthly Notices Roy. Astron. Soc. 126, 67
(1963).
90. Roxburgh, I.W., I.A.U. Symp. #22, Stellar and Solar Magnetic Fields p. 102 (Lust, R., ed., North Holland Pub. Co., 1965).
91. Roxburgh, I.W., Monthly Notices Roy. Astron. Soc. 132, 201
(1966).
92. Roxburgh, I.W., Monthly Notices Roy. Astron. Soc. 132, 347
(1966).
93. Roxburgh, I.W., The Magnetic and Related Stars p. 45
(Cameron, R.C. ed., Mono Book Corp., Baltimore, Md., 1967).

94. Roxburgh, I.W., Griffith, J.S., and Sweet, P.A., Zeitschr. f. Astrophys. 61, 203 (1965).
95. Roxburgh, I.W. and Strittmatter, P.A., Zeitschr. f. Astrophys. 63, 15 (1965).
96. Sackmann, I.-J., and Anand, S.P.S., Astrophys. Journ. 162, 105 (1970).
97. Sanderson, A.D., Connon Smith, R., and Hazelhurst, J., Astrophys. Journ. 159, 169 (1970).
98. Schwarzschild, M., Structure And Evolution of the Stars, rpt. Dover, New York (1965).
99. Schwarzschild, M., Astrophys. Journ. 112, 222 (1950).
100. Smith T.S., Astrophys. Journ. 139, 767 (1964).
101. Stepien, K., Astrophys. Journ. 154, 945 (1968).
102. Stibbs, D.W.N., Monthly Notices Roy. Astron. Soc. 110, 395 (1950).
103. Strittmatter, P.A., and Norris, J., Astron. Astrophys. 15, 239 (1971).
104. Stothers, R. and Chin, C.-W., Astrophys. Journ. 180, 901 (1973).
105. Tayler, R.J., Monthly Notices Roy. Astron. Soc. 161, 365 (1973).
106. Trasco, J.D., Astrophys. Journ. 161, 633 (1970).
107. Trasco, J.D., Astrophys. Journ. 171, 569 (1972).
108. Trehan, S.K., and Uberoi, M.S., Astrophys. Journ. 175, 161 (1972).
109. Vandakurov, Yu.V., Soviet Astron. AJ 16, 265 (1972).
110. Van der Borgh, R., Australian Journ. Phys. 20, 643 (1967).
111. Weiss, N.O., Proc. Roy. Soc. London A293, 310 (1966).
112. Wentzel, D.G., Astrophys. Journ. 133, 170 (1961).
113. Wentzel, D.G., Astrophys. Journ. Supp. Ser. 5, 187 (1966).
114. Wolff, S.C. and Wolff, R.J. Astron. Journ. 76, 422 (1971).

- 115. Woltjer, L., Astrophys. Journ. 130,400 (1959).
- 116. Woltjer, L., Astrophys. Journ. 131,227 (1960).
- 117. Woltjer, L., Astrophys. Journ. 135,235 (1962).
- 118. Wright, G.A.E., Monthly Notices Roy. Astron. Soc.
146,197 (1969).
- 119. Wright, G.A.E., Monthly Notices Roy. Astron. Soc.
162,339 (1973).

APPENDIX I: STELLAR STRUCTURE EQUATIONS

By assumption the potential can be decomposed as

$$\begin{aligned}\Phi &= \phi + \psi, \\ &= \phi_0 + \psi_0 + (\phi_2 + \psi_2) P_2(\mu),\end{aligned}$$

where $\phi_0 \gg \psi_0, \psi_2$, and ϕ_2 .

(A1.1)

And all quantities can be expanded like

$$Q(r, \theta) = Q_0(r_0) + Q_2(r_0) P_2(\mu).$$

(A1.2)

where $Q_0(r_0)$ is the quantity evaluated on the line $P_2(\cos\theta)=0$, where r_0 is the distance from the centre to that point on the surface. Note all quantities $Q_0(r_0)$ are constant on the equipotential surface $\Phi=\text{constant}$. Substituting the expanded variables into Poisson's equation we obtain,

$$\nabla^2 (\phi_0 + \phi_2 P_2(\mu)) = 4\pi G (\rho_0 + \rho_2 P_2(\mu)).$$

(A1.3)

Expressing this in spherical polar coordinates and integrating over θ on the shell $r=r_0$, the P_2 terms drop out and,

$$\frac{1}{r^2} \frac{d}{dr} \left(r^2 \frac{d\phi_0}{dr} \right) = 4\pi G \rho_0.$$

(A1.4)

Integrating this over r gives,

$$\phi_0 = -\frac{G M_r}{r_0^2},$$

(AI.5)

$$\text{where } M_r = 4\pi \int_0^r \rho_0 r^2 dr,$$

(AI.6)

To determine the shape of the surfaces of constant potential we make a second order Taylor's expansion of the total potential about the point $(r, P_2(\cos\theta)=0)$,

$$\begin{aligned} \Phi(r, \theta) = \Phi(r_0, P_2=0) &+ \left. \frac{\partial \Phi}{\partial r} \right|_{r=r_0} (r-r_0) + \left. \frac{\partial^2 \Phi}{\partial r^2} \right|_{r=r_0} (r-r_0)^2 \\ &+ \left. \frac{\partial \Phi}{\partial P_2} \right|_{P_2=0} P_2(u). \end{aligned} \quad (\text{AI.7})$$

We want a surface of constant potential so that

$$\Phi(r, \theta) = \Phi(r_0, P_2=0).$$

(AI.8)

Putting this all together with the expanded potential we have

$$\frac{\partial^2 \Phi}{\partial r^2} (r-r_0)^2 + \frac{\partial \Phi}{\partial r} (r-r_0) + \Phi_2 P_2 = 0. \quad (\text{AI.9})$$

which is a quadratic equation in $(r-r_0)$. Using the binomial expansion with the quadratic equation we obtain $(\Phi_2 > \Phi)$,

$$r-r_0 = \frac{\Phi_2 P_2}{\frac{\partial \Phi}{\partial r}} - \frac{\frac{\partial^2 \Phi}{\partial r^2} \Phi_2 P_2^2}{\left(\frac{\partial \Phi}{\partial r}\right)^3}. \quad (\text{AI.10})$$

Which can be written as

$$r = r_0 [1 + \bar{e}(r_0) P_2(u) + \bar{s}(r_0) P_2^2(u)],$$

(AI.11)

$$\text{where } \bar{e} = -\frac{1}{r_0} \frac{\Phi_2}{\frac{\partial \Phi_0}{\partial r}}, \quad \bar{s} = -\frac{1}{r_0} \frac{\frac{\partial^2 \Phi_0}{\partial r_0^2} \Phi_2^2}{\left(\frac{\partial \Phi_0}{\partial r}\right)^3}.$$

(AI.12)

To first order this is simply

$$r = r_0 [1 + e(r_0) P_2],$$

$$\text{where } e(r_0) = -\frac{1}{r_0} \frac{\phi_2 + \psi_2}{e_{mr}/r_0^2}.$$

(AI.13)

The volume inside an equipotential surface, V_{Φ} is easily obtained

$$V_{\Phi} = \int_{\mu=-1}^{\mu=+1} \int_{\varphi=0}^{2\pi} \int_{r=0}^{r_{\Phi}} r^2 dr d\mu d\varphi.$$

(AI.14)

Evaluating this with the radius given to second order by (AI.11) gives,

$$V_{\Phi} = \frac{4\pi r_0^3}{3} \left[1 + \frac{3}{5} \bar{s} + \frac{3}{5} \bar{e}^2 \right].$$

(AI.15)

Note that to first order $V = 4/3 \pi r_0^3$, and that

$$\frac{dV_{\Phi}}{dr_0} = 4\pi r_0^2 \left[1 + \frac{3}{5} \bar{s} + \frac{3}{5} \bar{e}^2 \right] + \frac{4\pi}{5} r_0^3 \left[\frac{d}{dr_0} \bar{e}^2 + \frac{d}{dr_0} \bar{s} \right].$$

(AI.16)

The area of the surface $\Phi = \text{constant}$ is also easily deter-

mined

$$A_{\Sigma} = 2\pi \int_{u=0}^{+1} \sqrt{1 + \frac{1}{r^2} \frac{dr}{d\theta}} d\mu,$$

(AI.17)

$$= 4\pi r_0^2 \int_{u=0}^{+1} [1 + 2\bar{e} P_2 + 2\bar{s} P_2^2 + \bar{e}^2 P_2^2 + \frac{2}{3} k^2 (1-u^2) \bar{e}] d\mu,$$

(AI.18)

$$= 4\pi r_0^2 \left[1 + \frac{2}{3} \bar{s} + \frac{4}{3} \bar{e}^2 \right].$$

(AI.19)

The Larson-Demarque scheme for the solution of the stellar structure equations requires as the independent variable the mass fraction inside the volume with radius r , here given by the mass inside the equipotential surface with radius r along the line $P_2=0$. This mass M_{Σ} is,

$$M_{\Sigma} = \int_{V_{\Sigma}} \rho dV_{\Sigma}$$

(AI.20)

$$= 4\pi \int_{\mu=0}^{+1} (\rho_0 + \rho_1 P_2) 4\pi r_0^3 (1 + O(\epsilon^2)) dr d\mu,$$

(AI.21)

$$M_{\Phi} = M_{r_0} + O(\epsilon^2),$$

(AI.22)

$$\text{where } M_{r_0} = 4\pi \int_0^{r_0} \rho_0 r^2 dr.$$

(AI.23)

To develop the perturbed equations of stellar structure, we follow the formalism of the J^2 method. The dependent variable will be r_0 .

First the radiative transfer equation,

$$\vec{F} = -\frac{4ac}{3\kappa\rho} T^3 \nabla T.$$

(AI.24)

This is easily integrated over a surface of constant Φ , since all quantities except the gradient are constant on $\Phi = \text{constant}$.

$$\int_{\Phi} \vec{F} \cdot d\vec{\Sigma} = -\frac{4ac}{3\kappa\rho} T^3 \frac{dT}{dr_0} \int_{\Phi} \nabla r_0 \cdot d\vec{\Sigma}.$$

(AI.25)

L_{Φ} is defined as the total energy released inside the volume V_{Φ} .

$$L_{\Phi} = \int_{V_{\Phi}} \epsilon_p dV_{\Phi}.$$

(AI.26)

Although the models discussed here do not have circulation, the J^2 method easily deals with it, in fact it drops out of the

structure equations. To show this, the above expression is re-written using the energy balance equation of FRS (11)

$$L\Phi = \int_{\Phi} (\nabla \cdot \vec{F} + c_v \rho \vec{v} \cdot \nabla T + p \nabla \cdot \vec{v}) dV_{\Phi} \quad (\text{AI.27})$$

Then with Gauss' Theorem and the simplifying expression of FRS

$$L\Phi = \int_{\Phi} (\vec{F} + \rho \vec{v} (c_p T + \Phi)) \cdot d\vec{\Sigma} \quad (\text{AI.28})$$

But since $c_p T + \Phi$ is constant on constant Φ surfaces, and the mass inside an equipotential surface must be constant, this simplifies to

$$L\Phi = \int \vec{F} \cdot d\vec{\Sigma} \quad (\text{AI.29})$$

Now the equation of radiative equilibrium, with a little rearranging becomes

$$\frac{\int \nabla r \cdot d\vec{\Sigma}}{4\pi r_0^2} \frac{dT}{dr_0} = \frac{-3\tau \kappa \rho}{16\pi a c r_0^2} \frac{L\Phi}{T^3} \quad (\text{AI.30})$$

The other equations are recast into the J² format analogously, with greater ease. The equation of hydrostatic equilibrium,

$$\frac{\nabla P}{\rho} = -\nabla \Phi, \quad (\text{AI.31})$$

is integrated over a surface of constant potential, and

Poisson's equation with Gauss' Theorem is used to transform the integral over the gravitational potential to one over the density.

$$\frac{1}{\rho} \frac{d\rho}{dr_0} \frac{\int \nabla r_0 \cdot d\vec{\Sigma}}{4\pi r_0^2} = \frac{-4\pi G \int \rho dV}{4\pi r_0^2} - \frac{\int \nabla \phi \cdot d\vec{\Sigma}}{4\pi r_0^2} \quad (\text{AI.32})$$

The equation of mass conservation is simply,

$$\frac{dM_r}{dr_0} = 4\pi r_0^2 \rho \frac{dV_\phi}{dr} / 4\pi r_0^2. \quad (\text{AI.33})$$

And similarly energy conservation is,

$$\frac{dL_\phi}{dr} = 4\pi r_0^2 \epsilon \rho \frac{dV_\phi}{dr} / 4\pi r_0^2. \quad (\text{AI.34})$$

To evaluate the modifying factors, the f 's, we simply need to evaluate a few integrals. The first is

$$f_1 = \frac{\int \nabla r_0 \cdot d\vec{\Sigma}}{4\pi r_0^2}. \quad (\text{AI.35})$$

Since $d\vec{\Sigma}$ is a vector perpendicular to the constant potential surface, ∇r and $d\vec{\Sigma}$ are parallel. Hence $d\vec{\Sigma}$ can be written

$$d\vec{\Sigma} = \frac{\nabla r_0}{|\nabla r_0|} r_0 \sqrt{1 + \frac{1}{r_0^2} \left(\frac{dr}{d\theta} \right)^2} dr d\theta \quad (\text{AI.36})$$

On surfaces of constant potential, the distortion factor $\epsilon(r_0)$ is constant, so that the gradient ∇r_0 is,

$$\nabla r_0 = \left(\frac{1}{1 + \epsilon P_2}, \frac{3\epsilon \cos\theta \sin\theta}{1 + \epsilon P_2}, 0 \right).$$

(AI.37)

To first order

$$|\nabla r_0| = \frac{1}{1 + \epsilon P_2}.$$

(AI.38)

Now f_1 is

$$f_1 = \frac{4\pi}{4\pi r_0^2} \int_{\mu=0}^{+1} |\nabla r_0| \sqrt{1 + \frac{1}{r_0^2} \frac{dr}{d\theta}} d\mu.$$

(AI.39)

Substituting the various quantities and integrating gives

$$f_1 = 1 - \frac{2}{3} \epsilon^2.$$

(AI.40)

The factor for the perturbing potential is

$$f_2 = \frac{- \int_{\Sigma} \nabla \psi \cdot d\mathbf{\Sigma}}{4\pi r_0^2}.$$

(AI.41)

Using the expressions developed above, we have

$$f_2 = \frac{-1}{4\pi r_0^2} \int \left(\frac{\partial \psi_0}{\partial r} + \frac{\partial \psi_2}{\partial r} P_2, \frac{3\psi_2}{r_0} \cos\theta \sin\theta, 0 \right) \cdot (1, 3\epsilon \cos\theta \sin\theta, 0) r_0^2 (1 + 2\epsilon P_2) d\mu.$$

$$f_z = -\frac{\partial \psi_0}{\partial r_0} + \mathcal{O}(\epsilon^2)$$

(AI.42)

With this the equation of hydrostatic equilibrium is

$$\frac{1}{\rho} \frac{d\rho}{dr_0} = -\frac{Gm_r}{r_0^2} - \frac{d\psi}{dr_0}.$$

(AI.43)

We define

$$\lambda = \frac{d\psi/dr_0}{Gm_r/r_0^2}.$$

(AI.44)

So the hydrostatic equation is now,

$$\frac{1}{\rho} \frac{d\rho}{dr_0} = -\frac{Gm_r(1+\lambda)}{r_0^2}$$

(AI.45)

This use of λ restricts us to potentials that give a bounded λ at the origin. The condition for the validity of all these expansions is then

$$|\lambda| \ll 1 \text{ everywhere.}$$

(AI.46)

This λ factor is the only effect, to first order, that we see of the perturbing force, so that the modification to a calculation of stellar structure involves only computing an effective mass

$$m_{\text{eff}} = m_r (1 + \lambda)$$

(AI.47)

Putting this all together we have, in the J^2 format

$$f_1 \frac{1}{r} \frac{dP}{dr_0} = - \frac{G M_r (1 + \lambda)}{r_0^2},$$

(AI.48)

$$\frac{dM_r}{dr_0} = 4\pi r_0^3 \rho f_3,$$

(AI.49)

$$\frac{dL_\Phi}{dr_0} = 4\pi r_0^2 \rho e f_3,$$

(AI.50)

$$f_1 \frac{dT}{dr_0} = - \frac{3T\rho L_\Phi}{16\pi ac T^3}, \text{ radiative}$$

(AI.51)

$$\frac{d \ln T}{d \ln P} = \frac{\Gamma - 1}{\Gamma}, \text{ convective}$$

(AI.52)

$$\text{where } f_1 = - \frac{\int \nabla r_0 \cdot d\vec{\Sigma}}{4\pi r_0^2}, \text{ to first order } = 1,$$

(AI.53)

$$f_3 = \frac{dV_0}{dr_0} / 4\pi r_0^2, \text{ to first order } = 1,$$

(AI.54)

$$\lambda = \frac{d\psi_0/dr_0}{\epsilon m_1/r_0^2}.$$

(AI.55)

APPENDIX II: THE DISTORTION TERMS

The variables expanded as (AI.2) are substituted in to stellar structure equations, and the first order terms are equated. From the equation of state we obtain

$$\frac{-p_2}{p_0} = \frac{T_2}{T_0} - \frac{p_2}{p_0} . \quad (\text{AII.1})$$

The radial component of the equation of hydrostatic equilibrium gives

$$\frac{1}{p_0} \frac{d p_2}{d r_0} + \frac{p_2}{p_0} \frac{d p_0}{d r_0} = -\frac{d \phi_2}{d r_0} - \frac{d \psi_2}{d r_0} . \quad (\text{AII.2})$$

And the tangential component

$$\frac{p_2}{p_0} = -\phi_2 - \psi_2 . \quad (\text{AII.3})$$

Equating p_2 terms in Poisson's equation

$$\frac{1}{r^2} \frac{d}{d r} \left(r^2 \frac{d \phi_2}{d r} \right) - \frac{6 \phi_2}{r^2} = 4 \pi G p_2 . \quad (\text{AII.4})$$

We use this set of equations to obtain an equation in ϕ_2 alone,

$$\frac{d^2 \phi_2}{d r^2} + \frac{2}{r} \frac{d \phi_2}{d r} - \frac{6 \phi_2}{r^2} + 4 \pi G p_0 \frac{d p_0}{d p_0} \phi_2 = 4 \pi G p_0 \frac{d p_0}{d p_0} \psi_2 . \quad (\text{AII.5})$$

No attempt was made to solve for T_2 , p_2 , or p_2 , since all

the information about the distribution of T, f , and P is given once the equipotential surfaces are known. These are determined by ϵ , a function of ψ_2 and ϕ_2 , which are now known.

Since we want the potential to match an external solution of Laplace's equation

$$\nabla^2 \phi = 0,$$

(AII.6)

which has a general solution

$$\phi = \sum_{n=0}^{\infty} \frac{\phi_n P_n(\mu)}{r^{2n+1}}.$$

(AII.7)

this gives the boundary condition on $r = R_*$,

$$3\phi_2 + R_* \frac{d\phi_2}{dr} = 0.$$

(AII.8)

at the centre all forces vanish, so $\phi_1(0)=0$, and $\phi_2'(0)=0$.

APPENDIX III: THE LARSON-DEMARQUE EQUATIONS

The Larson-Demarque (47) variables are:

$$S = \frac{\Gamma}{R_0} , \quad (\text{AIII.1})$$

$$q = \frac{L \Phi \left(1 + \frac{a}{x^2} \right)}{L * L_0} , \quad (\text{AIII.2})$$

$$P = \frac{10^3 P}{T^{2.5}} , \quad (\text{AIII.3})$$

$$t = \frac{T}{10^7} . \quad (\text{AIII.4})$$

The density is eliminated from all equations by using the equation of state,

$$p = \frac{\mu H}{k} 10^{9.5} \beta p t^{1.5} , \quad (\text{AIII.5})$$

with

$$\beta = 1 - \frac{a}{3} 10^{11.5} \frac{t^{1.5}}{P} \quad (\text{AIII.6})$$

The mass function, defined as,

$$f(x) = \frac{M_{\Phi}}{M_*}, \quad (\text{AIII.7})$$

for upper main sequence stars with radiative surface, reduces from LD's general expression to

$$f(x) = \left[1 - (1-x)^{\sigma} \right]^3. \quad (\text{AIII.8})$$

The opacity was calculated from

$$\kappa = \kappa_s + \kappa_t$$

$$\text{where } \kappa_s = .195 (1+x),$$

$$\kappa_t = .245 \left(\frac{1-x}{2-z} \right)^{.67} \rho^{\alpha} t^{-\beta},$$

$$\alpha = .667,$$

$$\beta = 3.214.$$

(AIII.9)

Quantities used in the calculation are

$$\eta \equiv \frac{\partial \log \kappa_t}{\partial \log \rho} = \alpha,$$

$$\theta \equiv - \frac{\partial \log \kappa_t}{\partial \log t} = \beta - \frac{3}{2} \alpha,$$

$$\sigma = \frac{4 + \alpha + \beta}{1 + \alpha}.$$

(AIII.10)

The energy generation rate is given by

$$\epsilon = \epsilon_{pp} + \epsilon_{cn}$$

(AIII.11)

where

$$\begin{aligned} \epsilon_{pp} &= \epsilon_I + \epsilon_{II} + \epsilon_{III}, \\ \epsilon_I &= \epsilon_I' (1 - \gamma), \\ \epsilon_{II} &= \epsilon_I' \frac{1.968}{1 + w}, \\ \epsilon_{III} &= \epsilon_I' \frac{1.46w}{1 + w}, \\ \epsilon_I' &= 4.44 \times 10^5 f_{II} g_{II} X^2 \rho t^{-3/2} e^{-15.693 t^{-1/2}}, \\ \gamma &= 1.94 \times 10^4 \left(\frac{Y}{4X} \right)^2 e^{-46.414 t^{-1/2}}, \\ w &= 8.31 \times 10^{15} f_{71} g_{71} \frac{X}{1 + X} t^{-1/6}, \\ f_{II} &= 1 + .0079 \rho^{1/2} t^{-3/2}, \\ f_{71} &= 1 + .0316 \rho^{1/2} t^{-3/2}, \\ g_{II} &= 1.027 + .033t, \\ g_{71} &= 1, \\ \epsilon_{cn} &= 1.711 \times 10^{37} f_{14,1} g_{14,1} X X_{14} \rho t^{2/3} e^{-70.697 t^{-1/3}}, \\ f_{14,1} &= 1 + .0553 \rho^{1/2} t^{-1/2}, \\ g_{14,1} &= .995 - .008t, \\ X_{14} &= \begin{cases} .585 Z & t \geq 1.6 \\ .188 Z & t < 1.6 \end{cases} \end{aligned}$$

(AIII.12)

The mean molecular weight μ is defined as

$$\frac{1}{\mu} = 2X + \frac{3}{4}Y + \frac{1}{2}Z.$$

(AIII.13)

With these substitutions, the spherical part of the equations of stellar structure become

$$DS = \frac{ds}{dx} = \frac{M_X}{4\pi R_0^3} \frac{k}{\mu H 10^{9.5}} \frac{f'(x)}{\beta \rho t^{1.5}} s^2,$$

(AIII.14)

$$(n+1)_{\text{rad}} = \frac{16\pi ac}{3L_* L_0} \frac{10^{11.5} t^{1.5} f(x) (1+\lambda) (1 + \frac{q}{\lambda_2})}{g P \kappa},$$

(AIII.15)

$$(n+1)_{\text{em}} = 4 - \frac{3/2 \beta^2}{4 - 3\beta},$$

(AIII.16)

$$(n+1) = \max((n+1)_{\text{rad}}, (n+1)_{\text{em}}),$$

(AIII.17)

$$DT = \frac{dt}{dx} = - \frac{GM_X^2}{4\pi R_0^4} \frac{10^{-11.5} f(x) (1+\lambda) f'(x)}{s^4 (n+1) \rho t^{1.5}},$$

(AIII.18)

$$DP = \frac{dp}{dx} = \frac{p}{t} \frac{dt}{dx} \left[(n+1) - \frac{\xi}{2} \right],$$

(AIII.19)

$$DU = \frac{M_*}{L_* L_0} \left(1 + \frac{a}{x^2} \right) f'(x) \epsilon,$$

(AIII.20)

$$DV = \frac{2 a q}{x^3 + a x},$$

(AIII.21)

$$DQ = DU - DV.$$

(AIII.22)

The various partial derivatives are taken and the difference coefficients are formed in the same manner as LD.

The boundary conditions at the centre are as in LD, with a few minor modifications. For small x

$$f'(x) = 3\sigma^3 x^2.$$

(AIII.23)

Since $\lim_{x \rightarrow 0} s=0$, and $\lim_{x \rightarrow 0} q=0$, at the centre,

$$DS_1 = \left[\frac{M_*}{4\pi R_0^3} \frac{k}{\mu H 10^{9.5}} \frac{3\sigma^3}{\beta_P T^{1.5}} \right]^{1/3},$$

(AIII.24)

$$DU_1 = \frac{M_*}{L_* L_0} 3\sigma^3 \epsilon, \quad (\text{AIII.25})$$

$$DQ_1 = \frac{1}{3} DU_1, \quad (\text{AIII.26})$$

$$DV_1 = 2 DQ_1, \quad (\text{AIII.27})$$

$$DT_1 = 0, \quad (\text{AIII.28})$$

$$DP_1 = 0, \quad (\text{AIII.29})$$

For a radiative surface the radiative zero ($T \rightarrow 0$, $P \rightarrow 0$ at surface) boundary conditions are used boundary conditions. As shown by Schwarzschild (98), these are appropriate .

The inclusion of radiation pressure introduces some minor problems. The effective polytropic index is

$$\begin{aligned}
 (n+1) &\equiv \frac{T}{P} \frac{dP}{dT} , \\
 &= \frac{T\beta}{P_g} \frac{d\left(\frac{P_g}{\beta}\right)}{dT} .
 \end{aligned}$$

(AIII.30)

In the surface layers of a star in radiative equilibrium $P_g = T^*$. Substituting this into the above expression gives for the surface value of $(n+1)$

$$(n+1)_{\text{rad}} = \beta\sigma + 4(1-\beta).$$

(AIII.31)

The β_{new} used in this expression was set equal to the β_n of the previous layer.

The outer boundary conditions then are

$$DS = \frac{-10^7 R_0}{GM_*} \frac{h}{\mu H} \frac{(n+1)s^2}{1+\lambda} \frac{DT}{\beta},$$

(AIII.32)

$$DT = \left\{ \frac{-3\sigma \frac{GM_*^2}{4\pi R^4} (1+\lambda)}{s^4 (n+1) \left[\frac{(1+\lambda) \frac{GM_*^2}{4\pi R_0^4} (1+e)}{(n+1)q \left[\frac{\beta \mu H 109.5}{h} \right]^\kappa 10^{-7} (\beta - \frac{3}{2}\kappa)} \right]} \right\}^{\frac{1}{1+\kappa}} \frac{1}{\sigma}$$

(AIII.33)

$$DP = 0,$$

(AIII.34)

$$DU = 0,$$

(AIII.35)

$$DV = \frac{2aq}{1+a},$$

(AIII.36)

$$DQ = -DV$$

(AIII.37)

APPENDIX IV: THE GREY ATMOSPHERE

There are two basic equations for a grey atmosphere. Radiative transfer

$$\mu I_\nu(0, \mu) = \int_0^\infty B_\nu(T) e^{-\tau \mu} d\tau, \quad (\text{IV. 1})$$

where: μ is the cosine of the angle between the line of sight and the normal to the surface,

$$B_\nu(T) \text{ is the Planck function, } \propto \frac{\nu^3}{e^{\frac{h\nu}{kT}} - 1},$$

$$T^4 = T_e^4(\theta) \left(\tau + \frac{2}{3} \right).$$

The absolute flux detected by the observer is,

$$F_\nu(i) = \int_\Sigma \mu I_\nu(\mu, 0) d\Sigma \quad (\text{IV. 2})$$

where i is the angle between the line of sight and the axis of symmetry of the star, and the integral is done over the observable surface.

The diagram below explains the geometry

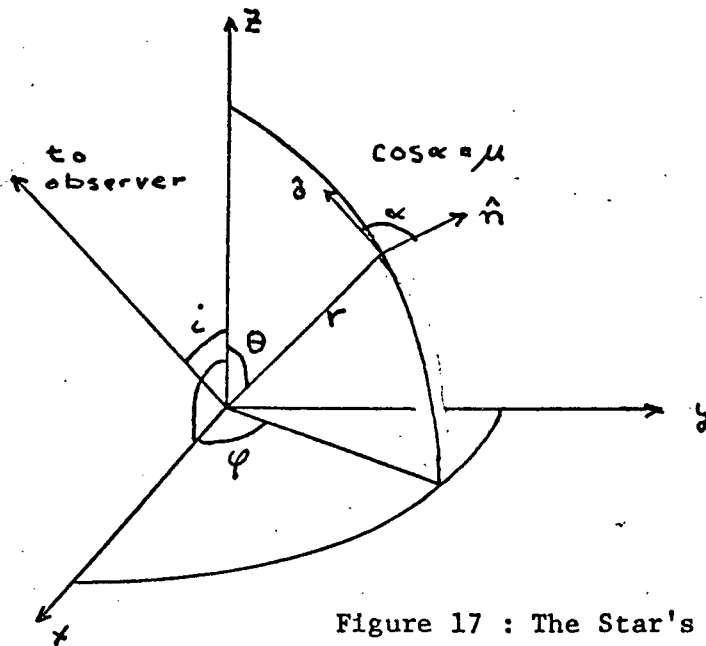


Figure 17 : The Star's Geometry

The temperature distribution $T_e(\theta)$ is found from Von Zeipel's Theorem, which states

$$F \propto |\vec{g}|,$$

(IV.3)

where g is the local effective acceleration. Since $F = T_e^4$, and $|\vec{g}| = |\nabla \Phi|$, where the total potential is given by,

$$\Phi = -\frac{GM}{r} + kb + (\phi_2 - kb) P_2(\cos \theta).$$

(IV.4)

In spherical coordinates we have

$$|\vec{g}| = \left| \left(\frac{GM}{r} + kb' + (\phi_2' - kb') P_2, \frac{\phi_2 - kb}{r} \frac{\partial P}{\partial \theta}, 0 \right) \right|.$$

(IV.5)

The surface of the star is given by

$$r = r_0 \left(1 + \epsilon(r_0) P_2(\cos \theta) \right).$$

(IV.6)

Consequently the gravity to first order is

$$g(\theta) = \frac{GM}{r_0(1+\epsilon P_2)^2} + \frac{3}{2} kb' \sin^2 \theta + \phi_2' P_2(\mu).$$

(IV.7)

The effective temperature average is defined as

$$\sigma T_e^4 = \frac{L_*}{4\pi R_*^2}.$$

(IV.8)

So we have for the temperature distribution,

$$T_e(\theta) = T_e(\theta_0) \left[\frac{g(\theta)}{g(\theta_0)} \right]^{\frac{1}{4}}.$$

(IV.9)

To determine μ , the angle between the observer's line of sight and the normal to the surface, we note that the surface is given to first order by,

$$r_0 = \frac{r}{1 + \epsilon P_2} \quad (IV.10)$$

The normal to the surface is given by

$$\hat{n} = \frac{\nabla r_0}{|\nabla r_0|} \quad (IV.11)$$

Calculating this out we find

$$\begin{aligned} \nabla r_0 = \frac{1}{1 + \epsilon P_2} & \left[\sin \theta \cos \phi \left\{ 1 + \frac{\epsilon}{1 + \epsilon P_2} (1 + 2P_2) \right\} \hat{x} \right. \\ & + \sin \theta \sin \phi \left\{ 1 + \frac{\epsilon}{1 + \epsilon P_2} (1 + 2P_2) \right\} \hat{y} \\ & \left. + \cos \theta \left\{ 1 + \frac{\epsilon}{1 + \epsilon P_2} (-2 + 2P_2) \right\} \hat{z} \right], \end{aligned} \quad (IV.12)$$

and

$$|\nabla r_0| = \frac{1}{1 + \epsilon P_2} \quad (IV.13)$$

Therefore the normal is

$$\hat{n} = \left[\left(1 + 3\epsilon \cos^2 \theta \right) \sin \theta \cos \phi, \left(1 + 3\epsilon \cos^2 \theta \right) \sin \theta \sin \phi, (1 - 3\epsilon \sin^2 \theta) \cos \theta \right]. \quad (IV.14)$$

Now μ can be determined simply from the dot product be-

tween the vector to the line of sight and the normal vector.
The vector to the observer is

$$\hat{o} = (\sin i, 0, \cos i),$$

(IV.15)

so we have

$$\mu = \hat{n} \cdot \hat{o} = (1 + 3\epsilon \cos^2 \theta) \sin \theta \cos \phi \sin i + (1 - 3\epsilon \sin^2 \theta) \cos \theta \cos i.$$

(IV.16)

Note that μ is an even function in ϕ .

Now to integrate this intensity over the visible part of the stars surface. The flux is then given by

$$F_2(i) = \int_{\theta=0}^{\pi/2} \int_{\phi=0}^{\pi} r_0^2 \mu(\theta, \phi) I(\mu, 0) (1 + \epsilon P_2)^3 \sin \theta d\theta d\phi.$$

(IV.17)

The numerical solutions are based on a number of quadrature formulas for doing the integrations. Over θ Legendre-Gauss is used, over ϕ Chebyshev-Gauss, and over τ Laguerre-Gauss. The above formula for the flux becomes

$$F_2(i) = \frac{K \pi^2}{4} \sum_{i=1}^m \frac{2}{(1 - \mu_i)^2 [P'_n(\mu_i)]^2} \sum_{j=1}^{\tilde{m}} \frac{\pi}{n} \mu(u_i, v_j) I(\mu, 0) (1 + \epsilon P_2)^3 \sin\left(\frac{\pi}{2} u_i\right).$$

(IV.18)

where $u_i = \text{zeros of } P_m$, the Legendre polynomial of degree m ,
degree m .

$v_j =$ zeros of T_n , the Chebyshev polynomial of degree n ,

$$\theta_i = \frac{\pi}{2} v_i,$$

$$\phi_j = \frac{\pi}{2} v_j,$$

Similarly the intensity is given by

$$\mu(u, v_j) I(\mu, 0) = K' \nu^3 \sum_{k=1}^N \mu \frac{1}{\exp\left(\frac{h\nu}{\lambda T_c(\theta)(x_k + \frac{2}{\pi})}\right) - 1} \frac{1}{x_k [L_N^y(x_k)]^2}.$$

(IV.19)

where $x_k \equiv \tau_{\mu}$ are the zeros of L_N , the Laguerre polynomial of degree N .

It is necessary to make a simple transformation between the coordinates in the observer's system to one in the stars system. These are (primed quantities are in star's system)

$$\cos \theta' = \cos \theta \sin i + \sin \theta \cos \phi \cos i,$$

(IV.20)

$$\tan \phi' = \frac{\sin \theta \sin \phi}{\sin \theta \cos \phi \sin i - \cos \theta \cos i}.$$

(IV.21)

Magnitudes are computed from

$$m_\nu = -2.5 \log F_\nu$$

(IV.22)

These magnitudes were taken at roughly the centres of the V and B bands ($V=5530\text{\AA}$ and $B=4350\text{\AA}$ about). The V and $(B-V)$ indices were then calculated to see what the observational effects of the magnetic field might be.

APPENDIX V: COMPUTER PROGRAMS

The first program listed is the calculation of stellar structure. As input it requires an initial model on unit 3 and the specification of certain NAMELIST variables:

M0 the mass of the model,
 X1, Z1 the abundances of hydrogen and metals respectively,
 ERCP, etc. The maximum allowed relative change in P,T,S
 and Q from one model to the next,
 H0 the magnetic field in gauss.

There are also a variety of parameters to control the amount of output, the calculation of certain quantities, and a few variable parameters in the stellar model. All of these have default values.

The magnetic field is found by calling the subroutine BFIELD. The main program also requires:

STEMP to calculate effective surface temperatures,
 ENGEN calculates the energy generation rate,
 SMAX finds the maximum of a ratio,
 LAGINS is a Lagrangian interpolation, supplied by Dr.
 A.J. Barnard,
 FLUXPO calculates the flux for a poloidal field,
 TANB calculates the tangential component of the magnetic
 field at any point in the equatorial plane,
 KAPPA is an optional opacity table look up (not used),
 ENPOLE calculates the field energy for a poloidal magnetic
 field,
 FH calculates the magnetic energy in a mass shell,
 FG calculates the gravitational energy in a mass shell.

Next the subroutine COLOUR calculates the grey atmosphere. It is called from STEMP and requires input from the initial NAMELIST statement of the number of inclination angles to be evaluated and the initial B and V indices. All integrals are approximated by sixteenth order polynomials.

There are three versions of the subroutine BFIELD. The first calculates the field for the flux penetrating the core, the second for the flux excluded from the core, and the last the flux penetrates the core and the model is in uniform rotation. All of these use a Runge-Kutta routine provided by the UBC Computing Centre to find a particular solution to the pseudo-polytropic equation for the magnetic field. This routine DRK requires an auxiliary routine AUXRK to specify the differential equation. The BFIELD for the rotating magnetic star calls EROTAT and FROT to calculate the energy of rotation.


```

$C STAR(1,767) TO *SINK*@NOCC
C THIS IS A MODEL OF A MAGNETIC STAR
C NANG=NUMBER OF INCLINATION ANGLES COLOUR IS TO EVALUATE
C COL(1&2) ARE THE B AND V INDICES OF INITIAL STAR
  IMPLICIT REAL*8 (A-H,O-Z)
  DIMENSION AX(100),AS(100),AQ(100),AP(100),AT(100),ABETR(100),ARHO(
1100),AN1(100),AFX(100),ALAM(100)
  REAL*8 MAG(100),DMAG(100),POT2(100)
  DIMENSION SOLY(9)
  REAL*8 KAPPA(100)
  DIMENSION A(8,4,100),B(4,100),AUX(6400),BAUX(400),IP(400)
  DIMENSION IPASS(5),PASS(5),COL(2)
  REAL*4 OP(30,10)
  INTEGER TITLE(20)
  REAL*8 KAPS,KAPT,KAP,L1,M0,LOGLO,LOGTO
  REAL*4 TME,SCLOCK
C OUTPUT=T FOR FINAL MODEL OF ITERATION SEQUENCE ON UNIT 7
C OLDMOD=T IF REREAD INITIAL MODEL FOR NEW SERIES OF ITERATIONS
C INTER=TRUE FOR DUMP OF DETAILED MODEL PARAMETERS ONTO UNIT 0
C DUMP=T TO OUTPUT A MODEL WHICH DID NOT CONVERGE
  LOGICAL CONVG,MAGON,QUIT,OUTPUT,OLDMOD,INTER,SHORT,DUMP,PREV
  LOGICAL SECOND,MAGOUT,CURFIT
  COMMON /DAT/ SECOND
  COMMON /MAINB/ MAG,DMAG,ALAM,SOLY,H0,M0,OMEGA,ICVCT
1,NMASS,PASS,IPASS,SHORT,MAGOUT,ICONUM,ICVG
2,MCVCT,CURFIT
  COMMON /MAINRK/ AN1,ABETR,AT
  COMMON /ALL/ AS,ARHO,NP
  COMMON /MASS/ AFX
  COMMON /CMAIN/ COL,SINI,NANG
  COMMON /ETC/ WT,QUIT
C MASS FUCTIONS
  FM(Y)=(1.D0-(1.D0-Y)**SIG)**3
  FP(Y)=3.D0*SIG*((1.D0-(1.D0-Y)**SIG)**2)*(1.D0-Y)**(SIG-1.D0)
  NAMELIST/PARAM/M0,L1,AL,X1,Z1,NP,ERCP,ERCT,ERCS,ERCQ,ICMAX
1,ALPHA,BETA,H0,MAGON,PCON,SURFC,OUTPUT,CONVG,NMASS,
2PASS,ICONUM,IPASS,OLDMOD,INTER,SHORT,DUMP,MAGOUT
3,NANG,OMEGA,COL,MCVCT,SINI,CURFIT,LOGLO,LOGTO
C OPACITY TABLE ON UNIT 1
C   REWIND 1
C   READ(1,5001) NOP
C5001 FORMAT(I2)
C   READ (1,5000) ((OP(I,J) J=1,10),I=1,NOP)
C5000 FORMAT(E8.3,F8.0,8E8.3)
  REWIND 7
  OLDMOD=.FALSE.
  SECOND=.FALSE.
1001 CONTINUE
  REWIND 3
  DO 67 I=1,5
    PASS(I)=0.D0
67 IPASS(I)=0
C INPUT PARAMETERS AND COMPUTE CONSTANTS
  AL=1.D-2
  NP=81
  ERCQ=5.D-3

```

```

ERCT=0.D0
ERCP=0.D0
ERCS=0.D0
PCON=10.D0
PREV=.FALSE.
DUMP=.FALSE.
SHORT=.FALSE.
CONVG=.TRUE.
MAGOUT=.FALSE.
H0=1.D5
NMASS=0
SINI=0.D0
OMEGA=1.111111D-4
LOGLO=0.D0
LOGTO=0.D0
MCVCT=0
NANG=5
CURFIT=.FALSE.
INTER=.FALSE.
ICMAX=5
OUTPUT=.FALSE.
CONVG=.FALSE.
MAGON=.TRUE.
SURFC=1.D-5

```

C ICONUM=# OF TIMES BFIELD CALLED FOR CALCULATING STRUCTURE.

C NOTE THAT BFIELD CALLED ONCE MORE FOR FINAL OUTPUT

```

ICONUM=1
READ(3,PARAM)
READ(3,3000) (AX(I),AS(I),AQ(I),AP(I),AT(I),I=1,NP)
WRITE(6,PARAM)
IF(OLDMOD) GO TO 1002

```

C

C INITIALIZATION

C

```

1000 CONTINUE
READ(5,2305,END=999) TITLE
2305 FORMAT(20A4)
QUIT=.FALSE.
NT=1
READ(5,PARAM)
IF(OLDMOD) GO TO 1001
1002 OLDMOD=.FALSE.
NP1=NP-1
ML=5
NU=5
LCM=2*ML+NU
LC=LCM+1
LK=ML+NU+1-LC
LT=4*NP1*LC
IF(ERCT.EQ.0.D0) ERCT=ERCQ
IF(ERCP.EQ.0.D0) ERCP=ERCQ
IF(ERCS.EQ.0.D0) ERCS=ERCQ
ETA=ALPHA
THETA=BETA-1.5D0*ALPHA

```

C FROM SACKMANN-ANAND

```

RKO=.245D0*((1.D0+X1)/(2.D0-Z1))**.67D0
KAPS=.195D0*(1.D0+X1)
SIG=(4.D0+ALPHA+BETA)/(1.D0+ALPHA)
IF(SHORT) GO TO 71
WRITE(6,2200)

```

```

WRITE (6,2203)
WRITE (6,2204) (AX(I),AS(I),AQ(I),AP(I),AT(I),I=1,NP)
2203 FORMAT('1',12X,'X',20X,'S',20X,'Q',20X,'P',20X,'T'/)
2204 FORMAT(1X,5F21.8)
71  PALT=PCON/10.D0
CONA=.01225392567D0*M0*PALT
CONB=.02828907204D0*M0*M0*PALT
CONU=41.50255393D0*M0/L1*PALT
CONRP=7.974157461D-4*PALT
CONE=.5179687500*M0/L1
Y1=1.D0-(X1+Z1)
WT=1.D0/(2.D0*X1+.75D0*Y1+.5D0*Z1)
CONRHO=38.31089742/PALT*WT

```

C INITIAL LOGIC

```

ICVG=0
IF(CONVG) ICVG=1
IF(PREV.AND.MAGON) GO TO 900
ICVCT=101
DO 66 I=1,100
ALAM(I)=0.D0
ARHO(I)=0.D0
ABETR(I)=1.D0
AN1(I)=0.D0
ITOT=0
CONTINUE
ITOT=ITOT+1
ICOUNT=1

```

SQPT SQPT SQPT

CONTINUE

```
DO 10 I=1,NP
DO 10 J=1,4
DO 10 K=1,8
A(K,J,I)=0.DO
```

CENTRAL BOUNDARY CONDITIONS ASSUMING CONVECTION

```

I=1
S3=SIG*SIG*SIG
X=AX(I)
S=AS(I)
Q=AQ(I)
P=AP(I)
T=AT(I)
T3=T**.3333333333333333
T32=T*DSQRT(T)
KAPPA(1)=0.D0
BETR=1.D0-CONRP*T32/P
ABETR(1)=BETR
RHO=CONRHO*BETR*P*T32
ARHO(1)=RHO
AN1(I)=4.D0-1.5D0*BETR*BETR/(4.D0-3.D0*BETR)
AFX(I)=0.D0
DS=(CONA*3.D0/(WT*BETR*P*T32))**.3333333333333333
DS=SIG*DS

```

E=EP+EC

DUK=CONE*AL*S3

DUP=3.D0*EP*DUK

DUC=3.D0*EC**DUK

DQ=DUK*E

DV=2.D0*DQ

DC=0.D0

DR=0.D0

DU=DUP+DUC

DT=0.D0

DP=0.D0

IF(SHORT) GO TO 72

WRITE(6,4001)

WRITE(6,4002)

4001 FORMAT('1',10X,'ENERGY GENERATION CHECK'//)

4002 FORMAT(5X,'EP',10X,'EC',10X,'DS',8X,'DQ',8X,'DP',8X,'DT',7X,'ENR'
1,7X,'ENC',7X,'KAP',6X,'BETR',5X,'ALPHA',6X,'BETA')

WRITE(6,4003) EP,EC,DS,DQ,DP,DT

72 A(3,1,I)=.5D0*DS/(P*BETR)

A(4,1,I)=.75D0*DS/T*((2.D0*BETR-1.D0)/BETR)

A(3,2,I)=-.5D0*DU/(P*BETR)

BTF=1.5D0*(1.D0-BETR)/BETR

TRM1=.8333333333333333+5.231D0/T3-BTF

TRM2=.8333333333333333+23.566D0/T3-BTF

A(4,2,I)=-.5D0*(DUP*TRM1+DUC*TRM2)/T

DX=1.D0/(AX(I+1)-AX(I))

A(3,3,I)=-DX

A(4,4,I)=-DX

SL=S

QL=Q

PL=P

TL=T

DXL=DX

DSL=DS

DQL=DQ

DPL=DP

DTL=DT

C
C
C

SHELLS BETWEEN CENTRE AND SURFACE

NP1=NP-1

DO 100 I=2,NP1

X=AX(I)

X2=X*X

S=AS(I)

S2=S*S

S4=S2*S2

Q=AQ(I)

P=AP(I)

T=AT(I)

T3=T**.3333333333333333D0

T32=T*DSQRT(T)

BETR=1.D0-CONRP*T32/P

ABETR(I)=BETR

RHO=CONRHO*BETR*P*T32

ARHO(I)=RHO

AFX(I)=FM(X)

FPE=FP(X)

AMASS=(1.D0+ALAM(I))*AFX(I)

```

DS=CONA*FPE/(WT*S2*P*T32*BETR)
EC=0.D0
EP=0.D0
IF(T.LE..5D0) GO TO 19
CALL ENGEN (P,T,EP,EC,X1,Z1,WT,RHO,T3,T32)
19 CONTINUE
E=EP+EC
DUE=CONE*FPE*(1.D0+AL/X2)
DUP=DUE*EP
DUC=DUE*EC
DU=DUP+DUC
DV=2.D0*AL*Q/((X2+AL)*X)
DQ=DU-DV
C OPACITY USING KRAMERS FORMULA
KAPT=RKO*(RHO**ALPHA/T**BETA)
KAP=KAPS+KAPT
KAPPA(I)=KAP
C OPACITY USING TABLE LOOK UP
C IF(T.LE.2.D-3) GO TO 68
C CALL KAPPA(OP,RHO,T,KAP,KAP0,ALPHA,BETA,NT)
C ETA=ALPHA
C THETA=BETA-1.5D0*ALPHA
C KAPT=KAP-.2004D0*(1.D0+X1)
C SIG=(4.D0+ALPHA+BETA)/(1.D0+ALPHA)
C RKO=KAP0
C68 CONTINUE
ENR=CONU*AMASS*T32*(1.D0+AL/X2)/(KAP*Q*P)
ENC=4.D0-1.5D0*BETR*BETR/(4.D0-3.D0*BETR)
DTB=-CONB*AMASS*FPE/(S4*P*T32)
IF(ENC.GT.ENR) GO TO 18
DT=DTB/ENR
DR=DT
EN1=ENR
IF(ICVCT.GT.I) ICVCT=I
GO TO 17
18 DT=DTB/ENC
DC=DT
EN1=ENC
17 AN1(I)=EN1
DP=P/T*DT*(EN1-2.5D0)
IF(SHORT) GO TO 73
WRITE(6,4003) EP,EC,DS,DQ,DP,DT,ENR,ENC,KAP,BETR,ALPHA,BETA
4003 FORMAT(1X,2D11.3,4D10.3,6F10.4)
C
C
C THE DIFFERENCE EQUATION COEFFICIENTS
73 DX=1.D0/(AX(I+1)-AX(I))
IM=I-1
K=4
11 CONTINUE
A(K+1,1,IM)=DXL+DS/S
A(K+2,1,IM)=0.D0
A(K+3,1,IM)=.5D0*DS/(P*BETR)
A(K+4,1,IM)=.75D0*DS/T*(2.D0*BETR-1.D0)/BETR
A(K+1,2,IM)=0.D0
A(K+2,2,IM)=DXL+.5D0*DQ/Q
A(K+3,2,IM)=-.5D0*DU/(P*BETR)
BTF=1.5D0*(1.D0-BETR)/BETR
TRM1=.8333333333333333D0+5.231D0/T3-BTF
TRM2=.8333333333333333D0+23.566D0/T3-BTF

```

```

A(K+4,2,IM)=-.5D0*(DUP*TRM1+DUC*TRM2)/T
A(K+1,3,IM)=2.D0*DP/S
IF(ENR-ENC) 20,20,21
20 A(K+2,3,IM)=0.D0
   DBR=2.D0*(EN1-4.D0)*(EN1-4.D0-BETR)*(1.D0-BETR)/(BETR*BETR*EN1)
   A(K+3,3,IM)=DXL+1.25D0*DT*DBR/T
   A(K+4,3,IM)=1.25D0*DP/T-1.875D0*P*DT*DBR/(T*T)
   GO TO 22
21 A(K+2,3,IM)=1.25D0*P*DR/(T*Q)
   TKAP1=ETA*KAPT/KAP/BETR
   A(K+3,3,IM)=DXL+1.25D0*DR*(1.D0+TKAP1)/T
   TKAP2=KAPT/KAP*(THETA+ETA*BTF)
   A(K+4,3,IM)=1.25D0*DP/T-1.25D0*DR*P*(1.5+TKAP2)/(T*T)
22 CONTINUE
   A(K+1,4,IM)=2.D0*DT/S
   IF(ENR-ENC) 30,30,31
30 A(K+2,4,IM)=0.D0
   A(K+3,4,IM)=.5D0*DC/P*(1.D0-DBR)
   A(K+4,4,IM)=DXL+.75D0*DC/T*(1.D0+DBR)
   GO TO 32
31 A(K+2,4,IM)=-.5D0*DR/Q
   A(K+3,4,IM)=-.5D0*DR*TKAP1/P
   A(K+4,4,IM)=DXL+.5D0*DR*(3.D0+TKAP2)/T
32 CONTINUE
   IF(IM.EQ.I) GO TO 40
   IM=I
   K=0
   DXP=DXL
   DXL=-DX
   GO TO 11
40 CONTINUE
   IM=I-1
C RIGHT HAND SIDES
   B(1,IM)=-DXP*(S-SL)+.5D0*(DS+DSL)
   B(2,IM)=-DXP*(Q-QL)+.5D0*(DQ+DQL)
   B(3,IM)=-DXP*(P-PL)+.5D0*(DP+DPL)
   B(4,IM)=-DXP*(T-TL)+.5D0*(DT+DTL)
   SL=S
   QL=Q
   PL=P
   TL=T
   DXL=DX
   DSL=DS
   DQL=DQ
   DPL=DP
   DTL=DT
100 CONTINUE
C
C BOUNDARY CONDITIONS FOR A RADIATIVE SURFACE
C
   I=NP
   X=AX(I)
   S=AS(I)
   S2=S*S
   S4=S2*S2
   Q=AQ(I)
   P=AP(I)
   T=AT(I)
   KAPPA(NP)=0.D0
   ABETR(I)=BETR

```

```

ARHO(I)=0.D0
AFX(I)=1.D0
EN1=BETR*SIG+4.D0*(1.D0-BETR)
ENR=EN1
AN1(I)=EN1
AMASS=1.D0+ALAM(I)
CONK=RKO*(WT*BETR*CONRHO)**ALPHA
CQ=CONU*(1.D0+AL)/CONK
POW=1.D0/(1.D0+ALPHA)
P2=1.D0/SIG
DT=-(3.D0*SIG*CONB*AMASS/(EN1*(AMASS*CQ/(EN1*Q))**POW*S4))**P2
DS=-.4331681737/M0*EN1*S2*DT/(WT*AMASS*BETR)
DP=0.D0
DUP=0.D0
DUC=0.D0
DU=0.D0
DV=2.D0*AL*Q/(1.D0+AL)
DQ=-DV
IF(SHORT) GO TO 74
WRITE(6,4003) EP,EC,DS,DQ,DP,DT,ENR,ENC,KAPT,BETR
74 A(5,1,NP1)=DXL+DS/S
   A(6,1,NP1)=0.D0
   A(5,2,NP1)=0.D0
   A(6,2,NP1)=DXL+.5D0*DV/Q
   A(5,3,NP1)=2.D0*DP/S
   A(6,3,NP1)=0.D0
   A(5,4,NP1)=2.D0*DT/S
   A(6,4,NP1)=-.5D0*DT/Q
   B(1,NP1)=-DXL*(S-SL)+.5D0*(DS+DSL)
   B(2,NP1)=-DXL*(Q-QL)+.5D0*(DQ+DQL)
   B(3,NP1)=-DXL*(P-PL)+.5D0*(DP+DPL)
   B(4,NP1)=-DXL*(T-TL)+.5D0*(DT+DTL)
C
C SOLVE DIFFERENCE EQUATIONS FOR CORRECTIONS
C
DO 150 L=1,LT
150 AUX(L)=0.D0
DO 200 I=1,NP1
DO 200 J=1,4
NR=4*I+J-4
BAUX(NR)=B(J,I)
KS=1
KF=8
IF(I.EQ.1) KS=3
IF(I.EQ.NP1) KF=6
DO 200 K=KS,KF
NC=4*I+K-6
KK=NC*LC+NR-NC+LK
AUX(KK)=A(K,J,I)
200 CONTINUE
NEQ=4*NP1
C TME=SCLOCK(0.0)
CALL DGBAND(AUX,BAUX,NEQ,ML,NU,1,IP,DET,NCN)
C TME=SCLOCK(TME)
IF(DET.NE.0.D0) GO TO 250
WRITE(6,2300)
2300 FORMAT('1',10X,'DETERMINANT IS ZERO')
GO TO 1000
250 CONTINUE
DO 340 I=1,NP1

```

```

AS (I+1)=AS (I+1)+BAUX (4*I-1)
AQ (I+1)=AQ (I+1)+BAUX (4*I)
AP (I)=AP (I)+BAUX (4*I-3)
AT (I)=AT (I)+BAUX (4*I-2)
340  CONTINUE
C
C
C  OUTPUT      OUTPUT      OUTPUT
      IF (SHORT) GO TO 82
83    WRITE (6,2306) TITLE
2306  FORMAT ('1',9X,20A4//)
      WRITE (6,2000) M0
2000  FORMAT (10X,'THIS IS A ',F7.2,' SOLAR MASS MODEL'//)
      RLUM=L1*AQ (NP)/(1.D0+AL)
      WRITE (6,2001) RLUM
2001  FORMAT (10X,'THE LUMINOSITY OF THIS MODEL IS',F10.4,' SOLAR UNITS'/
1/)
      WRITE (6,2010) ALPHA,BETA,SIG
2010  FORMAT (10X,'KRAMERS OPACITY: ALPHA=',F8.4,', BETA=',F8.4,', SIGM
1A=',F8.4//)
      TCNT=AT (1)*1.D7
      PCNT=AP (1)*(TCNT)**2.5D0/PCON
      WRITE (6,2008) AS (NP),TCNT,PCNT,ARHO (1)
2008  FORMAT (10X,'R=',F10.8,10X,'T CENTRE=',F10.0,10X,'P CENTRE=',D13.6,
110X,'RHO CENTRE=',F10.7//)
C
      WRITE (6,2004) TME
2004  FORMAT (10X,'EXECUTION TIME FOR SOLUTION OF MATRIX IS',F10.4//)
      T0=(RLUM*1.1146D+15/(AS (NP)*AS (NP)))**.25D0
      WRITE (6,3500) T0
3500  FORMAT (10X,'THE EFFECTIVE SURFACE TEMPERATURE IS',F9.2,' DEGREES'
1///)
      HRT=DLOG10 (T0)
      HLOGL=DLOG10 (RLUM)
      HRL=4.734D0-2.5D0*HLOGL
      WRITE (6,2206) HRL,HRT,HLOGL
2206  FORMAT (10X,'M BOL 0=',F10.6,5X,'LOG (T EFF)=',F10.6,
$ 10X,'LOG (L)=',F10.7///)
      IF (LOGLO.EQ.0.D0) GO TO 2408
      DLOGL=HLOGL-LOGLO
      DLOGT=HRT-LOGT0
      WRITE (6,2409) DLOGL,DLOGT
2409  FORMAT (10X,'CHANGE IN LOG (L)',D12.5,10X,'CHANGE IN LOG (T EFF)',D12.5//)
2408  CBV=COL (1)-COL (2)
      WRITE (6,2207) COL (2),CBV
2207  FORMAT (10X,'THE COLOURS OF THE INITIAL MODEL ARE: V=',F10.6,10X,
# 'B-V=',F10.6///)
      WRITE (6,2205) ITOT
2205  FORMAT (10X,'THIS IS THE',I3,' ITERATION')
      IF (MAGON) WRITE (6,2211) H0
2211  FORMAT (10X,'H0=',F9.0)
      IF (OMEGA.NE.1.111111D-4) WRITE (6,2212) OMEGA
2212  FORMAT ('-',9X,'OMEGA=',D12.5)
      WRITE (6,2200)
2200  FORMAT ('1',10X,'THE NEW STARTING MODEL FOLLOWS'//)
      WRITE (6,PARAM)
      WRITE (6,2201)
2201  FORMAT (6X,'FX',11X,'S',11X,'Q',11X,'P',11X,'T',12X,'RHO',9X,
1'N+1',10X,'LAMBDA',10X,'KAPPA'//)
      WRITE (6,2202) (AFX (I),AS (I),AQ (I),AP (I),AT (I),ARHO (I),AN1 (I),ALAM
1 (I),KAPPA (I),I=1,NP)

```


2202 FORMAT(1X,5F12.6,D13.5,F12.6,F20.16,F12.6)
 IF(QUIT.AND.SHORT) GO TO 84

107

C

C INTERMEDIATE OUTPUT INTERMEDIATE OUTPUT INTERMEDIATE OUTPUT

82 IF((.NOT.INTER).OR.(ITOT.GT.2)) GO TO 860
 WRITE(0,2401) H0,M0,WT,ICVCT,NMASS,NP,QUIT
 WRITE(0,2400) (AFX(I),MAG(I),DMAG(I),ALAM(I),AN1(I),ABETR(I),AT(I),
 1 AS(I),ARHO(I),I=1,NP)
 2400 FORMAT(9D25.16)
 2401 FORMAT(6D25.16,3I3,L1)
 WRITE(0,2402) PASS,IPASS
 2402 FORMAT(5D25.16,5I10)
 860 CONTINUE

C

C CONVERGENCE TESTS CONVERGENCE TESTS
 CALL SMAX(BAUX,400,0,AQ,NP,1,RMAXCQ,IXQ)
 IF(RMAXCQ.GT.ERCQ) GO TO 310
 CALL SMAX(BAUX,400,-1,AS,NP,1,RMAXCS,IXS)
 IF(RMAXCS.GT.ERCS) GO TO 310
 CALL SMAX(BAUX,400,-3,AP,NP,0,RMAXCP,IXP)
 IF(RMAXCP.LE.ERCP) GO TO 308
 BXP=DABS(BAUX(4*IXP-3))
 IF(BXP.LT.SURFC) GO TO 308
 GO TO 310
 308 CALL SMAX(BAUX,400,-2,AT,NP,0,RMAXCT,IXT)
 IF(RMAXCT.LE.ERCT) GO TO 320
 BXT=DABS(BAUX(4*IXT-2))
 IF(BXT.LT.SURFC) GO TO 320

C

C FINAL LOGIC LOGIC LOGIC LOGIC

C

310 CONVG=.FALSE.
 ITOT=ITOT+1
 ICOUNT=ICOUNT+1
 IF(ICOUNT.LE.ICMAX) GO TO 2
 WRITE(6,2301)
 2301 FORMAT('1',10X,'CONVERGENCE TOO SLOW, NO NEW OUTPUT MODEL PRODUCED
 1')
 IF(.NOT.DUMP) GO TO 999
 WRITE(7,PARAM)
 WRITE(7,3000) (AX(I),AS(I),AQ(I),AP(I),AT(I),I=1,NP)
 999 STOP
 320 CONVG=.TRUE.
 ICVG=ICVG+1
 IF(ICVG.LE.ICONUM) GO TO 850
 QUIT=.TRUE.
 IF(SHORT) GO TO 83
 84 IF(.NOT.OUTPUT) GO TO 870
 WRITE(7,PARAM)
 WRITE(7,3000) (AX(I),AS(I),AQ(I),AP(I),AT(I),I=1,NP)
 3000 FORMAT(5D25.16)
 870 CONTINUE
 IF(MAGON) GO TO 900
 GO TO 1000
 850 IF(.NOT.MAGON) GO TO 1

C

C

C

C THE CALCULATION OF THE MAGNETIC FIELD STRUCTURE

C

```

900  CONVG=.FALSE.
      CALL BFIELD
      IF (.NOT.QUIT) GO TO 1

```

108

```

C
C
C  EFFECTIVE SURFACE TEMPERATURES

```

```

      CALL STEMP(RLUM,T0,AS(NP))
      WRITE(6,3125)
3125  FORMAT('1')
      PREV=.TRUE.
      SECOND=.TRUE.
      GO TO 1000
      END
      SUBROUTINE STEMP(RLUM,T0,S)
      IMPLICIT REAL*8 (A-H,O-Z)
      DIMENSION PASS(5),COL(2),B(20),V(20)
      DIMENSION ANG(20)
      COMMON /CMAIN/ COL,SINI,NANG
      COMMON /CTEMP/ DPOT2,HLAM,ROT,E
      S2=S*S
      DEN=1.D0+HLAM-ROT
      CP=(1.D0/(1.D0+E)**2+DPOT2)/DEN
      CE=(1.D0/(1.D0-.5D0*E)**2+1.5D0*(HLAM-ROT*(1-.5D0*E))-.5D0*DPOT2)
      $ /DEN
      TPOL=T0*CP**.25D0
      TEQU=T0*CE**.25D0
      WRITE(6,3120) T0,TPOL,TEQU
3120  FORMAT('0','THE SURFACE TEMPERATURE IS',F19.12,' DEGREES ON P2=0'
1/28X,F18.12,' DEGREES AT THE POLE'/28X,F18.12,' DEGREES AT THE EQU
2ATOR')
      RD=1.5D+2*E
      TDIFF=TPOL-TEQU
      WRITE(6,200) TDIFF,RD
200  FORMAT(1X,'TEMPERATURE DIFFERENCE=',F12.5,10X,'RADIUS DIFFERENCE P
1OLE-EQUATOR=',F12.8,'%')
      WRITE(6,100) DPOT2
100  FORMAT(1X,'(DPOT2/DR)/(GM/R*R)=DPOT2=',D15.7)
      WRITE(6,300) DPOT2,HLAM,ROT,E
300  FORMAT(1X,4D25.15)
      IF(NANG.EQ.0) RETURN
      IF(SINI.GE.0.D0) ANG(1)=SINI
      WRITE(6,400)
400  FORMAT('- ',9X,'THE UBV COLOURS ARE'/'- ','I DEGREES',7X,'V ',20X,
# 'B-V'//)
      CALL COLOUR(S,T0,B,V,ANG)
      DO 20 K=1,NANG
20  B(K)=B(K)-V(K)
10  WRITE(6,500) (ANG(K),V(K),B(K),K=1,NANG)
500  FORMAT(1X,F6.2,2D20.10)
      RETURN
      END
      SUBROUTINE ENGEN(P,T,EP,EC,X,Z,WT,RHO,T3,T32)
      IMPLICIT REAL*8 (A-H,O-Z)
      Q=DSQRT(RHO)/T32
      RHOH=RHO/(T3*T3)
      Y=1.D0-(X+Z)
      AL=39.336631D0-46.416D0/T3+2.D0*(DLOG(Y)-DLOG(X))
      DA=DEXP(AL)
      DG=DA*(DSQRT(1.D0+2.D0/DA)-1.D0)
      EF11=1.D0+.79D-2*Q

```

```

EF71=1.D0+3.16D-2*Q
G11=1.037D0+.33D-1*T
G71=1.D0
EPT=13.003580D0-15.693D0/T3
EPH=DEXP (EPT)
EPS=EPH*RHOH*EF11*G11*X*X
WTH=36.656236D0-47.623D0/T3
WTH=WTH+DLOG (EF71)+DLOG (G71)
WTH=WTH- (.16666666666666667*DLOG (T))
WTH=WTH+DLOG (X)-DLOG (1.D0+X)
DW=DEXP (WTH)
DG1=1.D0-DG
DGW1=DG/(1.D0+DW)
GW1=1.96D0*DGW1
GW2=1.46D0*DGW1*DW
EP1=EPS*DG1
EP2=EPS*GW1
EP3=EPS*GW2
EP=EP1+EP2+EP3
EF141=1.D0+5.33D-2*Q
G141=.995D0-8.D-3*T
ECT=62.706876D0-70.697D0/T3
ECH=DEXP (ECT)
X14=.585D0*Z
IF (T.LT.1.6D0) X14=.188D0*Z
EC=ECH*EF141*G141*X*X14*RHOH
RETURN
END
SUBROUTINE SMAX(XN,NN,KN,XD,ND,KD,Q,IX)
IMPLICIT REAL*8 (A-H,O-Z)
DIMENSION XN(NN),XD(ND)
Q=0.D0
NF=ND-1
DO 10 I=1,NF
QQ=DABS(XN(4*I+KN)/XD(I+KD))
IF(QQ.LE.Q) GO TO 10
Q=QQ
IX=I
CONTINUE
RETURN
END
SUBROUTINE LAGINS(XV,FV,X,F,N,NL,NMIN,NMAX,ND)
IMPLICIT REAL*8(A-H,O-Z)
DIMENSION XV(ND),FV(ND)
DIMENSION CV(10)
DO 10 K=NMIN,NMAX
M=K
IF(X.LT.XV(K)) GO TO 20
10 CONTINUE
20 NMIN=M
N=M-NL/2-1
ENTRY LAGINC(XV,FV,X,F,N,NL,ND)
DO 60 I=1,NL
CV(I)=1.D0
DO 50 J=1,NL
IF(J.EQ.I) GO TO 50
CV(I)=CV(I)*(X-XV(J+N))/(XV(I+N)-XV(J+N))
50 CONTINUE
60 CONTINUE
ENTRY LAGINT(XV,FV,F,N,NL,ND)

```

```

F=0.
DO 80 I=1,NL
80 F=F+CV(I)*FV(I+N)
RETURN
END
SUBROUTINE FLUXPO(NP,H0,RC,R0,FLUX)
IMPLICIT REAL*8 (A-H,R)
COMMON /LAG/ NL,NMIN,NMAX
EXTERNAL TANB
NL=4
NMIN=NL/2+1
NMAX=NP-(NL-1)/2
SRC=SNGL(RC)
SR0=SNGL(R0)
FLUX=H0*3.04367D+22*DBLE(SQUANK(TANB,SRC,SR0,.001,TOL,TF))
RETURN
END
FUNCTION TANB(R)
REAL*8 AS(100),ARHO(100),WT,HT(100),DTANB,DR
REAL*8 HR(100)
LOGICAL QUIT
COMMON /ALL/ AS,ARHO,NP
COMMON /HFLUX/ HT,HR
COMMON /LAG/ NL,NMIN,NMAX
DR=DBLE(R)
CALL LAGINS(AS,HT,DR,DTANB,N,NL,NMIN,NMAX,NP)
TANB=SNGL(DTANB)*R
RETURN
END
SUBROUTINE KAPPA(OP,RHO,T,KAP,KAPO,ALPHA,BETA,NT)
IMPLICIT REAL*8 (A-H,O-Z)
REAL*4 OP(30,10)
REAL*4 TL,RLOG
TL=T*10.
RLOG=SNGL(DLOG10(RHO))
DO10 I=NT,30
IF(TL.LT.OP(I,1)) GO TO 20
CONTINUE
10 NT=I
20 NR=IFIX(RLOG-OP(NT,2))+3
ALPHA=DLOG10(DBLE(OP(NT,NR+1)/OP(NT,NR)))
NR1=IFIX(RLOG-OP(NT-1,2))+3
BETA=DLOG10(DBLE(OP(NT-1,NR1)/OP(NT,NR)))
BETA=-BETA/DLOG10(DBLE(OP(NT-1,1)/OP(NT,1)))
KAPO=OP(NT,NR)*(.1*OP(NT,1))**BETA/(OP(NT,2)**ALPHA)
KAP=KAPO*(RHO**ALPHA)/(T**BETA)
RETURN
END
SUBROUTINE ENPOLE(B,DB,H0,M0,ER,EG)
IMPLICIT REAL*8 (A-H,O-Z)
REAL*8 M0
DIMENSION B(100),DB(100),HR(100),HT(100),RATIO(100),AS(100)
1 ,AFX(100),ARHO(100)
REAL*4 SQUANK,TOL,FIF,FG,FH,S0
COMMON /ENERG/ RATIO
COMMON /LAG/ NL,NMIN,NMAX
COMMON /HFLUX/ HT,HR
COMMON /ALL/ AS,ARHO,NP
COMMON /MASS/ AFX
EXTERNAL FH,FG

```

```

      RATIO(1)=0.D0
      SS0=AS(NP)
C    CONSTANT = R/(24*PI*G*MSUN)
      C=.69601364D-17*H0*H0/M0
      S2=SS0*SS0
      S22=S2/2.D0
      NP1=NP-1
      RATIO(1)=3.D0*HR(1)*HR(1)
      DO 10 I=2,NP1
      HR(I)=-S2*B(I)/(AS(I)*AS(I))
      HT(I)=S22*DB(I)/AS(I)
      RATIO(I)=(HR(I)*HR(I)+2.D0*HT(I)*HT(I))
10    CONTINUE
      HR(NP)=1.D0
      HT(NP)=.5D0
      RATIO(NP)=1.5D0
      NL=4
      NMIN=NL/2+1
      NMAX=NP-(NL-1)/2
      S0=SNGL(SS0)
      EH=DBLE(SQUANK(FH,0.,S0,.00001,TOL,FIF))
      NMIN=NL/2+1
      S0=SNGL(SS0)
      EG=DBLE(SQUANK(FG,0.,S0,1.E-7,TOL,FIF))
      ER=C*EH/EG
      RATIO(1)=0.D0
      RATIO(NP)=0.D0
      DO 20 I=2,NP1
20    RATIO(I)=C*RATIO(I)*AS(I)/(AFX(I)*ARHO(I))
      RETURN
      END
      FUNCTION FH(S)
      REAL*8 RATIO(100),AS(100),ARHO(100),RAT,SS
      COMMON /ALL/AS,ARHO,NP
      COMMON /ENERG/ RATIO
      COMMON /LAG/ NL,NMIN,NMAX
      SS=DBLE(S)
      CALL LAGINS(AS,RATIO,SS,RAT,N,NL,NMIN,NMAX,NP)
      FH=SNGL(RAT*SS*SS)
      RETURN
      END
      FUNCTION FG(S)
      REAL*8 AS(100),ARHO(100),AFX(100),SS,MR,RHO
      COMMON /ALL/ AS,ARHO,NP
      COMMON /MASS/ AFX
      COMMON /LAG/ NL,NMIN,NMAX
      SS=DBLE(S)
      CALL LAGINS(AS,AFX,SS,MR,N,NL,NMIN,NMAX,NP)
      CALL LAGINT(AS,ARHO,RHO,N,NL,NP)
      FG=SNGL(MR*RHO*SS)
      RETURN
      END

```

\$C *SKIP

```

$C STAR(768) TO *SINK*@NOCC
      SUBROUTINE COLOUR(S0,TE0,B,V,ANG)
C   SINI IS SIN(ANG OF MAGNETIC AXIS WRT LINE OF SIGHT; I.E. 0=POLE ON)
C   INTEGRATION DONE WITH Z AXIS DEFINED AS LINE OF SIGHT
C   THETA=ANGLE BETWEEN POINT ON SURFACE OF STAR AND LINE OF SIGHT
C   PHI=ANGLE AROUND Z AXIS
C   BY SYMMETRIES 0<=THETA<=PI AND 0<=PHI<=PI/2; I.E. HALF OF VISIBLE SURFA
C   THETA PRIME IS ANGLE WRT TO SYMMETRY AXIS (MAGNETIC AXIS) OF STAR
C   I.E. IF SINI=0, THEN THETA=THETA PRIME.
      IMPLICIT REAL*8 (A-H,O-Z)
      DIMENSION COSPHI(8),SINT(8),SINPHI(8)
      INTEGER*4 THETA,PHI,THETA2
      DIMENSION HLGNDR(8),HLAGUE(8)
      DIMENSION ALGND(8),ALAG(8)
      DIMENSION B(20),V(20),COL(2),ANG(20)
      LOGICAL SECOND
      COMMON /DAT/ SECOND
      COMMON /CTEMP/ DPOT2,HLAM,ROT,E
      COMMON /CMAIN/ COL,SINI,NANG
      DATA ALGND /.095012509837637D0,.281603550779258D0,
# .458016777657227D0,.617876244402643D0,.755404408355003D0,
# .865631202387831D0,.944575023073232D0,.989400934991649D0/
      DATA HLGNDR /.189450610455068D0,.182603415044923D0,
# .169156519395002D0,.149595988816576D0,.124628971255533D0,
# .095158511682492D0,.062253523938647D0,.027152459411754D0/
      DATA ALAG /.170279632305D0,.903701776799D0,
# 2.251086629866D0,4.266700170288D0,7.045905402393D0,
# 10.758516010181D0,15.740678641278D0,22.863131736889D0/
      DATA HLAGUE /3.69188589342D-1,4.18786780814D-1,
# 1.75794986637D-1,3.33434922612D-2,2.79453623523D-3,
# 9.07650877336D-5,8.48574671627D-7,1.04800117487D-9/
      PI2=3.141592653589793D0/2.D0
      POSNEG=-1.D0
      TERED4=.75D0*TE0**4/(1.D0+HLAM-ROT)
      S2=S0*S0
      NLAGUE=8
      NLGNDR=8
      IF(SECOND) GO TO 2
C   ALGND=COS(THETA) AND PI2*ALGND=PHI
      DO 1 K=1,NLGNDR
      SINT(K)=DSQRT(1.D0-ALGND(K)*ALGND(K))
      COSPHI(K)=DCOS(PI2*ALGND(K))
      SINPHI(K)=DSIN(PI2*ALGND(K))
1   CONTINUE
2   DO 5 K=1,NANG
      IF(NANG.EQ.1) GO TO 100
      FR=(K-1)/DFLOAT(NANG-1)
      SINI=DSIN(PI2*FR)
      ANG(K)=90.D0*FR
100  COSI=DSQRT(1.D0-SINI*SINI)
      FLUXB=0.D0
      FLUXV=0.D0
      DO 10 THETA=1,NLGNDR
      DO 20 THETA2=1,2
      POSNEG=-POSNEG
      DO 30 PHI=1,NLGNDR

```

```

TPHI=SINT(THETA)*SINPHI(PHI)/(SINT(THETA)*COSPHI(PHI)*COSI
$      -POSNEG*ALGND(THETA)*SINI)
CPHIP=1.D0/DSQRT(1.D0+TPHI*TPHI)
IF(TPHI.LT.0.D0) CPHIP=-CPHIP
CTHEP=+POSNEG*ALGND(THETA)*COSI+SINT(THETA)*COSPHI(PHI)*SINI
CO2=CTHEP*CTHEP
P2=(3.D0*CO2-1.D0)*.5D0
SI2=1.D0-CO2
STH=DSQRT(SI2)
AMU=- (1.D0+3.D0*E*CO2)*STH*CPHIP*SINI+(1.D0-3.D0*E*SI2)*CTHEP*COSI
AMU=DABS(AMU)
TET=TERED4*(1.D0/(1.D0+E*P2)**2+1.5D0*(HLAM-ROT*(1.D0+E*P2))*STH
#      +DPOT2*P2)
HNKTB=.1196811276D+19/TET
E3=(1.D0+E*P2)**3
FIUB=0.D0
FIUV=0.D0
DO 50 ILAG=1,NLAGUE
TEMP=ALAG(ILAG)*AMU+.6666666666666666D0
ARG4=(HNKTB/TEMP)**.25D0
DENB=DEXP(ARG4)-1.D0
DENV=DEXP(ARG4*.78661844484D0)-1.D0
50  FIUB=FIUB+HLAGUE(ILAG)/DENB
    FIUV=FIUV+HLAGUE(ILAG)/DENV
    FIUB=FIUB*AMU
    FIUV=FIUV*AMU
C   BIS CALCULATED AT 4350A AND V AT 5530A
    FLUXB=FLUXB+HLGNDR(THETA)*HLGNDR(PHI)*FIUB*E3
    FLUXV=FLUXV+HLGNDR(THETA)*HLGNDR(PHI)*FIUV*E3
30  CONTINUE
20  CONTINUE
10  CONTINUE
C   COL FINDS DIFFERENCE FROM INITIAL BV COLOURS
    B(K)=-2.5D0*DLOG10(S2*FLUXB)-COL(1)
C   CONSTANT=-2.5*LOG10((4350/5530)**3)
    V(K)=-2.5D0*DLOG10(S2*FLUXV)-COL(2)+.7817690578D0
5   CONTINUE
    RETURN
    END

```

\$C *SKIP

```

$C NORM TO *SINK*@NOCC
  SUBROUTINE BFIELD
    IMPLICIT REAL*8 (A-H,O-Z)
    REAL*8 AS(100), ARHO(100), AN1(100), MAG(100), DMAG(100)
    1, EPS(100), ALAM(100), POT2(100), PP(100), PH(100), AFX(100)
    2, HR(100), HT(100), RATIO(100)
    REAL*8 MO
    LOGICAL QUIT, MAGOUT, SHORT, CURFIT
    DIMENSION IPASS(5), PASS(5)
    DIMENSION SOLY(9), SOLF(9), SOLQ(9)
    DIMENSION CONPAT(25)
    COMMON /MAINB/ MAG, DMAG, ALAM, SOLY, HO, MO, OMEGA, ICVCT
    1, NMASS, PASS, IPASS, SHORT, MAGOUT, ICONUM, ICVG
    2, MCVCT, CURFIT
    COMMON /ALL/ AS, ARHO, NP
    COMMON /RKB/ CON1, CON2, RHOAV, SC
    COMMON /HFLUX/ HT, HR
    COMMON /MASS/ AFX
    COMMON /ETC/ WT, QUIT
    COMMON /LAG/NL, NMIN, NMAX
    COMMON /ENERG/ RATIO
    COMMON /CTEMP/ DPOT2, HLAM, ROT, E
    SURF=AS(NP)
    S2=SURF*SURF
    S3=SURF*S2
    RHOAV=1.408376669*MO/S3
    DO 910 I=1,9
      SOLY(I)=0.D0
      SOLY(1)=AS(2)-AS(1)
      MAG(1)=0.D0
      DMAG(1)=0.D0
      POT2(1)=0.D0
      PP(1)=0.D0
      PH(1)=0.D0
      SOLY(2)=SOLY(1)*SOLY(1)
      SOLY(4)=SOLY(2)
      SOLY(6)=SOLY(2)
      SOLY(8)=SOLY(2)
      SOLY(3)=2.D0*SOLY(1)
      SOLY(5)=SOLY(3)
      SOLY(7)=SOLY(3)
      SOLY(9)=SOLY(3)
      MAG(2)=SOLY(8)
      DMAG(2)=SOLY(9)
      POT2(2)=SOLY(8)
      PP(2)=SOLY(8)
      PH(2)=SOLY(8)
      CON1=4.917521412D0
      CLAM=.69603164D-17*(SURF**4*HO*HO/(RHOAV*MO))
      CON2=CON1*CLAM
      NP1=NP-1
      NL=4
      NMIN=NL/2+1
      NMAX=NP-(NL-1)/2
      DO 920 J=2, NP1
        I=J+1

```



```

H=AS (J+1) -AS (J)
CALL DRK (SOLY,SOLF,SOLQ,H,9,1)
MAG (I)=SOLY (2)
DMAG (I)=SOLY (3)
IF (.NOT.QUIT) GO TO 920
PH (I)=SOLY (4)
PP (I)=SOLY (6)
POT2 (I)=SOLY (8)
920 CONTINUE
BCB=-(MAG (NP)+SURF*DMAG (NP))/(3.D0*SURF*SURF)
CNORM=DABS (MAG (NP)+BCB*AS (NP)*AS (NP))
DO 930 I=1,NP
MAG (I)=(BCB*AS (I)*AS (I)+MAG (I))/CNORM
DMAG (I)=(2.D0*BCB*AS (I)+DMAG (I))/CNORM
930 CONTINUE
CLAM=CLAM/CNORM
CONPAT (ICVG)=CLAM
ALAM (1)=2.D0*S3*RHOAV*CLAM*(BCB+1.D0)/(CNORM*ARHO (1))
DO 940 I=2,NP
940 ALAM (I)=CLAM*DMAG (I)*AS (I)*AS (I)/AFX (I)
IF ((.NOT.QUIT).AND.SHORT) RETURN
HR (1)=-(BCB+1.D0)/CNORM*SURF*SURF
HT (1)=-HR (1)
CALL ENPOLE (MAG,DMAG,H0,M0,ER,EG)
SC=0.D0
CALL FLUXPO (NP,H0,SC,SURF,FLUX)
WRITE (6,3200)
3200 FORMAT ('1',10X,'THE STREAM FUNCTION FOR THE MAGNETIC FIELD'//)
WRITE (6,3250) CLAM,CNORM,FLUX
3250 FORMAT (1X,'CLAM=',D10.3,10X,'CNORM=',D10.3,10X,'FLUX=',D10.3)
WRITE (6,3208) ER,H0
3208 FORMAT (1X,'ENERGY RATIO=',D10.3,10X,'H0=',F9.0,'GAUSS'//)
WRITE (6,3210)
3210 FORMAT (12X,'S',19X,'B',19X,'DB/DS',15X,'H RAD',15X,'H TAN',15X,
1 'ENERGY RATIO'//)
WRITE (6,3220) (AS (I),MAG (I),DMAG (I),HR (I),HT (I),RATIO (I),I=1,NP)
3220 FORMAT (1X,5F20.6,D20.6)
IF (.NOT.QUIT) RETURN

C
C
C
C THE P2 TERM OF THE GRAVITATION POTENTIAL
BCPOT=-(3.D0*(PP (NP)+BCB*PH (NP))+SURF*(SOLY (7)+BCB*SOLY (5)))
C2=CNORM*CNORM
BCPOT=BCPOT/(3.D0*POT2 (NP)+SURF*SOLY (9))/C2
EPS (1)=-(BCPOT+(1.D0+BCB)/C2-CLAM)*RHOAV*S3/ARHO (1)
DO 950 I=2,NP
POT2 (I)=BCPOT*POT2 (I)+(PP (I)+BCB*PH (I))/C2
950 EPS (I)=-AS (I)*(POT2 (I)-CLAM*MAG (I))/AFX (I)
WRITE (6,4000)
4000 FORMAT ('-', 'THE PATH OF CLAM WAS:')
WRITE (6,3999) (I,CONPAT (I),I=1,ICONUM)
3999 FORMAT (1X,I5,D20.5)
WRITE (6,3110)
3110 FORMAT ('1',9X,'I',10X,'EPS',17X,'LAMBDA',18X,'S',15X,'POT2'//)
WRITE (6,3100) (I,EPS (I),ALAM (I),AS (I),POT2 (I),I=1,NP)
3100 FORMAT (1X,I10,2D20.5,F20.5,D20.5)
E=EPS (NP)
DPOT2=S2*(BCPOT*SOLY (9)+(SOLY (7)+BCB*SOLY (5))/C2)
HLAM=ALAM (NP)

```

```

ROT=0.D0
IF(MAGOUT) WRITE(7,1999) H0,M0
1999 FORMAT(10X,'NORMAL MAGNETIC FIELD: H0=',F9.0,10X,'FOR M0=',F4.1)
IF(MAGOUT) WRITE (7,2000) (AS(I),MAG(I),DMAG(I),I=1,NP)
2000 FORMAT(3D25.16)
RETURN
END
SUBROUTINE AUXRK(Y,F)
IMPLICIT REAL*8 (A-H,O-Z)
DIMENSION ABETR(100)
DIMENSION Y(9),F(9),ARHO(100),AS(100),AN1(100),AT(100)
LOGICAL QUIT
COMMON /RKB/ CON1,CON2,RHOAV,SC
COMMON /MAINRK/ AN1,ABETR,AT
COMMON /ALL/ AS,ARHO,NP
COMMON /LAG/ NL,NMIN,NMAX
COMMON /ETC/ WT,QUIT
X=Y(1)
X2=X*X
F(2)=Y(3)
CALL LAGINS(AS,ARHO,X,DEN,N,NL,NMIN,NMAX,NP)
F(3)=2.D0*Y(2)/X2+DEN/RHOAV*X2
IF(QUIT) GO TO 10
DO 5 I=4,9
5 F(I)=0.D0
RETURN
10 CONTINUE
C NOTE THAT POT2 IS A DIMENSIONLESS POTENTIAL
CALL LAGINT(AS,ABETR,BET,N,NL,NP)
CALL LAGINT(AS,AN1,EN1,N,NL,NP)
CALL LAGINT(AS,AT,T,N,NL,NP)
F(4)=Y(5)
F(6)=Y(7)
F(8)=Y(9)
IF (T.LE..0D0) GO TO 50
CALC=DEN*WT/T*((3.D0*BET-4.D0)/EN1+1.D0)
GO TO 60
50 CALC=0.D0
60 CPOT=CON1*CALC
CB=CON2*CALC
F(5)=-2.D0*Y(5)/X+6.D0*Y(4)/X2-CPOT*Y(4)+CB*X2
F(7)=-2.D0*Y(7)/X+6.D0*Y(6)/X2-CPOT*Y(6)+CB*Y(2)
F(9)=-2.D0*Y(9)/X+6.D0*Y(8)/X2-CPOT*Y(8)
RETURN
END

```

\$C *SKIP

```

$C CON TO *SINK*@NOCC
  SUBROUTINE BFIELD
    IMPLICIT REAL*8 (A-H,O-Z)
    REAL*8 AS (100), ARHO (100), AN1 (100), MAG (100), DMAG (100)
1, EPS (100), ALAM (100), POT2 (100), PP (100), PH (100), AFX (100)
    REAL*8 M0
    LOGICAL QUIT, MAGOUT, SHORT, CURFIT
    DIMENSION HR (100), HT (100), RATIO (100)
    DIMENSION SOLY (9), SOLF (9), SOLQ (9)
    DIMENSION COEF (3, 3), RHS (3)
    DIMENSION IPASS (5), PASS (5)
    DIMENSION CONPAT (25)
    COMMON /MAINB/ MAG, DMAG, ALAM, SOLY, H0, M0, OMEGA, ICVCT
1, NMASS, PASS, IPASS, SHORT, MAGOUT, ICONUM, ICVG
2, MCVCT, CURFIT
    COMMON /ALL/ AS, ARHO, NP
    COMMON /RKB/ CON1, CON2, RHOAV, SC3
    COMMON /HFLUX/ HT, HR
    COMMON /MASS/ AFX
    COMMON /ETC/ WT, QUIT
    COMMON /LAG/ NL, NMIN, NMAX
    COMMON /ENERG/ RATIO
    COMMON /CTEMP/ DPOT2, HLAM, ROT, E
C MCVCT MOVES THE FITTING POINT INTO THE INTERIOR
  NXT=ICVCT+(NMASS+1)/2-MCVCT
  NB=ICVCT-NMASS/2-MCVCT
  CW=AS(NXT)-AS(NB)
  SC=AS(ICVCT)
  SC3=SC*SC*SC
  SURF=AS(NP)
  S3=SURF**3
  RHOAV=1.408376669*M0/S3
  DO 910 I=1,9
910 SOLY(I)=0.D0
    ICVCT1=ICVCT+1
    DO 10 I=1,ICVCT1
    PP(I)=0.D0
    PH(I)=0.D0
    MAG(I)=0.D0
    DMAG(I)=0.D0
    POT2(I)=0.D0
    ALAM(I)=0.D0
10 EPS(I)=0.D0
    SOLY(1)=AS(ICVCT)
    SOLY(3)=3.D0*SC
    DMAG(ICVCT)=SOLY(3)
C WHEN POT2, B ARE SMALL POT2 GOES AS S**2-SC**5/S**3
    SOLY(5)=5.D0*SC
    SOLY(7)=SOLY(5)
    SOLY(9)=SOLY(5)
C CON1=4*PI*G*H*R*R/(K*1D7)
C CLAM CONSTANT=2/(3*16*PI)*R/(G*M) MASS OF STAR
    CON1=4.917521412
    CLAM=.69603164D-17*(SURF**4*H0*H0/(RHOAV*M0))
C H0 IS THE RADIAL MAGNETIC FIELD AT THE POLE
    CON2=CON1*CLAM

```

```

NP1=NP-1
NL=4
NMIN=NL/2+1
NMAX=NP-(NL-1)/2
DO 920 J=ICVCT,NP1
I=J+1
H=(AS(I)-AS(J))/2.D0
CALL DRK(SOLY,SOLF,SOLQ,H,9,2)
MAG(I)=SOLY(2)
DMAG(I)=SOLY(3)
IF(.NOT.QUIT) GO TO 920
PH(I)=SOLY(4)
PP(I)=SOLY(6)
POT2(I)=SOLY(8)
920 CONTINUE
BCB=-(MAG(NP)+SURF*DMAG(NP))/(3.D0*SURF*SURF)
CNORM=DABS(MAG(NP)+BCB*(AS(NP)*AS(NP)-SC3/AS(NP)))
DO 930 I=ICVCT,NP
S2=AS(I)*AS(I)
MAG(I)=(BCB*(S2-SC3/AS(I))+MAG(I))/CNORM
DMAG(I)=(BCB*(AS(I)*2.D0+SC3/S2)+DMAG(I))/CNORM
930 CONTINUE
C CURVE FITTING TO CONVECTIVE CORE
IF(.NOT.CURFIT) GO TO 50
W2=CW*CW
W3=W2*CW
W4=W3*CW
W5=W4*CW
COEF(1,1)=W3
COEF(2,1)=3.D0*W2
COEF(3,1)=6.D0*CW
COEF(1,2)=W4
COEF(2,2)=4.D0*W3
COEF(3,2)=12.D0*W2
COEF(1,3)=W5
COEF(2,3)=5.D0*W4
COEF(3,3)=20.D0*W3
RHS(1)=MAG(NXT)
RHS(2)=DMAG(NXT)
RHS(3)=2.D0*MAG(NXT)/(AS(NXT)*AS(NXT))+ARHO(NXT)*AS(NXT)*AS(NXT)
1/(RHOAV*CNORM)
CALL DSOLTN(COEF,RHS,3,3,DET)
DO 12 I=NB,NXT
X=AS(I)-AS(NB)
X3=X*X*X
MAG(I)=RHS(1)*X3+RHS(2)*X3*X+RHS(3)*X3*X*X
12 DMAG(I)=3.D0*RHS(1)*X*X+4.D0*RHS(2)*X3+5.D0*RHS(3)*X3*X
50 CLAM=CLAM/CNORM
CONPAT(ICVG)=CLAM
DO 940 I=NB,NP
940 ALAM(I)=CLAM*DMAG(I)*AS(I)*AS(I)/AFX(I)
IF((.NOT.QUIT).AND.SHORT) RETURN
HR(1)=-(BCB+1.D0)/CNORM
HT(1)=-HR(1)
CALL ENPOLE(MAG,DMAG,H0,M0,ER,EG)
CALL FLUXPO(NP,H0,SC,SURF,FLUX)
WRITE(6,3200)
3200 FORMAT('1',10X,'THE STREAM FUNCTION FOR THE MAGNETIC FIELD WITH CO
INVECTION'//)
WRITE(6,3250) CLAM,CNORM,NMASS,NB

```

```

3250  FORMAT(1X,'CLAM=',D10.3,10X,'CNORM=',D10.3,10X,'NUMBER OF MASS SHE
      ILLS IN CURRENT ZONE=',I3,10X,'BEGINNING AT #',I3)
      WRITE(6,3211) FLUX,ER,H0
3211  FORMAT(1X,'FLUX=',D10.3,10X,'ENERGY RATIO=',D10.3,10X,'H0=',F9.0,'
      1GAUSS'//)
      WRITE(6,3210)
3210  FORMAT(12X,'S',19X,'B',19X,'DB/DS',15X,'H RAD',15X,'H TAN',15X,
      1 'ENERGY RATIO'//)
      WRITE(6,3220) (AS(I),MAG(I),DMAG(I),HR(I),HT(I),RATIO(I),I=NB,NP)
3220  FORMAT(1X,5F20.6,D20.6)
      IF(.NOT.QUIT) RETURN
C
C  THE P2 TERM OF THE GRAVITATION POTENTIAL
C  BC IS 3*POT2+SURF*POT2=0
C
      BCPOT=-(3.D0*(PP(NP)+BCB*PH(NP))+SURF*(SOLY(7)+BCB*SOLY(5)))
      C2=CNORM*CNORM
      BCPOT=BCPOT/(3.D0*POT2(NP)+SURF*SOLY(9))
      DO 950 I=NB,NP
      POT2(I)=(BCPOT*POT2(I)+PP(I)+BCB*PH(I))/C2
950  EPS(I)=-AS(I)*(POT2(I)-CLAM*MAG(I))/AFX(I)
      EPS(NB)=0.D0
      E=EPS(NP)
      DPOT2=S2*(BCPOT*SOLY(9)+SOLY(7)+BCB*SOLY(5))/C2
      ROT=0.D0
      HLAM=ALAM(NP)
      WRITE(6,4000)
4000  FORMAT('-', 'THE PATH OF CLAM WAS:')
      WRITE(6,3999) (I,CONPAT(I),I=1,ICONUM)
3999  FORMAT(1X,I5,D20.5)
      WRITE(6,3110)
3110  FORMAT('I',9X,'I',10X,'EPS',17X,'LAMBDA',18X,'S',15X,'POT2'//)
      WRITE(6,3100) (I,EPS(I),ALAM(I),AS(I),POT2(I),I=1,NP)
3100  FORMAT(1X,I10,2D20.5,F20.5,D20.5)
      IF(MAGOUT) WRITE(7,1999) H0,M0
1999  FORMAT(1X,'CONVECTIVE CORE MAGNETIC FIELD: H0=',F9.0,10X,'FOR M0='
      $ ,F4.1)
      IF(MAGOUT) WRITE(7,2000) (AS(I),MAG(I),DMAG(I),I=1,NP)
2000  FORMAT(3D25.16)
      RETURN
      END
      SUBROUTINE AUXRK(Y,F)
      IMPLICIT REAL*8 (A-H,O-Z)
      DIMENSION ABETR(100)
      DIMENSION Y(9),F(9),ARHO(100),AS(100),AN1(100),AT(100)
      LOGICAL QUIT
      COMMON /RKB/ CON1,CON2,RHOAV,SC3
      COMMON /MAINRK/ AN1,ABETR,AT
      COMMON /ALL/ AS,ARHO,NP
      COMMON /LAG/ NL,NMIN,NMAX
      COMMON /ETC/ WT,QUIT
      X=Y(1)
      X2=X*X
      F(2)=Y(3)
      CALL LAGINS(AS,ARHO,X,DEN,N,NL,NMIN,NMAX,NP)
      F(3)=2.D0*Y(2)/X2+DEN/RHOAV*X2
      IF(QUIT) GO TO 10
      DO 5 I=4,9
      F(I)=0.D0
      RETURN

```

10 CONTINUE
 CALL LAGINT(AS,ABETR,BET,N,NL,NP)
 CALL LAGINT(AS,AN1,EN1,N,NL,NP)
 CALL LAGINT(AS,AT,T,N,NL,NP)
 F(4)=Y(5)
 F(6)=Y(7)
 F(8)=Y(9)
 IF (T.LE..0D0) GO TO 50
 CALC=DEN*WT/T*((3.D0*BET-4.D0)/EN1+1.D0)
 GO TO 60
 50 CALC=0.D0
 60 CPOT=CON1*CALC
 CB=CON2*CALC
 F(5)=-2.D0*Y(5)/X+6.D0*Y(4)/X2-CPOT*Y(4)+CB*(X2-SC3/X)
 F(7)=-2.D0*Y(7)/X+6.D0*Y(6)/X2-CPOT*Y(6)+CB*Y(2)
 F(9)=-2.D0*Y(9)/X+6.D0*Y(8)/X2-CPOT*Y(8)
 RETURN
 END

120

\$C *SKIP

```

$C ROT TO *SINK*@NOCC
  SUBROUTINE BFIELD
    IMPLICIT REAL*8 (A-H,O-Z)
    REAL*8 AS(100), ARHO(100), AN1(100), MAG(100), DMAG(100)
    1, EPS(100), ALAM(100), POT2(100), PP(100), PH(100), AFX(100)
    2, HR(100), HT(100), RATIO(100)
    REAL*8 M0
    LOGICAL QUIT, MAGOUT, SHORT, CURFIT
    DIMENSION IPASS(5), PASS(5)
    DIMENSION SOLY(9), SOLF(9), SOLQ(9)
    DIMENSION CONPAT(25)
    COMMON /MAINB/ MAG, DMAG, ALAM, SOLY, H0, M0, OMEGA, ICVCT
    1, NMASS, PASS, IPASS, SHORT, MAGOUT, ICONUM, ICVG
    2, MCVCT, CURFIT
    COMMON /ALL/ AS, ARHO, NP
    COMMON /RKB/ CON1, CON2, RHOAV, SC
    COMMON /HFLUX/ HT, HR
    COMMON /MASS/ AFX
    COMMON /ETC/ WT, QUIT
    COMMON /LAG/NL, NMIN, NMAX
    COMMON /CTEMP/ DPOT2, HLAM, ROT, E
    COMMON /ENERG/ RATIO
    SURF=AS(NP)
    S2=SURF*SURF
    S3=SURF*S2
    O2=OMEGA*OMEGA
    RHOAV=1.408376669*M0/S3
C  CROT CONSTANT= 2/3*RSUN**3/(G*MSUN)
    CROT=1.694751728D6*O2/M0
    CROT2=CROT/2.D0
    CON1=4.917521412D0
    CLAM=.69603164D-17*(SURF**4*H0*H0/(RHOAV*M0))
    CON2=CON1*CLAM
    NP1=NP-1
    NL=4
    NMIN=NL/2+1
    NMAX=NP-(NL-1)/2
    DO 910 I=1,9
910  SOLY(I)=0.D0
    SOLY(1)=AS(2)-AS(1)
    MAG(1)=0.D0
    DMAG(1)=0.D0
    POT2(1)=0.D0
    PP(1)=0.D0
    PH(1)=0.D0
    SOLY(2)=SOLY(1)*SOLY(1)
    SOLY(4)=CLAM*SOLY(2)
    SOLY(6)=CLAM*SOLY(2)
    SOLY(8)=CLAM*SOLY(2)
    SOLY(3)=2.D0*SOLY(1)
    SOLY(5)=CLAM*SOLY(3)
    SOLY(7)=CLAM*SOLY(3)
    SOLY(9)=CLAM*SOLY(3)
    MAG(2)=SOLY(2)
    DMAG(2)=SOLY(3)
    POT2(2)=SOLY(8)

```

```

PP(2)=SOLY(8)
PH(2)=SOLY(8)
DO 920 J=2,NP1
I=J+1
H=AS(J+1)-AS(J)
CALL DRK(SOLY,SOLF,SOLQ,H,9,1)
MAG(I)=SOLY(2)
DMAG(I)=SOLY(3)
IF(.NOT.QUIT) GO TO 920
PH(I)=SOLY(4)
PP(I)=SOLY(6)
POT2(I)=SOLY(8)
920 CONTINUE
BCB=-(MAG(NP)+SURF*DMAG(NP))/(3.D0*SURF*SURF)
CNORM=DABS(MAG(NP)+BCB*AS(NP)*AS(NP))
DO 930 I=1,NP
MAG(I)=(BCB*AS(I)*AS(I)+MAG(I))/CNORM
DMAG(I)=(2.D0*BCB*AS(I)+DMAG(I))/CNORM
930 CONTINUE
CLAM=CLAM/CNORM
CONPAT(ICVG)=CLAM
CROTC=CROT*S3*RHOAV/ARHO(1)
ALAM(1)=2.D0*S3*RHOAV*CLAM*(BCB+1.D0)/(CNORM*ARHO(1))-CROTC
DO 940 I=2,NP
940 ALAM(I)=(CLAM*DMAG(I)-CROT*AS(I))*AS(I)*AS(I)/AFX(I)
IF(.NOT.QUIT).AND.SHORT) RETURN
HR(1)=- (BCB+1.D0)/CNORM*SURF*SURF
HT(1)=-HR(1)
CALL ENPOLE(MAG,DMAG,H0,M0,ERM,EG)
CALL EROTAT(M0,OMEGA,EG,ERR)
ER=ERM+ERR
SC=0.D0
CALL FLUXPO(NP,H0,SC,SURF,FLUX)
WRITE(6,3200)
3200 FORMAT('1',10X,'THE STREAM FUNCTION FOR THE MAGNETIC FIELD'//)
WRITE(6,3250) CLAM,CNORM,FLUX
3250 FORMAT(1X,'CLAM=',D10.3,10X,'CNORM=',D10.3,10X,'FLUX=',D10.3)
WRITE(6,3208) ERM,ERR,H0
3208 FORMAT(1X,'MAG ENERGY RATIO=',D10.3,10X,'ROT E RATIO',D10.3,10X,
$ 'H0=',F9.0,'GAUSS'//)
RLAM=CLAM/CROT
WRITE(6,3209) CROT,RLAM,OMEGA
3209 FORMAT(1X,'CROT=',D12.5,10X,'LAM MAG/LAM ROT=',D12.5,
$ 10X,'OMEGA=',D12.5//)
WRITE(6,3210)
3210 FORMAT(12X,'S',19X,'B',19X,'DB/DS',15X,'H RAD',15X,'H TAN',15X,
1 'MAG ENERGY RATIO'//)
WRITE(6,3220) (AS(I),MAG(I),DMAG(I),HR(I),HT(I),RATIO(I),I=1,NP)
3220 FORMAT(1X,5F20.6,D20.6)
IF(.NOT.QUIT) RETURN

C
C
C
C THE P2 TERM OF THE GRAVITATION POTENTIAL
C2=CNORM*CNORM
CB2=BCB/C2-CROT2/CLAM*CNORM
BCPOT=-(3.D0*(PP(NP)/C2+CB2*PH(NP))+SURF*(SOLY(7)/C2+CB2*SOLY(5)))
BCPOT=BCPOT/(3.D0*POT2(NP)+SURF*SOLY(9))
EPS(1)=-((BCPOT+1.D0/C2-1.D0/CNORM+CB2)*CLAM*CNORM+CROT2)
$ *RHOAV*S3/ARHO(1)

```



```

DO 950 I=2,NP
POT2(I)=BCPOT*POT2(I)+PP(I)/C2+CB2*PH(I)
950 EPS(I)=-AS(I)*(POT2(I)-CLAM*MAG(I)+CROT2*AS(I)*AS(I))/AFX(I)
RATEQU=1.5D0*CROT*S3*(1-.5D0*EPS(NP))**3
WRITE(6,3111) RATEQU
3111 FORMAT(' ', 'ROTATIONAL FORCE/GRAV FORCE AT EQUATOR IS:', D12.5)
WRITE(6,4000)
4000 FORMAT(' ', 'THE PATH OF CLAM WAS:')
WRITE(6,3999) (I, CONPAT(I), I=1, ICONUM)
3999 FORMAT(1X, I5, D20.5)
WRITE(6,3110)
3110 FORMAT(' ', 9X, 'I', 10X, 'EPS', 17X, 'LAMBDA', 18X, 'S', 15X, 'POT2'//)
WRITE(6,3100) (I, EPS(I), ALAM(I), AS(I), POT2(I), I=1, NP)
3100 FORMAT(1X, I10, 2D20.5, F20.5, D20.5)
E=EPS(NP)
DPOT2=S2*(BCPOT*SOLY(9)+SOLY(7)/C2+CB2*SOLY(5))
HLAM=CLAM*DMAG(NP)*S2
ROT=CROT*S3
IF(MAGOUT) WRITE(7,1999) HO, MO, OMEGA
1999 FORMAT(1X, 'ROTATION', 27X, F9.0, 10X, 'FOR MO=', F4.1, 10X,
$ 'OMEGA=', D12.5)
IF(MAGOUT) WRITE(7,2000) (AS(I), MAG(I), DMAG(I), I=1, NP)
2000 FORMAT(3D25.16)
RETURN
END
SUBROUTINE AUXRK(Y,F)
IMPLICIT REAL*8 (A-H,O-Z)
DIMENSION ABETR(100)
DIMENSION Y(9), F(9), ARHO(100), AS(100), AN1(100), AT(100)
LOGICAL QUIT
COMMON /RKB/ CON1, CON2, RHOAV, SC
COMMON /MAINRK/ AN1, ABETR, AT
COMMON /ALL/ AS, ARHO, NP
COMMON /LAG/ NL, NMIN, NMAX
COMMON /ETC/ WT, QUIT
X=Y(1)
X2=X*X
F(2)=Y(3)
CALL LAGINS(AS, ARHO, X, DEN, N, NL, NMIN, NMAX, NP)
F(3)=2.D0*Y(2)/X2+DEN/RHOAV*X2
IF(QUIT) GO TO 10
DO 5 I=4, 9
5 F(I)=0.D0
RETURN
10 CONTINUE
C POT2 IS A DIMENSIONLESS POTENTIAL
CALL LAGINT(AS, ABETR, BET, N, NL, NP)
CALL LAGINT(AS, AN1, EN1, N, NL, NP)
CALL LAGINT(AS, AT, T, N, NL, NP)
F(4)=Y(5)
F(6)=Y(7)
F(8)=Y(9)
IF (T.LE..0D0) GO TO 50
CALC=DEN*WT/T*((3.D0*BET-4.D0)/EN1+1.D0)
GO TO 60
50 CALC=0.D0
60 CPOT=CON1*CALC
CB=CON2*CALC
F(5)=-2.D0*Y(5)/X+6.D0*Y(4)/X2-CPOT*Y(4)+CB*X2
F(7)=-2.D0*Y(7)/X+6.D0*Y(6)/X2-CPOT*Y(6)+CB*Y(2)

```

```

F(9)=-2.D0*Y(9)/X+6.D0*Y(8)/X2-CPOT*Y(8)
RETURN
END
SUBROUTINE EROTAT(M0,OMEGA,EG,ERR)
IMPLICIT REAL*8 (A-H,O-Z)
REAL*8 M0
REAL*4 SQUANK,TOL,FIF,FROT,S0
DIMENSION AS(100),ARHO(100)
COMMON /ALL/ AS,ARHO,NP
COMMON /LAG/ NL,NMIN,NMAX
EXTERNAL FROT
C  CONSTANT=1/3*RSUN**3/(G*MSUN)
C=8.473758642D+5*OMEGA*OMEGA/M0
NL=4
NMIN=NL/2+1
NMAX=NP-(NL-1)/2
S0=SNGL(AS(NP))
FROT=DBLE(SQUANK(FROT,0.,S0,0.0,TOL,FIF))
ERR=C*EROT/EG
RETURN
END
FUNCTION FROT(S)
REAL*8 AS(100),ARHO(100),SS,DF
COMMON /ALL/ AS,ARHO,NP
COMMON /LAG/ NL,NMIN,NMAX
SS=DBLE(S)
CALL LAGINS(AS,ARHO,SS,DF,N,NL,NMIN,NMAX,NP)
FROT=SNGL(DF)*S**4
RETURN
END

```

\$C *SKIP